THE PHOTOCHEMISTRY OF ATMOSPHERIC OZONE

by

B.G. Hunt, B.Sc.

A THESIS

PRESENTED FOR THE DEGREE OF

MASTER OF SCIENCE

IN THE

UNIVERSITY OF ADELAIDE

MARCH, 1965.

CONTENTS

SUMMARY

This thesis is primarily concerned with the photochemistry of atmospheric ozone subjected to the somewhat artificial limitation of an oxygen atmosphere at rest. In order to relate the photochemical results to the actual ozone distribution in the earth's atmosphere a brief review is presented of our knowledge of atmospheric ozone and its variations and connections with other atmospheric effects. This is followed by a discussion of the likely effect on the photochemical ozone distribution of removing the limitation of an oxygen atmosphere, and including reactions involving atomic hydrogen and atomic nitrogen. These reactions would only affect the ozone distribution in the mesosphere and it is concluded that reactions involving atomic nitrogen can probably be safety neglected, but that those of atomic hydrogen are likely to be of some importance.

The photochemistry of an oxygen atmosphere in which it is assumed that photochemical equilibrium has been attained is then considered at some length. The values of the absorption coefficients of ozone and molecular oxygen, the spectral intensity of solar radiation and the various rate constants which are required for the photochemical calculations are discussed and tabulated. The likely photochemical reactions in an oxygen atmosphere are listed, and those of importance are taken to be representative of the processes actually occurring in the atmosphere. The methods used to calculate photochemical ozone profiles are outlined, and the results of such calculations are presented for the height range 10 to 80 km. The effect on the ozone profile of possible variations or alternatives to the selected values of the data are investigated, and regions in which uncertainties exist are defined. The conclusion arrived at is that the biggest uncertainty in the calculations involves the value of the rate constant for the reaction of atomic oxygen with ozone. The derived ozone profiles are compared with previous ozone calculations and it is shown that essentially the same results can be obtained by selecting the most suitable data.

The validity of the assumption that equilibrium ozone and atomic oxygen profiles are obtained at high levels in the atmosphere is subsequently investigated. The characteristic times for these gases in the atmosphere are calculated, and the possible consequences of these times on the attainment of equilibrium are discussed. Numerical methods are developed which permit the integration of the differential equations defining the atomic oxygen and ozone variations with time, allowance being made for the variation of the solar zenith angle with time of day. On applying these methods it is found that photochemical equilibrium cannot be expected to be attained above about 60 km in the atmosphere, and the extent of the departure from equilibrium and its variation with height are illustrated. The reasons for the departure from equilibrium are explained, and the likely effects of latitudinal and seasonal variations on the results are discussed. The extent of the diurnal photochemical variation of the total ozone amount in the atmosphere is given and compared with experimental observations.

The numerical methods developed for the above study are then applied to the determination of the variations which occur in the photochemical ozone profile in the mesosphere during an eclipse of the sun. Methods of representing the variation of the solar radiation intensity during an eclipse are developed both for the case where limb darkening of the sun is neglected as well as when it is included. The results obtained indicate that an increase in the ozone concentration occurs above about 50 km but that the total ozone variation is very small, and should not be observable from the ground. The reasons for the disagreement between theory and observation as regards this ozone increase are discussed, and attributed to instrumental deficiencies.

Finally the whole of the ozone reaction scheme in an oxygen atmosphere is re-examined in view of recent laboratory experiments on the rate of destruction of ozone by atomic oxygen. Using the standard reaction scheme it is shown that these laboratory results imply that very high ozone concentrations and total ozone amounts should be observed in the atmosphere, in disagreement with the known facts. Possible ways of modifying the ozone reaction scheme so that more realistic photochemical results are obtained are examined. It is shown that very satisfactory total ozone amounts and ozone profiles in the stratosphere can be obtained by allowing for the destruction of ozone by electronically excited atomic oxygen. High ozone concentrations are still obtained in the mesosphere but it is thought that allowing for reactions of atomic hydrogen would remove this discrepancy. The validity of the results obtained however depends on the rate at which the electronically excited atomic oxygen is deactivated in the atmosphere, which is unknown at present. Reactions involving electronically and vibrationally excited molecular oxygen are concluded to be unimportant as far as the photochemistry of ozone is concerned.

PREFACE

To the best of the author's knowledge and belief this thesis contains no material previously published or written by another person except when due reference has been made in the text.

Portions of Chapter 3 and the investigations presented in Chapters 4, 5 and 6 are claimed as original contributions. All programming of the equations for the IBM 7090 computer required for the calculations presented in this thesis was the work of the author.

This thesis contains no material which has been presented by the author for the award of any other degree or diploma in any university.

ACKNOWLEDGEMENTS

Most of the investigations reported in this thesis were carried out as part of my duties as a member of Flight Projects Group of the Weapons Research Establishment, and I am indebted to the Public Service Board for the opportunities presented for this work. I would also like to acknowledge the assistance of my supervisors, Professor J.H. Carver and Mr. B. Rofe, in the production of this thesis. In addition I am indebted to Mr. L.A. Nicholls of W.R.E. for several enlightening discussions on the application of the Runge-Kutta numerical integration technique to the problems arising in Chapters 4, 5 and 6.

Finally I would like to thank the various members of Publications Section of W.R.E. who assisted in the production of the finished form of this thesis, in particular Miss Robertson and Mr. Chambers who so willingly undertook the brunt of the work.

CHAPTER 1

A BRIEF REVIEW OF THE PRESENT STATE OF KNOWLEDGE OF THE OZONOSPHERE

1.1 General

Ozone, O_3, is an allotropic form of molecular oxygen, O_2, which occurs naturally in the atmosphere from ground level up to about 90km. The amount of ozone present in the atmosphere is minute, at ground level it is very variable with a relative concentration of about 1 part in 10^8 (10^{-2}p.p.m.), while its maximum relative concentration occurs in the middle stratosphere and is only about 10 p.p.m. The total amount of ozone in a vertical column of the atmosphere varies from about 2mm STP to 5mm STP compared with a total atmospheric thickness of about 8km STP. In view of this small amount of ozone one might well ask what is its importance and why is there so much interest in ozone. As will be shown below there are many reasons for such interest, ranging from air-conditioning of supersonic aircraft to the formation of airglow, but it does not seem an overstatement to say that ozone is undoubtedly the most important minor constituent in the atmosphere below 100km.

Simply as a constituent of the atmosphere ozone is of intrinsic interest since it differs from other constituents of the homosphere in that its absolute concentration increases with height initially, reaching a peak at about 25 to 30km and then decreasing again at higher altitudes. Some fairly typical vertical ozone distributions are given in figure 1, these were obtained by Johnson et al. (1952) from rocket flights at White Sands in America. This unusual vertical distribution is due to the way ozone is formed in the atmosphere by photochemical reactions and will be discussed in detail in the body of this thesis. It is this vertical distribution of ozone together with its absorption properties which produce many effects of particular interest to meteorologists, and this has resulted in a large effort being invested in measuring ozone variations both with latitude and season and also height.

1.2 Ozone variations and the circulation of the atmosphere

It is found at any one place that the total ozone amount undergoes a seasonal variation with a maximum in late winter and spring and a minimum in autumn. Latitudinally an increase in the total ozone amount is observed from the equator to the pole in winter and spring in the northern hemisphere but in autumn the maximum is situated at about 60°N. In the southern hemisphere the distribution is different with the maximum occurring at about 55°S for the major part of the year. A compilation of ozone measurements made prior to 1942, mainly for the northern hemisphere, has been made by Craig (1950) who illustrates some of the above variations. MacDowall (1960) has presented a composite diagram, reproduced in figure 2, of ozone measurements made during the I.G.Y. from seventeen stations distributed over the globe. The considerable difficulty which has

been experienced in explaining the observed ozone distribution and its seasonal variation has given rise to the term of "the ozone problem". The basic difficulty has been to account for the discrepancy between theory and observation. On the basis of the photochemical theory of ozone, which attributes the formation of ozone in the atmosphere to the dissociation of oxygen by the sun's ultraviolet radiation in the first instance, one would expect the maximum total ozone amount to be observed at the equator, the minimum at the poles, and also that the seasonal maximum would appear in summer and the minimum in winter. In order to explain this discrepancy Brewer (1949), Craig (1950) and others have postulated that circulations in the atmosphere are removing air, and thus ozone, from the equatorial regions where it is most readily formed and transporting it polewards where it accumulates in the lower stratosphere. As a result of the way variations in the total ozone amount are related to air movements, the concept has arisen of using ozone as a "tracer" in the atmosphere to study such movements. This concept is now so well established that MacDowall (1960) on the basis of a comparison of the total ozone distributions in the northern and southern hemispheres has stated that these indicate profound changes must exist in the circulations of the two hemispheres.

The transport of ozone in the atmosphere has now been extensively studied and Newell (1963), in particular, has gained considerable insight into the transport processes operating by using ozone data. He has shown that net polewards transport of ozone occurs by means of large scale eddies and not by the simple meridional circulation postulated previously, such a circulation in any case being unable to balance the angular momentum budget of the atmosphere. Newell found that these large scale eddies reach a maximum in winter and spring and he explains the ozone build up at this time of year in the polar regions as due to transport of ozone polewards and downwards from the ozone source region of about 20 to 30 km in the atmosphere over the equator. Since the ozone descends as it travels polewards it is protected from the sun's dissociating radiation and hence has an indefinite life which gives it the tracer properties. Further recent work of note on the ozone problem has been carried out by Godson (1960), who confined his discussion to the north polar region and showed that ozone increases correspond to injections of stratospheric air which travel northwards and downwards in agreement with Newell's conclusions. The essential difficulties of the ozone problem now appear to have been overcome although much further work is required to understand the detailed processes which occur.

The important function that the tropopause has in isolating the troposphere from the stratosphere and preventing mass-exchange between these two regimes has been greatly amplified by ozone studies. Newell (1963) has used a combination of the tracer properties of ozone and those of radioactive debris from nuclear bomb tests in the atmosphere to study these mass-exchange processes. He found that such exchange must occur principally in the region of the tropopause breaks in the sub-tropics (30°-35° Latitude), and is associated with the jet stream which is a feature of these breaks. Direct supporting evidence that mass transfer does actually occur in

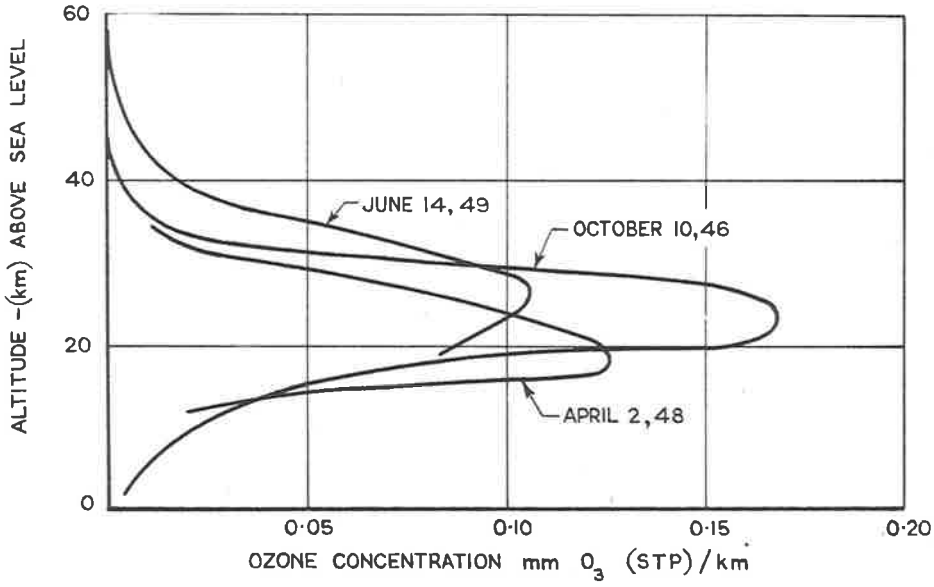

FIGURE 1. VERTICAL DISTRIBUTION OF O_3 FROM THREE NRL ROCKET FLIGHTS (AFTER JOHNSON, PURCELL, WATANABE AND TOUSEY, 1952)

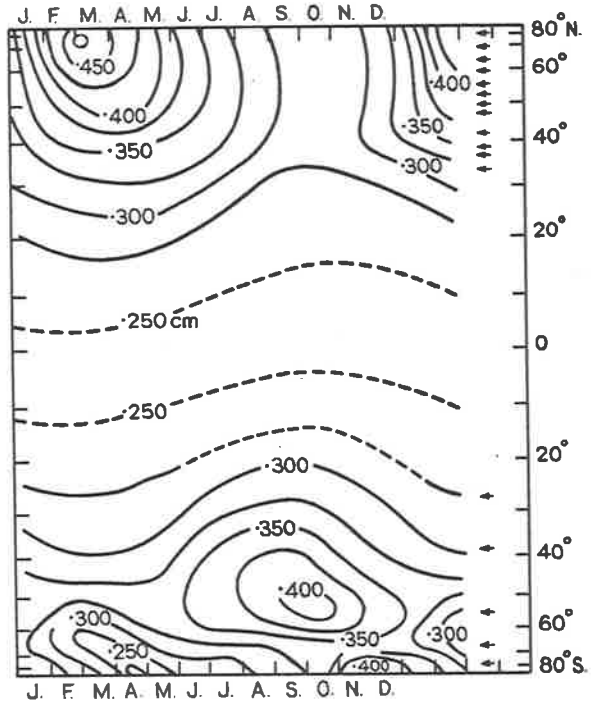

FIGURE 2. SMOOTHED OZONE RESULTS OF SEVENTEEN STATIONS DURING THE I.G.Y. ARE USED TO SHOW HOW THE NATURE OF THE OZONE DISTRIBUTION DIFFERS IN THE TWO HEMISPHERES. (AFTER MACDOWALL, 1960)

the neighbourhood of the tropopause gap has been provided by aircraft flights made by Briggs and Roach (1963) in the region of the temperate latitude jet stream. They found on several occasions that "tongues" of ozone rich air from the stratosphere had penetrated into the troposphere through the tropopause gap. It is thought that it is the presence of the jet stream which actually dominates the transfer process. The radical changes which are produced in the vertical ozone distribution due to the presence of the jet stream for stations very close in latitude, one being in the region of the sub-tropical tropopause gap, Salisbury 35°S, and the other Aspendale 38°S, just polewards of it, are illustrated in figure 3 which is taken from Hunt (1964). Although the profiles are for the same total ozone amount they are remarkably different, whereas for a given station the ozone profile in general is very similar for the same total ozone amounts regardless of the time of year, and this difference has been attributed to the transfer of ozone by the jet stream from the stratosphere to the troposphere through the tropopause gap for the station at Salisbury. The station at Aspendale is assumed to be free from this direct transfer process because of its position just south of the tropopause break. The variation of the monthly mean total ozone amounts for Salisbury and Aspendale also supports the hypotheses that the mass-exchange between the stratosphere and troposphere in winter and spring is a maximum.

The effect of the tropopause on the vertical distribution of ozone with latitude can best be illustrated by means of figure 4 taken from Ramanathan and Kulkarni (1960). It can be seen that the amount of ozone above 30 km remains virtually constant for all seasons and is the same for all latitudes. Below 30 km large changes occur in the vertical ozone distribution with the overall effect being that the large increases in the total ozone amount in the polar regions in spring are accommodated in the lower stratosphere. Mateer and Godson (1960) have found that in Canada three-quarters of the seasonal or daily changes in the total ozone are attributable to changes in the ozone content between 12 and 24 km. Increases in the total ozone amount in general result in a decrease in the height of the ozone centre of gravity as can be deduced from figure 4, the increase in the ozone amount taking place almost entirely below the height of the ozone maximum. Figure 4 also illustrates that the latitudinal gradient of ozone concentration in the stratosphere and troposphere is gradual in summer but in winter there is a steep rise at 30°N. This sudden increase at 30°N can be related to the change of the tropopause from equatorial, with a height of about 16 km, to polar with a height of about 10 km. Since the tropopause acts as a barrier to mass exchange the height range available for ozone storage in the stratosphere is greatly increased at latitudes with a polar tropopause thus permitting the accumulation of the large ozone amount resulting from the increase in stratospheric transport in the winter and spring. In contrast with this is the stability of the ozone in the tropics where it is mainly stored around 30 km, there being little change in the total ozone amount with season. Ozone cannot be stored in the troposphere because it

undergoes decomposition at the earth's surface and is also washed out by rain. In fact very little ozone is normally present in the troposphere and a sudden discontinuity is observed in the ozone profile at the tropopause as Brewer and Milford (1960) have shown from ozone sonde measurements, of which a typical one is reproduced in figure 5.

With the advent of a network of ozone sonde stations operating on a synoptic basis, it is to be hoped that a more comprehensive picture of the principal atmospheric circulations will be obtained and our knowledge of the atmosphere improved.

1.3 Ozone and the weather

In addition to variations with latitude and season ozone shows a marked variation with weather, which has been shown conclusively by Dobson et al. (1929) to be related to the local synoptic pressure situation in the atmosphere. As a result of this relation there is an appreciable day-to-day change in the total ozone amount which can be greater than the difference between the maximum and minimum monthly means for the entire year. The greatest day-to-day ozone variations take place in spring when both the total ozone amount and the latitudinal ozone gradient are a maximum. At one time it was thought that the ozone variations might be causing the weather changes. A close similarity was found by Dobson et al. (1929) between departures of the ozone content from its monthly mean and the isobaric pattern of the surface weather map, as indicated in figures 6 (a) and 6 (b). These show that positive ozone departures are associated with a cyclonic pressure distribution at the surface, while negative departures are associated with anti-cyclonic activity, the highest ozone deviations being to the west of the pressure centres. Later Dobson et al. (1946) reported that they could observe the effects on the total ozone amount of an advancing warm front several hundred miles before the front arrived at the surface. A reduction in the ozone content was observed for the passage of a warm front and the reverse for a cold front. The prior notice given by a warm front is due to the front sloping forward at an angle of about 1/150, since a cold front is normally much steeper than a warm front and also slopes backwards the change in the ozone amount occurs a short time after the passage of the front at the surface.

The variation of the ozone amount with weather has resulted in a considerable study of the processes occuring in the atmosphere which lead to this variation, and many correlations have been made between ozone variations and the height of the tropopause, various pressure levels, potential temperature etc. Probably the most important work in this regard was carried out by Normand (1953) who found that for day-to-day deviations from the monthly means there was a negative correlation between the ozone departure and the height of the tropopause and the thickness of the 500 to 300mb layer as shown in figure 7. It is apparent that there is a significant correspondence between these variables although the detailed variations are not perfect, as would be expected. Johansen (1957) found for ozone observations at Tromso

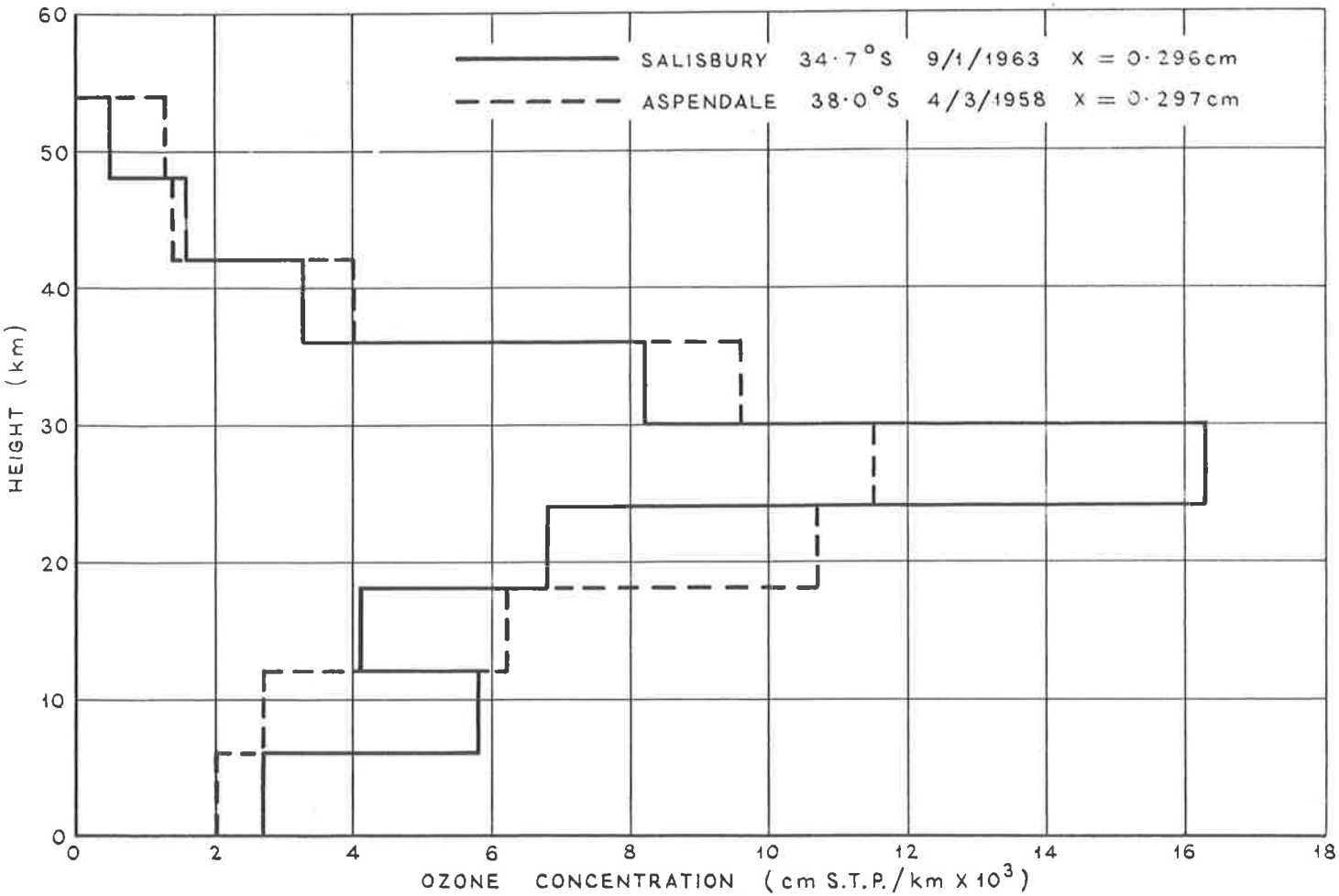

FIGURE 3. COMPARISON OF VERTICAL OZONE DISTRIBUTIONS FOR ASPENDALE AND SALISBURY

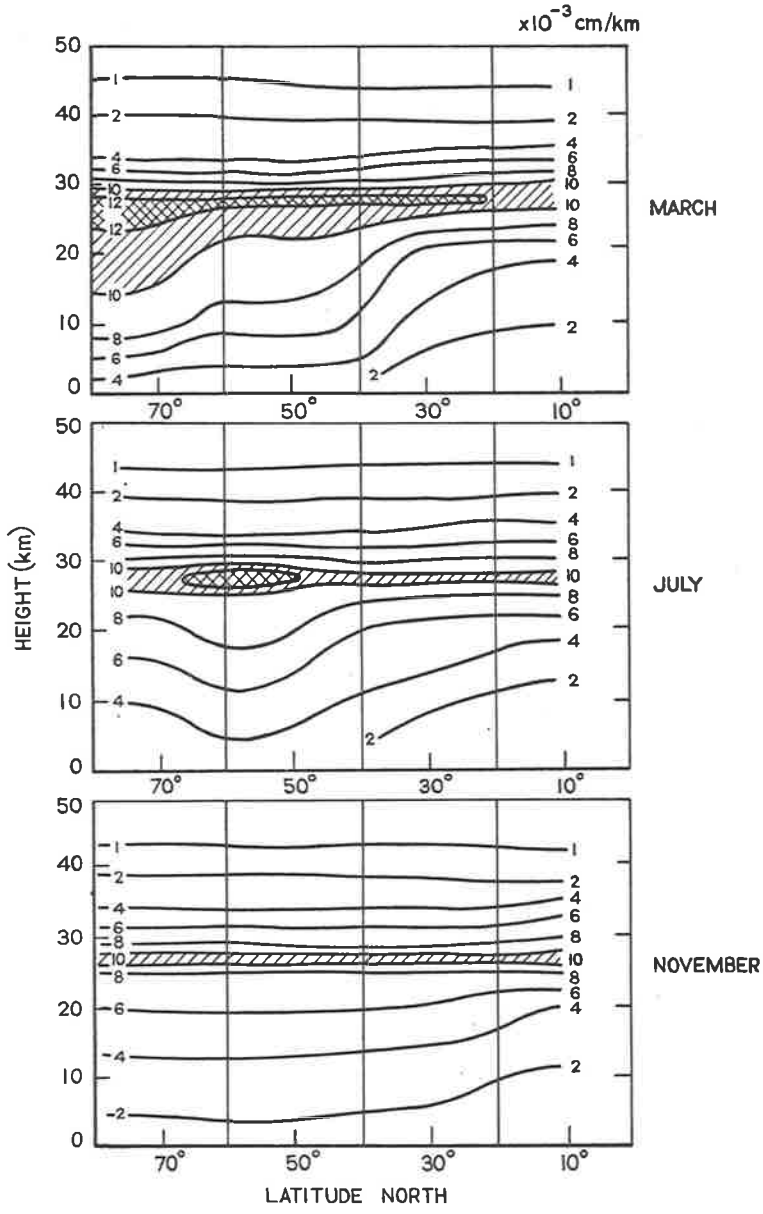

FIGURE 4. MEAN VERTICAL DISTRIBUTION OF OZONE IN MARCH, JULY AND NOVEMBER (10^3 CM KM^{-1} WITH NYE AND CHOONG'S α). (AFTER RAMANATHAN AND KULKARNI, 1960)

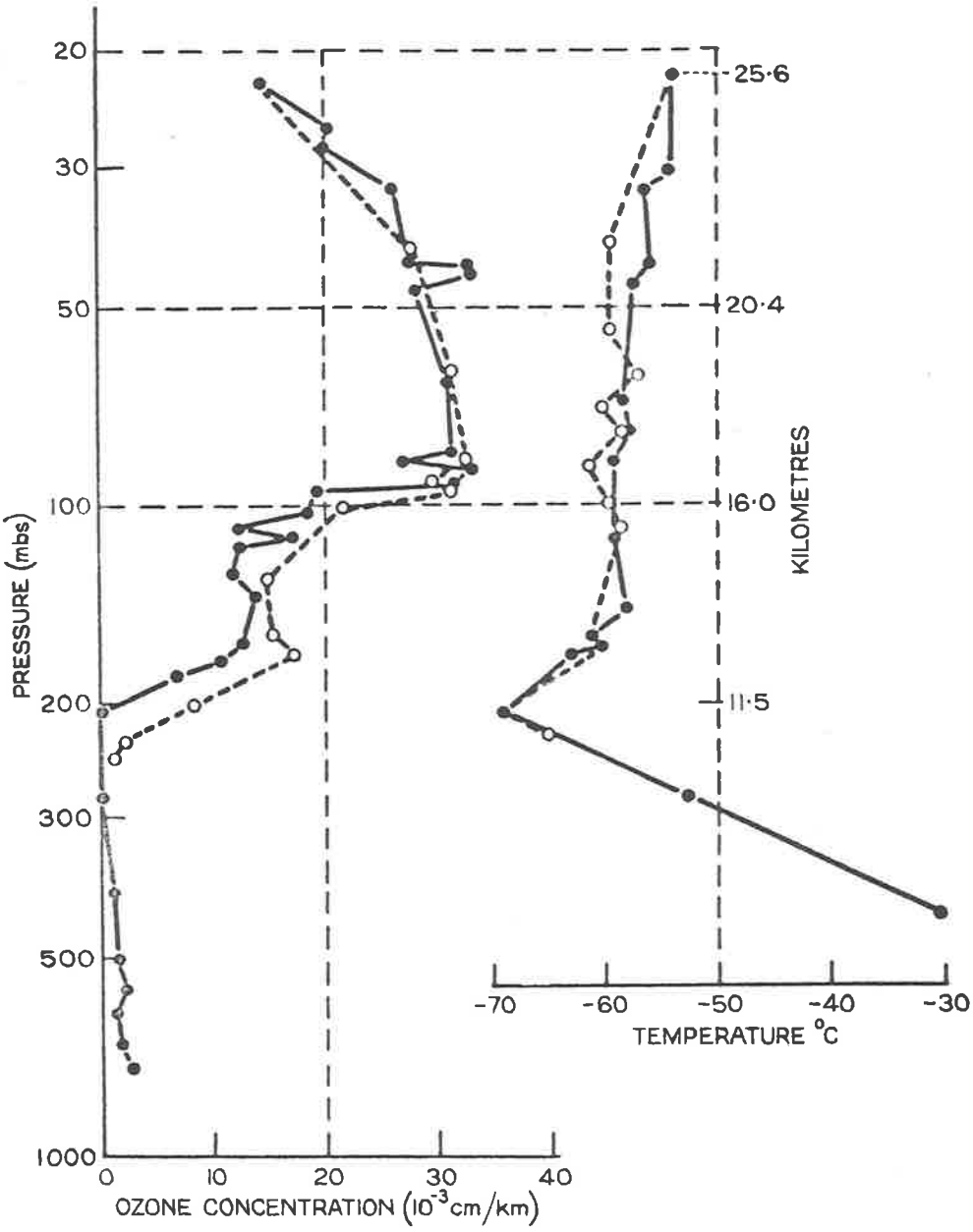

FIGURE 5. LIVERPOOL ASCENT, 14 APRIL 1958
(AFTER BREWER AND MILFORD, 1960)

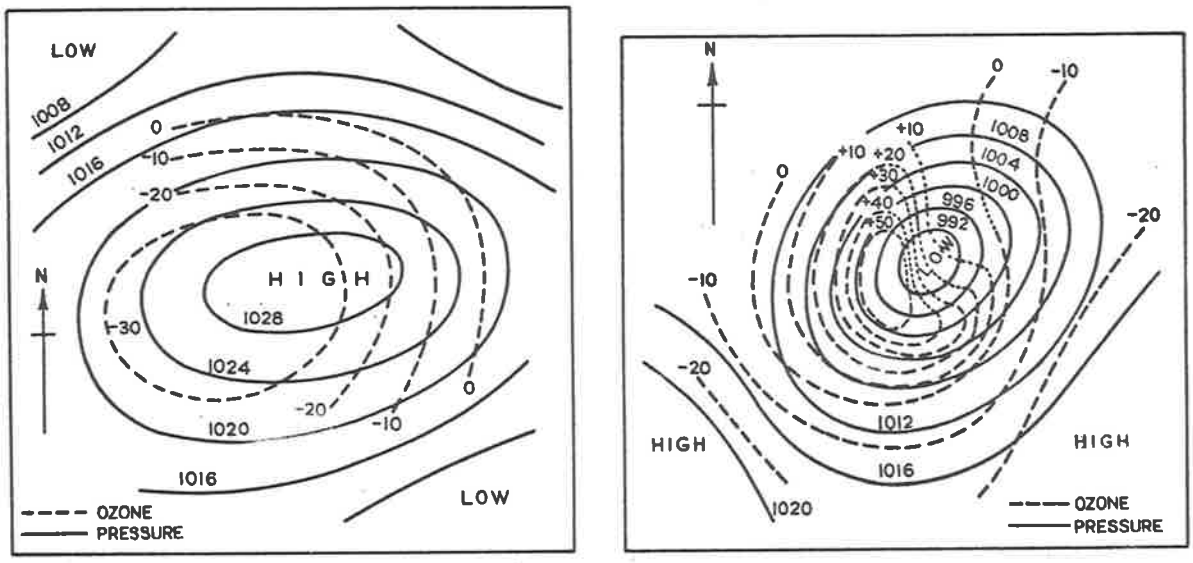

(a) (b)

FIGURE 6. ILLUSTRATING HOW THE AMOUNT OF OZONE IS RELATED TO PRESSURE DISTRIBUTION IN CYCLONE AND ANTICYCLONE. CONTINUOUS LINES ARE ISOBARS; THE DASHED CURVES ARE LINES OF EQUAL OZONE CONTENT. THE NUMBERS INDICATE DEPARTURES FROM THE MONTHLY OZONE-VALUES. THEY ARE POSITIVE OR NEGATIVE ACCORDING AS THE OBSERVED VALUE IS GREATER OR LESS THAN THE MONTHLY MEAN VALUE. (AFTER DOBSON, HARRISON AND LAWRENCE, 1929)

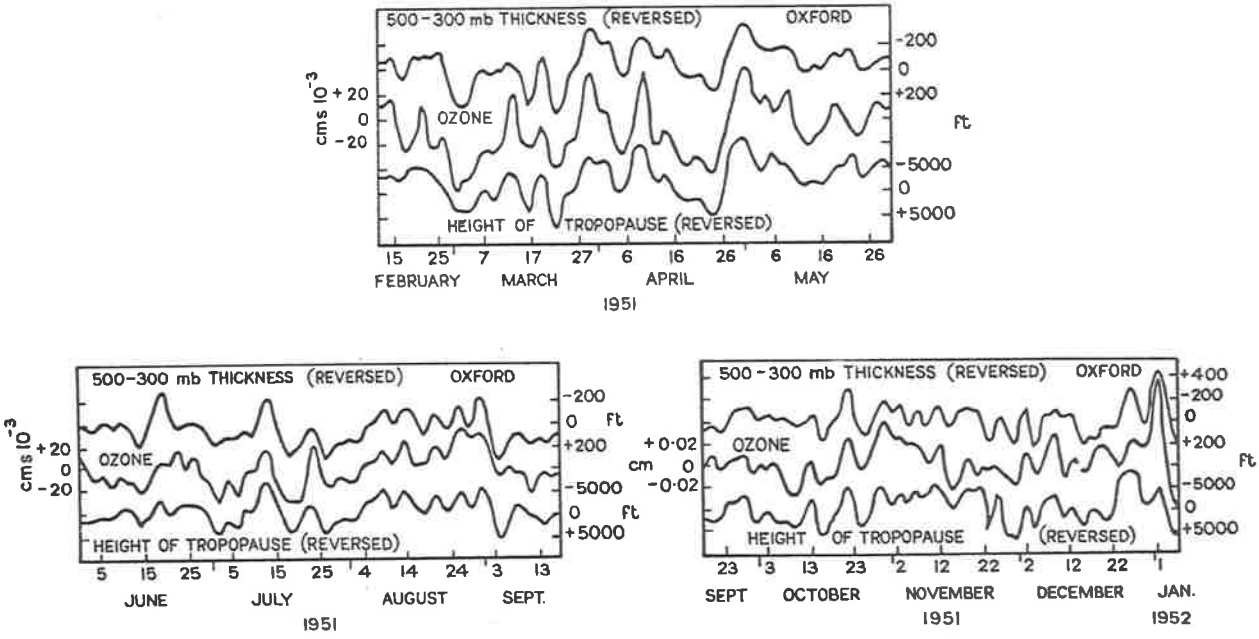

FIGURE 7. THE DEPARTURE FROM THE MONTHLY MEANS OF SMOOTHED DAILY OBSERVATIONS OF OZONE CONTENT, HEIGHT OF THE TROPOPAUSE AND THE THICKNESS OF THE 500-300 MB LAYER. THE DIRECTIONS OF THE DEPARTURES OF THE LAST TWO VARIABLES ARE REVERSED FOR CONVENIENCE. (AFTER NORMAND, 1953)

that there was a seasonal variation for correlations of this type, the correlation coefficient being small in mid-winter and highest during April and May. Ohring and Muench (1960) however, in a similar type of investigation obtained no signs of a definite seasonal variation of ozone correlation coefficients, although there were indications of a latitudinal variation with a maximum at 50°N.

Reed has investigated theoretically day-to-day ozone variations and their correlations with meteorological parameters, and has found that the observed variations can be explained by considering the high-level pressure troughs and ridges in the atmosphere. He, moreover, was able to calculate that a maximum ozone change of only about 0.04 cm STP can be expected to result from vertical air motions, this being made up of a positive deviation of 0.024 cm STP due to subsidence and a negative deviation of 0.017 cm STP due to divergence. As a result of these calculations Reed concluded that vertical motions in the atmosphere can account for, at the most, one-third of the observed ozone changes, the remainder must be attributed to advection. Thus to a large extent the relationship between ozone and weather variations is now understood.

A point that may be mentioned in passing is the large increase in ozone reported by Dobson et al. (1946) during a thunderstorm. Vassy (1951) has studied the ozone increase which occurs at ground level in relation to thunderstorms and claims that the electric potential gradient inside the thundercloud can be assumed to be responsible for the increase. Since the formation of ozone by this process is confined to the troposphere any ozone formed in this way would have only a local effect.

1.4 The relationship of atmospheric ozone and solar activity

As is well known the sun is not a quiescent radiator but undergoes an approximate 11 year cycle in which its activity varies greatly. The extent of this activity is normally measured at the earth's surface by means of the relative sunspot number or the earth's geomagnetic index. Since solar radiation is responsible for the formation of ozone it might be thought that variations could be observed in the atmospheric ozone content which could be related to solar disturbances. Many attempts have been made using statistical methods to discover if such an effect is present, but as Craig (1950) has emphasized, any direct ozone variations due to solar effects must take place above 35 km, and they are not reflected directly by variations in the total ozone amount. Ahmed and Halim (1961) report that there is little correlation between the earth's geomagnetic activity and changes in the total ozone amount. They also found that the correlation coefficient between total ozone and the sunspot number was not significant, in agreement with the findings of Gotz (1951) who gives a correlation coefficient of 0.01. Ahmed and Halim, however, state that possible changes in the extra-terrestrial calibration constant of the observing instrument, the Dobson spectrophotometer, could hide any possible changes.

On the other hand Willett (1962) claims to have found a highly significant negative correlation between the relative sunspot number and the worldwide average of total ozone. His results have been

challenged by London and Haurwitz (1963) who claim that they could have arisen from the use of biased data. Further doubt has been raised by Dobson and Normand (1962) who point out that instrumental errors could have been responsible for Willett's results.

A different type of investigation has been carried out by Kulkarni (1963) who found that within about 24 hours of a severe geomagnetic disturbance the total ozone amount decreased in the region of 50° - 65°N and increased south of about 50°N, resulting in a marked drop in the latitudinal ozone gradient in this region. Within two or three days of the storm the latitudinal gradient had returned to normal. Kulkarni suggests that a redistribution of ozone must occur during a magnetic storm but no direct proof is available of course as to how such a redistribution occurs. If Kulkarni's findings are proved to be statistically significant then an important discovery will have been made, as this provides direct proof that variations in the Sun's radiation have resulting effects on the atmospheric circulation. It must nevertheless be emphasized that no significant correlation exists between the total ozone amount and solar activity.

1.5 The biennial variation of ozone

An unusual type of variation for the atmosphere has been observed in recent years in the tropics and sub-tropics. This is the biennial variation of ozone, which was first reported by Funk and Garnham (1962) for ozone stations at Brisbane (27°S) and Aspendale (38°S) in Australia. They found a variation in the total ozone monthly means which in addition to the normal seasonal cycle showed a variation from year to year in the overall maximum and minimum. A more extensive series of measurements has recently been examined by Ramanathan (1963) who showed that the biennial oscillation could be detected as far north as Rome (42°N), as illustrated in figure 8. As Ramanathan pointed out years of high ozone and low ozone occur simultaneously for both hemispheres if allowance is made for the phase difference in the seasons. At the equator, as represented by Kodiakanal 10°N, the ozone variation is of the opposite phase to that of the higher latitudes.

In addition to ozone variations a now well substantiated, Ebdon (1961), Reed and Rogers (1962), stratospheric wind cycle in the equatorial regions of approximately two years has also been found. It is natural to endeavour to relate these ozone and wind variations and Ramanathan (1963) has advanced the following surprisingly simple hypothesis. Easterly winds in the equatorial stratosphere, owing to their tendency to conserve angular momentum, produce slow descent of ozone from above which will warm up the lower equatorial stratosphere and change the stratospheric winds to westerly. This leads to an upward movement, outward flow of air to higher latitudes, a loss of ozone and subsequent cooling and re-establishment of equatorial easterly winds.

A further explanation of the biennial wind oscillation has been advanced by Staley (1963). He suggests that this cycle results from a fluctuation of solar radiation with a period of about 26 months, such a solar cycle having been noted by Shapiro and

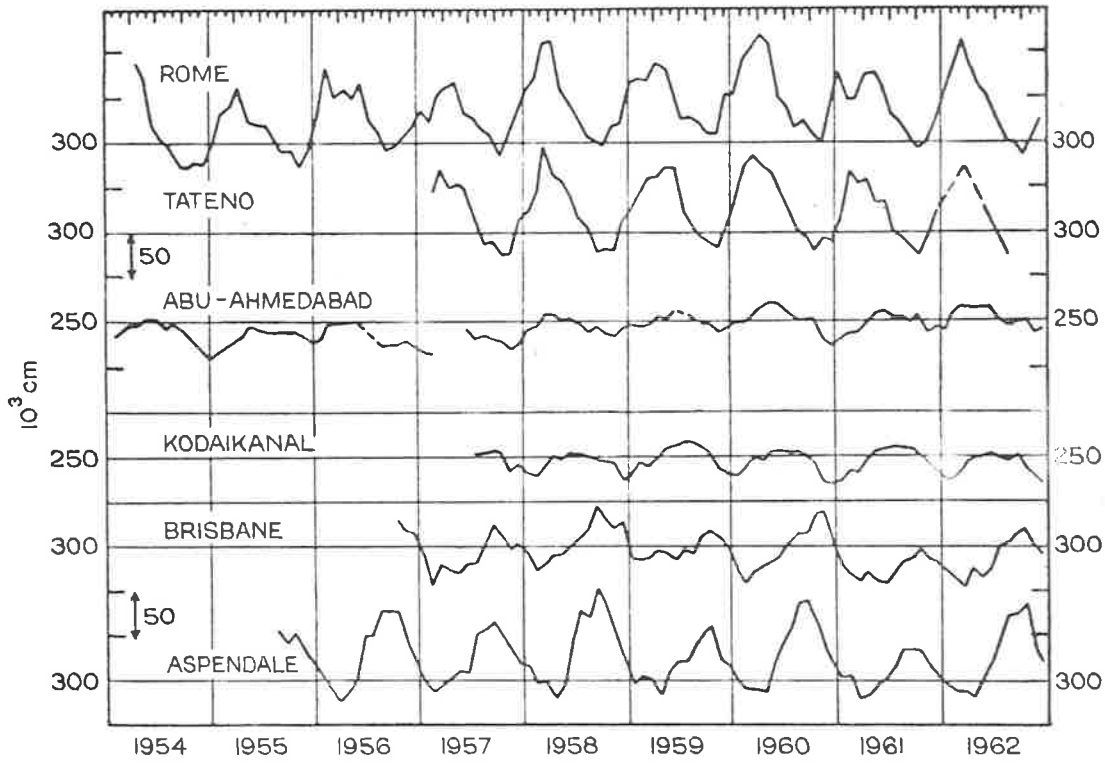

FIGURE 8. MONTHLY MEAN OZONE AMOUNTS
(AFTER RAMANATHAN, 1963)

Ward (1962). Ozone is presumed to be the most likely absorber, and the heat absorbed around 35 to 40 km is assumed to propagate downwards. Staley however does not directly relate the biennial cycles of ozone and wind as Ramanathan did, and his explanation does not appear to explain the facts as readily as Ramanathan's hypothesis. More data and more detailed calculations are needed to verify these ideas however.

1.6 Ozone and radiation

In spite of the wealth of information which has been revealed on atmospheric motions by the study of total ozone variations, the major geophysical interest in ozone arises from the effects of its absorption of radiation. Ozone has a very strong absorption spectrum in the near ultraviolet with a maximum at 2550Å and a rather weak absorption spectrum in the visible (these absorption spectra will be discussed again in more detail in Chapter 3). Further absorption bands lie in the near infrared at 4.7μ, 9.6μ and 14.1μ. The spectral cut-off at about 2900Å which occurs in the solar radiation received at ground level is due to ozone absorption in the atmosphere, and in fact without the protection of the ozone layer it seems unlikely that life in its present form could exist on this planet, because of the dangerous effects of the sun's ultraviolet radiation. The absorption of solar radiation in the ozonosphere results in the degradation of radiative energy to heat energy via the chemical reactions which take place in the photochemical reaction scheme of ozone. It is the absorption of solar ultraviolet radiation by ozone which is responsible for the temperature rise in the stratosphere shown in figure 9, where, according to the ARDC 1959 model atmosphere, a maximum temperature of 283°K occurs at the stratopause, which is approximately the same as that at ground level. Although the maximum ozone absorption is at about 30 km, in the region of the ozone maximum, the temperature peak occurs at about 50 km. This is because the temperature rise produced is proportional to the ratio of the absorbed energy and the atmospheric density, and this ratio is greatest at about 50 km since density falls with height. Gowan (1947a) has confirmed theoretically that ozone absorption can account for the observed temperature maximum at the stratopause by using an elementary model which assumes that radiative equilibrium exists. He obtained temperatures of the order of 400°K at 50 km, which are much too large, but these can be accounted for by the use of a more realistic model. Also he showed, Gowan (1947b), that the temperature maximum at 50 km persists throughout the night, as is now well known.

Several calculations, of which those by Murgatroyd and Goody (1958) are the most frequently quoted, have been made of the temperature changes which result from absorption of solar radiation in the ozonosphere. The net temperature changes per day at various heights as a function of latitude are given in figure 10 according to Murgatroyd and Singleton (1961). The heating is due almost entirely to ozone absorption in this region, except near 80 km where absorption by molecular oxygen becomes important, the long wavelength radiative cooling is by ozone and carbon dioxide,

water vapour being unimportant at these altitudes. Plass (1956a, 1956b) has calculated the heat loss due to ozone and carbon dioxide radiation in the atmosphere. Although the resulting temperature changes are quite small Murgatroyd and Singleton found that they were sufficient to give rise to meridional circulations of a significant order. The effect of latitudinal and seasonal changes on the temperature rises due to ozone absorption of solar radiation has been calculated by Pressman (1955), who found that strong temperature changes were to be expected. Johnson (1953) calculated the diurnal temperature change in the ozonosphere from ozone absorption taking data measured from a rocket flight and found that the maximum change was 5.3°K at 48 km. This temperature change is quite unremarkable but Butler and Small (1963) have claimed that diurnal heating of the ozonosphere must be responsible for the diurnal, semi-diurnal etc. pressure oscillations measured at the earth's surface.

Although most of the ozone absorption in the stratosphere is of solar ultraviolet radiation, at the lower levels adjacent to the tropopause absorption of terrestrial infrared radiation is considered to be important. Estimates of the amount of such radiation absorbed by ozone have been made by Dobson et al. (1946), who found that most of the energy emitted from the earth between 9 and 10μ is absorbed in the lower stratosphere. They related this absorption by ozone and its annual variation to the annual variation of the temperature in the lower stratosphere, which is reproduced in figure 11 together with corresponding temperatures in the troposphere. They consider that the tropospheric temperatures indicate that the lower troposphere is heated from the earth's surface, because of the temperature lag about the time of the solstice, and that the upper troposphere is heated from the lower because of the respective temperature lags. Since the maximum temperature in the lower stratosphere occurs at the time of the solstice they reasoned that the annual variation of ozone coupled with direct absorption of terrestrial radiation would result in just this type of temperature variation, as if it were heated from the troposphere a temperature lag would be apparent. The picture they present is an over-simplification and Goody (1954) states that in order to get the correct phase relations it is necessary to consider direct absorption of solar radiation by ozone also at these heights. Dobson et al. (1946) went on to generalize their premise to explain the annual and latitudinal variations of the height of the tropopause in terms of ozone absorption of terrestrial infrared radiation. Although their results are only qualitative and omitted absorption by water vapour and carbon dioxide, and also neglected convective motions in the troposphere, they probably are correct in the overall trends and they do serve to illustrate the importance of ozone to the radiation balance of the lower atmosphere.

Efforts have been made from time to time to find a connecting link between atmospheric variations in the stratosphere and troposphere, as such a connection might reveal that stratospheric variations have effects on conditions in the troposphere, and so

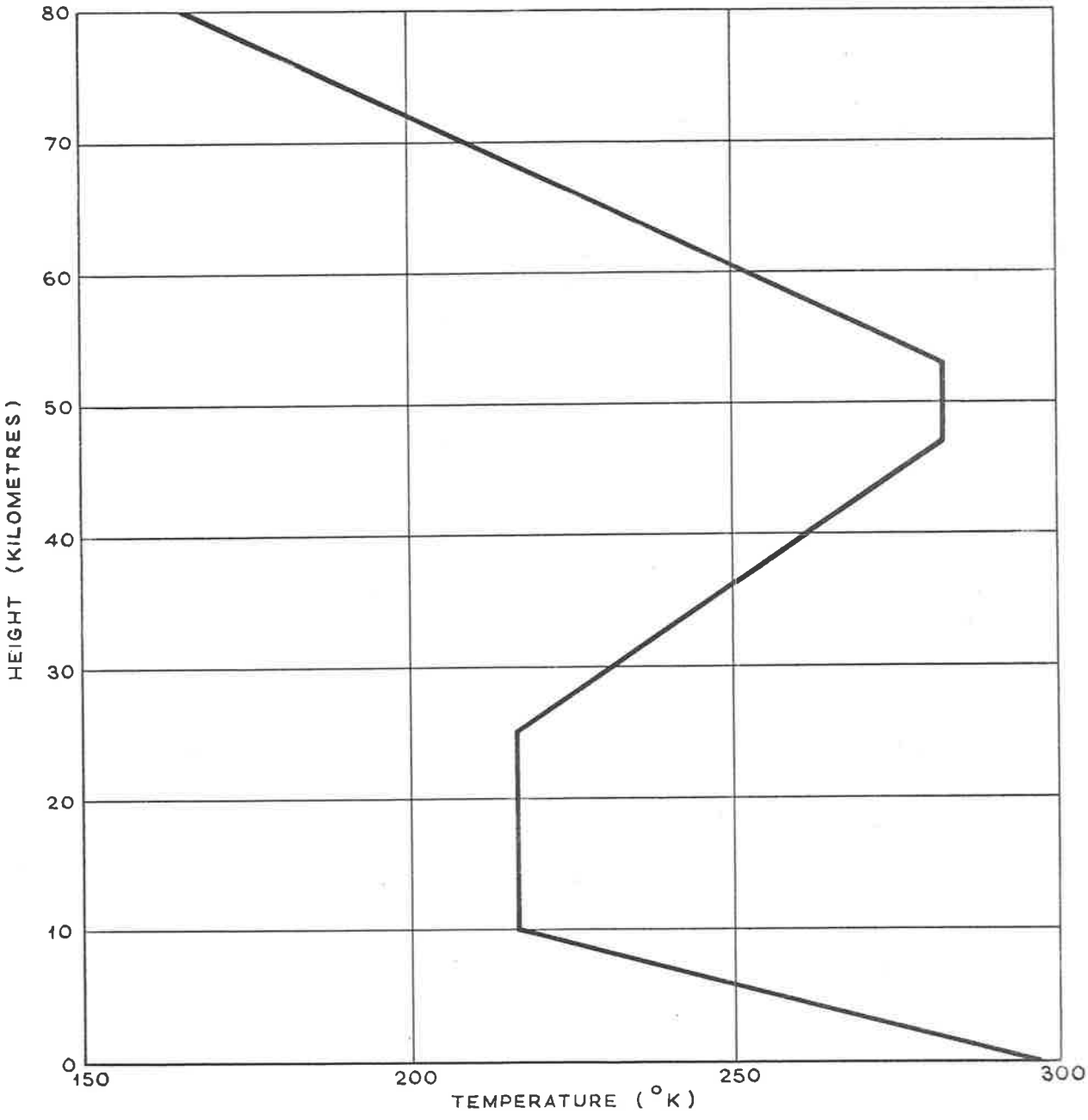

FIGURE 9. THE 1959 ARDC TEMPERATURE DISTRIBUTION UP TO 80 KM

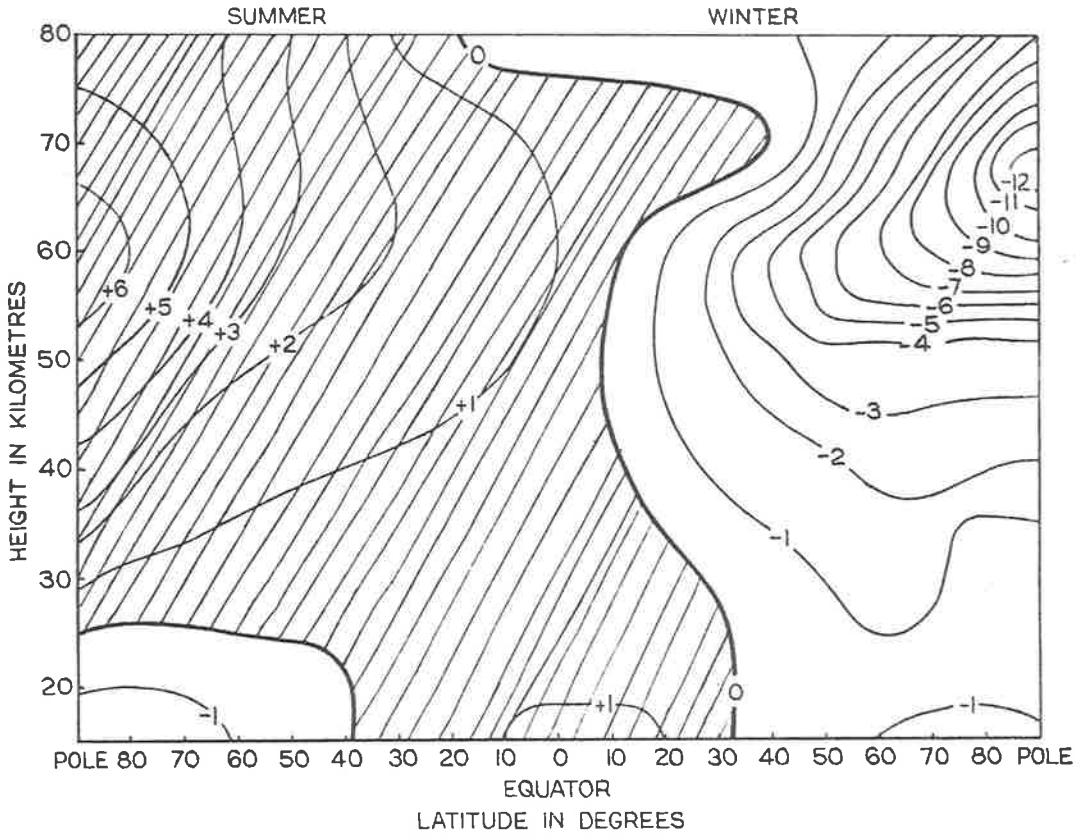

FIGURE 10. RADIATIVE HEADING AND COOLING $^{o}K\ DAY^{-1}$.
REGIONS OF HEATING ARE SHADED.
(MURGATROYD AND SINGLETON, 1961)

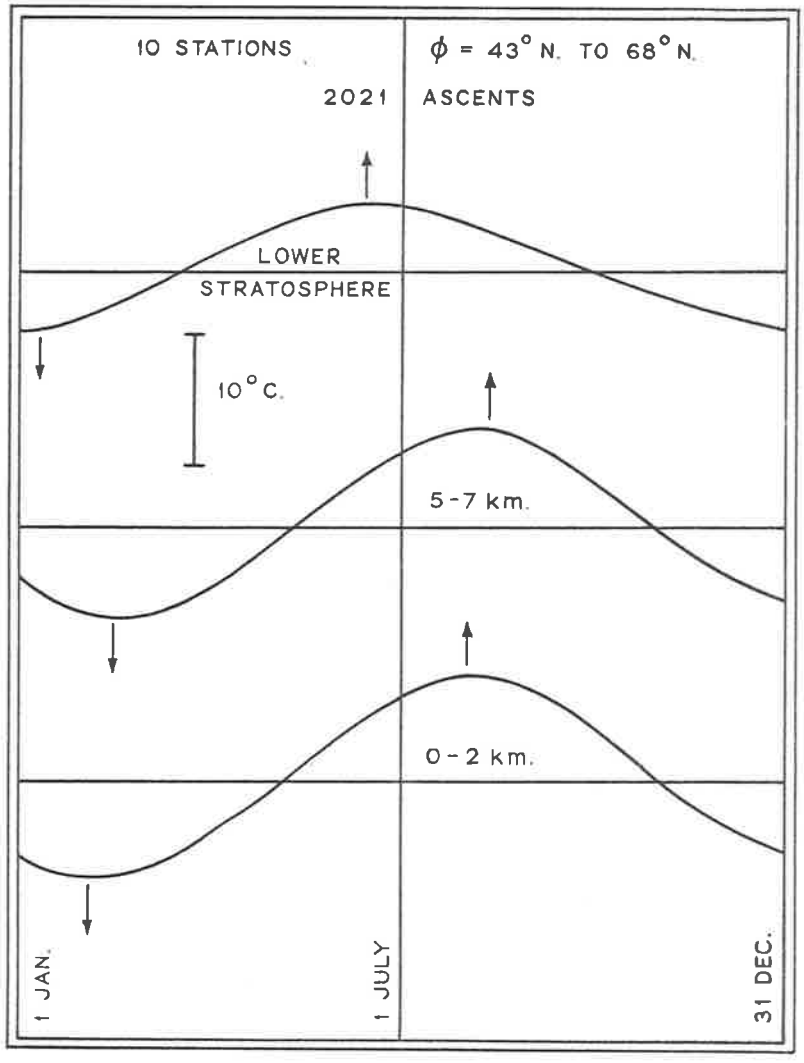

FIGURE 11. ANNUAL VARIATIONS OF TEMPERATURE IN THE TROPOSPHERE AND STRATOSPHERE (AFTER DOBSON ET AL., 1946)

could lead to a better understanding of dynamic processes in the atmosphere. It is possible that ozone might be important in this respect and also that ozone might provide a means by which the sun can influence our weather, although attempts to find any such effect have failed to date (Wexler, 1950). The interest in solar activity and ozone variations discussed previously arises to a large extent from the possibility that such activity might affect our weather. Ozone seems to provide the most suitable means by which solar variations can be transmitted into the atmospheric circulation system because of the way ozone is inextricably related to the atmosphere. It is possible that some of the atmospheric changes which are reflected by ozone variations are, if not actually initiated, at least require ozone for their maintenance. Thus the latitudinal and seasonal ozone distribution arises from atmospheric circulations which can be related back to absorption of solar radiation by ozone in the first instance, as demonstrated by Murgatroyd and Singleton (1961). A similar effect may occur with the biennial variations discussed in Section 1.5 if the explanation advanced by Ramanathan (1963) is correct. Again, the explanation given by Dobson et al. (1946) of the seasonal and latitudinal variations discussed in this section although superficial indicates that the lower height of the tropopause in high latitudes, which permits the accumulation of large ozone amounts, may in fact be largely due to the presence of the ozone itself. Hence, it appears that ozone has a peculiarity in that it may be responsible for many of the atmospheric effects whose consequences result in ozone variations. In the future the possibility of climate control via the adjustment of the atmosphere's ozone distribution will undoubtedly receive serious attention.

1.7 Ozone and the airglow

It does not generally seem to be appreciated that most of airglow luminosity arising in the atmosphere results from reactions involving ozone in some way. Thus the most intense source of airglow in the night sky arises from radiation emitted by vibrationally excited hydroxyl radicals in the ground electronic state. These radicals are formed according to Bates and Nicolet (1950) by the following reaction

$$H + O_3 \rightarrow OH^* + O_2$$

The radiation emitted by the excited radical as it returns to its normal state, $v'' = 0$, extends from the visible to the far infrared region of the spectrum and gives rise to an estimated airglow intensity of 4500 kR (Chamberlain 1961).

The above reaction has been challenged by Krassovsky (1955) who has advanced an alternative involving vibrationally excited oxygen.

$$O_2^* + H \rightarrow OH^* + O$$

The O_2^* presumably being formed by

$$O + O_3 \rightarrow O_2^* + O_2 \qquad \text{(see Chapter 6)}$$

In each case the cycle is completed via

$$OH + O \rightarrow O_2 + H$$

Krassovsky's reaction scheme has in turn been reputed in some detail by Bates and Moiseiwitsch (1956) and he has recently modified his original suggestions, as will be discussed in more detail in Chapter 2. It appears however that ozone is undoubtedly involved in the production of the hydroxyl airglow.

It also seems likely that at least part of the intensity of the Atmospheric airglow system of oxygen can be attributed to ozone. These bands arise from a radiative transition between an electronically excited state, $O_2(^1\Sigma_g^+)$ and the ground state of oxygen $O_2(^3\Sigma_g^-)$

$$O_2(^1\Sigma_g^+) \rightarrow O_2(^3\Sigma_g^-) + h\nu$$

The (0,0) band of this forbidden system is situated at 7619Å but is not observed at the surface because of atmospheric absorption, the (0,1) band at 8645Å is however observed (Chamberlain 1961). The formation of this band system can result either directly from the dissociation of ozone for wavelengths below 2670Å or indirectly by reaction of molecular oxygen with electronically excited atomic oxygen, see Chapter 6. The latter constituent, $O(^1D)$, can result from the dissociation of ozone below 3100Å or of oxygen below 1750Å. The following reaction is presumed to take place, Seaton (1958)

$$O(^1D) + O_2(^3\Sigma_g^-) \rightarrow O_2(^1\Sigma_g^+) + O(^3P)$$

The formation of the Infrared Atmospheric band system of oxygen has been discussed in some detail by Vallance Jones and Gattinger (1963). These bands arise from the forbidden electronic transition

$$O_2(^1\Delta_g) \rightarrow O_2(^3\Sigma_g^-) + h\nu$$

The (0,0) band at 1.27μ is again not observable at the surface because of atmospheric absorption. Vallance Jones and Gattinger assumed that the $O_2(^1\Delta_g)$ was formed principally by ozone dissociation below 3100Å together with the reaction

$$O(^1D) + O_2(^3\Sigma_g^-) \rightarrow O_2(^1\Delta_g) + O(^3P)$$

They were able to explain the twilight variation of this band system fairly satisfactorily with the complete reaction scheme which they considered.

Finally it may be mentioned that Ballif and Venkateswaran (1963b) have shown that the nightglow emitted by sodium may be due to reactions involving ozone, although at the present time they do not exclude the possibility of atomic hydrogen being more important than ozone in this reaction scheme.

1.8 Methods of measuring atmospheric ozone

Because of its convenient absorption spectrum the most widely used way of determining ozone amounts has been based on measuring the intensity of radiation of known initial strength after its traversal through a layer of ozone. This method has been selected for the Dobson spectrophotometer, Dobson (1957), which is the standard measuring instrument used throughout the world for total ozone determinations. This instrument uses a monochromator to isolate two wavelengths of interest, one being centred around 3100Å and the other at about 3300Å. The intensity of the radiation reaching the earth's surface at 3100Å is quite highly absorbed by ozone whereas that at 3300Å is only very weakly absorbed, hence the intensity of these two wavelengths is quite different. The radiation of the two wavelengths, after traversing a second monochromator to reduce effects due to scattered light, is then allowed to fall alternately on to a photomultiplier. The intensity of the stronger beam is reduced by means of a calibrated optical wedge until the photomultiplier indicates that the two beams are of equal intensity. The position of the wedge is noted, as is the time of the observation, and the total ozone amount, x, is calculated from the following formula

$$\log \frac{I_1}{I_2} = \log \frac{I_{1,0}}{I_{2,0}} - (\alpha_1 - \alpha_2)\mu x - (\beta_1 - \beta_2)M - (\delta_1 - \delta_2)\sec Z$$

where subscripts 1 and 2 refer to the short and long wavelengths respectively, α, β and δ being the coefficients of ozone absorption, Rayleigh scattering and particulate scattering respectively. μ, M and Z are very nearly identical and allow for the variation of the atmospheric pathlength with zenith angle. I is intensity of the radiation at the earth's surface and I_0 that outside the earth's atmosphere. The optical wedge reading on the spectrophotometer is related directly to the factor $N = \log \frac{I_{1,0}}{I_{2,0}} - \log \frac{I_1}{I_2}$ in tables supplied with each instrument. Various pairs of wavelengths can be selected on the instrument and in practice the A and D pairs are

used in the "difference method", Dobson (1957), in order to eliminate effects of particulate scattering. Observations are normally made on the direct sun, if possible, when an ozone measurement is being made, alternatively observations can be made on the zenith sky or cloud although a small correction must be made in these cases. Because of the various precautions taken in the design of the instrument and the method of observation the accuracy of total ozone measurements is quoted as 2%.

The Dobson spectrophotometer can also be used to provide a crude vertical ozone distribution, the data in figure 3 being obtained in this way, by what is known as the umkehr or inversion effect. Observations are made on the zenith sky with a single wavelength pair for a range of solar zenith angles, Z, as the sun is rising or falling, and it is found that if Z is plotted against N then a turning point is reached at about 86.5°. This variation can be explained in terms of the relative importance of absorption and scattering on the two wavelengths of interest, and the shape of the umkehr curve is related to the vertical ozone distribution in the atmosphere. The ozone profile obtained from the umkehr effect is not particularly accurate especially at the lower levels, and is generally analysed to give a "block" distribution for 9 layers each 6 km thick between 0 and 54 km. Because of the lack of any other suitable method it has nevertheless provided most of our information on the vertical distribution of ozone in the atmosphere.

In order to obtain more detailed ozone profiles, and to avoid the use of the cumbersome umkehr method, a large effort is at the present time being devoted to the development of a cheap, efficient means of measuring ozone concentrations from balloons using ozone sondes. These ozone sondes are normally standard meteorological radio sondes in which one of the recording channels transmits ozone data from an ozone sensor attached to the balloon.

The most widely used ozone sonde at the moment is the "bubbler" method devised by Brewer and Milford (1960). This method makes use of the following reaction

$$2KI + H_2O + O_3 \rightarrow 2KOH + I_2 + O_2$$

Now if electrodes are immersed in the solution and a small voltage is maintained between them then a current will flow, since at the cathode the free iodine is reduced to iodide

$$I_2 + 2e \rightarrow 2I^-$$

and at the anode iodine is reformed

$$2I^- - 2e \rightarrow I_2$$

The iodine reformed at the anode is removed from solution by making the anode of silver in which case silver iodide, AgI, is formed which is effectively insoluble in this solution.

In the ozone sonde air is pumped through the solution, which has a volume of only a few c.c.'s, and the resulting current is telemetered to the receiving station.

A variant of this type of sonde has been devised by Regener (1959) who makes use of a titration method of determining the amount of iodine present in the solution, based on the reaction of iodine with sodium thiosulphate, $Na_2S_2O_3$. This method does not give the fine structure of the ozone profile that is obtained with the Brewer method.

Paetzold and Kulcke (1957) have developed an optical ozone sonde which effectively makes use of the same principle as is used in the Dobson spectrophotometer. The wavelength regions of interest, in their case several hundred Å wide in the region of the Huggins absorption bands of ozone, are defined by means of optical filters, the intensity of the radiation passing through the filter being measured by a phototube and transmitted to the ground. This method of course does not measure the local ozone concentration as in the Brewer sonde but the amount of ozone between the sonde and the sun at various heights. Hence most of the detail in the ozone distribution cannot be obtained.

Many other types of ozone sonde are presently under development of which the chemi-luminescent type described by Kroening and Ney (1962) seems one of the most attractive. Various other means of measuring ozone concentrations ranging from the use of Krypton 85 clathrates to determine the heat released in the reaction of ozone with Hopcalite have been proposed, but no sonde produced to date appears to have found universal acceptance for various technical reasons.

The ozone profile in the atmosphere has of course been measured from rockets, the first such measurement being made by Johnson et al. (1951). They used a spectrograph to obtain a solar spectrum and recorded the variation in intensity of the incident radiation with height on film. Simpler methods are now under development by the British Meteorological Office and Adelaide University. The former have designed a spectrometer, which requires the rocket to roll in order to obtain the desired spectral range, the intensity of the radiation being measured with a photomultiplier. They have also used photocells, which is the method chosen by Adelaide University, in which the required spectral range is obtained by means of interference filters. By selecting different filters varying height ranges can be explored.

Ozone measurements have been reported from satellite observations by Rawcliffe et al. (1963), and further results should be forthcoming from the UK-2 satellite. The satellites normally will only measure ozone above about 40 km with the spectrometer methods used to date, but it is in the region from 40 to 90 km that such measurements are most lacking. Satellite measurements will undoubtedly provide much ozone data in the future.

CHAPTER 2

THE PHOTOCHEMISTRY OF THE ATMOSPHERE

2.1 The limitations and uses of photochemical calculations

The subsequent discussion will be limited to the neutral atmosphere, that is an atmosphere in which it is assumed that charged particles, either ions or electrons, are absent. In addition, partially because of this assumption, the discussion will be almost entirely restricted to levels below 100km. Only the D layer is present in this altitude range at a height of about 80km, the maximum electron density being about 10^3 cm^{-3}, and reactions involving charged particles can be omitted without incurring any noticeable error in the case of ozone. This is not necessarily true for other gases. Since the D layer is thought to consist normally of ionized nitric oxide, any account of the photochemistry of this gas should include the effects of charged particles in the atmosphere. The maximum height considered of 100km is also convenient, as up to about this height the atmosphere is well mixed and therefore 21% by volume of air can be taken to be molecular oxygen. A further restriction which is far from realistic for the actual atmosphere is that the model atmosphere assumed is considered to be at rest and hence no account is taken of diffusion, turbulence and winds.

In view of these restrictions it is as well to consider the value of photochemical calculations and their relevance to actual conditions in the atmosphere. Photochemical calculations are of interest, even subject to the above limitations, as they provide a quantitative check of any reaction scheme or mechanism by which the presence of atmospheric constituents may be explained, and therefore have an intrinsic interest of their own. Also a well developed theory, backed by good laboratory data required for the various terms in the photochemical equations, when compared with experimental measurements permits a study to be made of the influence of atmospheric effects, such as circulation processes, on the distribution of the gases under consideration. In addition a good theoretical knowledge of photochemical processes in the atmosphere aids analysis of any relevant experimental data and should give a clearer interpretation of the results. Once the theory is established it can then be applied to regions and conditions not amenable to experimental studies and, as with any worthwhile theory, it should be capable of predicting other effects thus leading the experimental work into new avenues and expanding our knowledge of the atmosphere.

2.2 The oxygen atmosphere

A further restriction on model atmospheres, which is almost invariably applied in photochemical ozone calculations, is to assume that only reactions involving oxygen need be considered, thus implying that no other gases react chemically with oxygen. This restriction is not as severe as it sounds and seems quite justified up to a height of about 60km, moreover, it greatly simplifies the reaction scheme and the photochemical calculations. Above 60km

reactions involving atomic nitrogen and hydrogen and their various oxides start to become important and result in lower ozone and atomic oxygen concentrations than those predicted for an oxygen atmosphere. Nevertheless, even above 60 km an oxygen atmosphere gives a good first approximation and is therefore of considerable value, especially when extending calculations from an oxygen atmosphere to a more realistic atmosphere. Again, since only a fraction of 1% of the total ozone amount is above 60 km this limitation is of no great importance as far as meteorological and many geophysical requirements are concerned.

The photochemical formation of ozone in the atmosphere results from the dissociation of molecular oxygen by solar ultra-violet radiation. The atomic oxygen formed is then able to combine with a molecule of oxygen in the presence of a third body to form a molecule of ozone. The reactions are

$$O_2 + h\nu \rightarrow O + O \quad \text{for } \lambda < 2424\text{Å} \qquad \text{R1}$$

and

$$O + O_2 + M \xrightarrow{k_2} O_3 + M \qquad \text{R2}$$

The wavelength limit of 2424Å is set by the dissociation energy of the oxygen molecule. In the three body reaction the third body, M, is necessary to satisfy energy and momentum requirements, k_2, being the rate constant for the reaction.

The formation of ozone in the atmosphere by means of the above reaction occurs theoretically in the altitude range 10 to 100 km, the maximum concentration being at about 25 km. The upper altitude limit results from the atmospheric pressure being so low that a three body interaction becomes extremely rare, and the formation of ozone is therefore negligible. The lower limit follows from the complete absorption of solar radiation of the requisite wavelengths for reaction R1.

The dissociation of ozone by solar radiation

$$O_3 + h\nu \rightarrow O + O_2 \quad \text{for } \lambda < 11\,800\text{Å} \qquad \text{R3}$$

can occur at all altitudes at which ozone exists, since radiation of wavelengths greater than about 3000Å reaches the ground. Ozone can also be destroyed by reaction with atomic oxygen to reform molecular oxygen

$$O + O_3 \xrightarrow{k_4} 2O_2 \qquad \text{R4}$$

Above about 60 km the recombination of atomic oxygen by means of a three body reaction needs to be considered.

$$O + O + M \xrightarrow{k_5} O_2 + M \qquad \text{R5}$$

Below 60 km the atomic oxygen concentration is so low that R5 can be safely neglected; if this reaction is also neglected for the higher altitudes a larger ozone concentration is obtained than that given when R5 is considered.

The above five reactions are those normally considered in photochemical ozone calculations, and, despite the simplicity of the reaction scheme, realistic ozone and atomic oxygen profiles can be obtained over most of the height range. It will be seen from these reactions that ozone is continually being formed and destroyed and hence a balance must occur at any given height which gives the resultant ozone concentration. The rate of change with time of the ozone and atomic oxygen concentrations can be shown by considering reactions R1 to R5 to be

$$\frac{d[O_3]}{dt} = k_2 [O][O_2][M] - k_4[O][O_3] - \alpha_3 q_3 [O_3] \qquad E1$$

$$\frac{d[O]}{dt} = 2\alpha_2 q_2 [O_2] + \alpha_3 q_3 [O_3] - k_2[O][O_2][M] - k_4[O][O_3] - 2k_5[O]^2[M] \qquad E2$$

The bracketed quantities represent the concentration of the gas considered per unit volume. α_2, q_2 and α_3, q_3 are the absorption coefficients and the number of quanta of radiation absorbed by oxygen and ozone respectively. It is implicit in the above two equations that each quantum of radiation absorbed dissociates a molecule.

If we assume equilibrium exists, i.e. that the net rate of change in E1 and E2 is zero, then solving for $[O_3]$ we obtain a cubic.

$$[O_3]^3\left\{\alpha_3 q_3 k_4^2\right\} + [O_3]^2\left\{\alpha_2 q_2 k_4^2 [O_2] - \alpha_3 q_3 k_2 k_4 [O_2][M] - \alpha_3^2 q_3^2 k_5 [M]\right\} - [O_3]\left\{2\alpha_2 q_2 k_2 k_4 [O_2]^2[M]\right\} + \alpha_2 q_2 k_2^2 [O_2]^3 [M]^2 = 0 \qquad E3$$

If the term representing R5 is neglected a much simpler, quadratic expression for $[O_3]$ is obtained

$$[O_3] = \frac{k_2}{k_4} \cdot [O_2][M] \cdot \frac{\alpha_2 q_2 [O_2]}{\alpha_2 q_2 [O_2] + \alpha_3 q_3 [O_3]} \qquad E4$$

For reasons explained previously this equation is valid below about 60 km, as R5 can be neglected because of the low atomic oxygen concentration.

Using either of the above two equations the photochemical ozone distribution in the atmosphere can be calculated.

Since this thesis is concerned solely with the photochemistry of an oxygen atmosphere it is convenient to outline the work of the thesis here. This work is presented in the four succeeding chapters which to a large extent are self contained, and represent the chronological development of the investigations carried out for the thesis.

In Chapter 3 the basis is set for the subsequent work in that the intensity of the incident solar radiation, the absorption coefficients of molecular oxygen and ozone and the rate constants for the various reactions are tabulated and discussed. Equilibrium calculations are presented for the different possible sets of data and the effects of the changes on the photochemical ozone profile in the atmosphere are illustrated. Other effects investigated are variations in the solar zenith angle, atmospheric temperature and possible errors in the ozone reaction scheme. The results are then compared with previous photochemical calculations and also with experimental ozone profiles.

The stipulation that photochemical equilibrium is attained in the atmosphere is investigated in Chapter 4, in which the diurnal photochemical variation of ozone and atomic oxygen are determined by integrating the relevant differential equations over a 24 hour period. New results are presented for the variations of these gases in the mesosphere.

In Chapter 5 the numerical methods developed in Chapter 4 are applied to investigate the changes which occur in the ozonosphere as a result of an eclipse of the sun, a study never previously attempted.

Finally in Chapter 6 the complete ozone reaction scheme for an oxygen atmosphere is reinvestigated in view of new laboratory data, and a revision of the photochemical ozone theory is suggested. This revision is required to bring otherwise completely unrealistic ozone profiles into agreement with experimental ozone profiles, and incidentally results in better agreement in the middle altitude range.

2.3 The nitrogen - oxygen atmosphere

When account is taken of reactions between nitrogen and oxygen in photochemical calculations it is necessary to consider a much larger reaction scheme. Bates (1954) has discussed the reactions of nitrogen and its oxides in some detail and lists over 20 possible reactions, luckily all of these reactions are not important in the atmosphere because of low concentration or very slow reaction rates. However, a major problem which exists with the nitrogen atmosphere is the difficulty of calculating precisely the atomic nitrogen concentration in the atmosphere. Nitrogen does not have a strong dissociation continuum in the spectral range where the sun's radiation is intense and atomic nitrogen is produced by

indirect procedures. By far the most important of these is dissociative recombination of ionised nitrogen.

$$N_2^+ + e \rightarrow N + N$$

which is expected to be an efficient mechanism in the F layer. This atomic nitrogen could be transported from the source region to lower layers according to Bates (1954) because of its long recombination time. Nicolet (1954) considers that about 10^3N atoms cm^{-3} sec^{-1} could be produced as low as 110 km by X-ray ionization followed by the above reaction. Nicolet also discussed the rate of atomic nitrogen formation in some detail and showed that diffusion was very important in determining the concentration attained at high altitudes. Below 100 km mixing is expected to be more important than diffusion as the time of diffusion is of the order of one month.

A further source of atomic nitrogen is the predissociation mechanism which was observed by Herzberg and Herzberg (1948) to occur in the wavelengths region 1200-1250Å. Since radiation at these wavelengths, principally Lyman alpha, penetrates deep into the atmosphere to about 70 km the Herzberg-Herzberg mechanism may be the principal source of atomic nitrogen at these altitudes despite its poor yield, depending on the importance of atmospheric mixing. Deb (1952) has calculated an atomic nitrogen profile corresponding to the above two dissociation processes, but, as Nicolet (1954) points out, because of atmospheric effects the actual profile cannot be expected to follow the theoretical distribution. Barth (1961) has studied the time variation of the concentrations of various nitrogen gases in the radiation free time at night, and considers that the following are the most important reactions in the night time nitrogen - oxygen reaction scheme, together with reactions R2, R4 and R5.

$$N + N + M \rightarrow N_2 + M$$
$$N + O + M \rightarrow NO + M$$
$$N + NO \rightarrow N_2 + O$$
$$N + O_2 \rightarrow NO + O$$
$$NO + O + M \rightarrow NO_2 + M$$
$$NO_2 + O \rightarrow NO + O_2$$

Barth also gives the relevant rate constants for these reactions. His study particularly emphasized the importance of NO in the nitrogen - oxygen atmosphere, and it can be seen that to a large extent NO acts as an intermediary in the recombination of O and N into their molecular forms. In his calculations Barth assumed initial concentrations of either 10^6 or 10^9N atoms cm^{-3} at all levels and then integrated the relevant equations to obtain the time variations. His principal results of interest are that below 80 km and above 120 km there was a reduction in the N concentration which in some cases rapidly led to exhaustion of the N supply. The NO concentration remained constant at all levels with a concentration of

between 10^5 and 10^7 molecules cm^{-3} and was, rather surprisingly, independent of the initial N concentration. The NO_2 concentration was small at all altitudes. These results are illustrated in figure 12. After its initial rise at sunset no change was observed in the ozone concentration, and it seems unlikely that including the nitrogen reactions affected the ozone. This arises because ozone only enters this reaction scheme through its reactions with atomic oxygen, whose concentration it controls to a large extent at night up to about 90 km. Reactions involving ozone directly such

$$N + O_3 \rightarrow NO + O_2$$

and

$$NO + O_3 \rightarrow NO_2 + O_2$$

have rate constants of 6×10^{-13} and 2×10^{-14} cm^3 $molecules^{-1}$ sec^{-1} respectively (Phillips and Schiff, 1962) and therefore proceed too slowly, because of the low concentrations, to be of much importance.

Compared with ozone relatively little is known about the concentrations, vertical distributions and variations of the various forms of nitrogen in the atmosphere. In the case of NO, Bates (1954) quotes a figure of less than 0.02 cm STP for its reduced thickness, based on the lack of NO absorption bands in the telluric spectrum in the infrared. This corresponds to a value of 5×10^{17} molecules cm^{-2} column. Jursa et al. (1959) from their failure to detect absorption by NO in a rocket flight estimated that between 63 and 87 km the NO concentration was less than 10^8 molecules cm^{-3}. Barth (1964) from an investigation of the NO dayglow using a scanning spectrometer mounted on a rocket has managed to determine an approximate NO profile. He found that above 83 km there were 2×10^{14} NO molecules cm^{-2} while above 125 km this had fallen to 0.15×10^{14}, resulting in a concentration of 6×10^7 molecules cm^{-3} from 76 to 90 km which fell to 10^7 molecules cm^{-3} at 100 km. These values agree approximately with the night time concentrations given by Barth (1961) in figure 12, but it must be remembered that the night values would be higher than the day values because of recombination after sunset. Barth (1961) also concluded from his study that the N atom concentration must be of the order of 10^6 cm^{-3} in order to account for the failure to detect NO airglow at the surface. In the case of NO_2 very little appears to be known about its concentration in the atmosphere. Bates (1954) infers from theoretical considerations that its total amount is even less than the 0.02 cm STP of NO, in agreement with Barth's results in figure 12.

During the day it is necessary to take account of the photodissociations

$$NO_2 + h\nu \rightarrow NO + O \quad \text{for } \lambda < 3700\text{Å}$$

and

$$NO + h\nu \rightarrow N + O \quad \text{for } \lambda < 1900\text{Å}$$

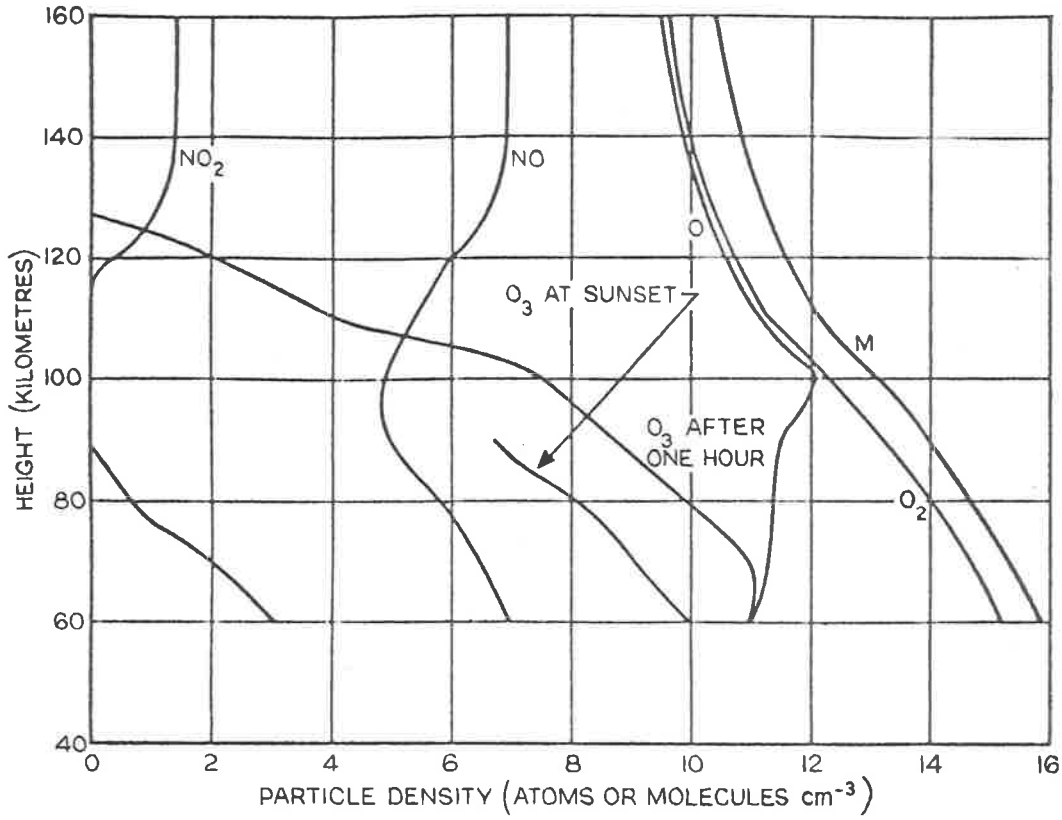

FIGURE 12. PARTICLE DENSITIES OF MODEL ATMOSPHERE (AFTER BARTH 1961)

The photoionization of NO

$$NO + h\nu \rightarrow NO^+ + e \quad \text{for } \lambda < 1300\text{Å}$$

has been shown to be responsible for the formation of the D layer, the ionization being due to the absorption of Lyman alpha radiation (see discussion by Nicolet and Aikin (1960)). Although this ionization removes NO from the photochemical reaction scheme this should not cause any significant reduction in the effective NO concentration, if Barth's (1964) results are valid, as only about 1% of the NO needs to be ionized to account for the D layer electron concentration. The results of Nicolet and Aikin, who gave NO concentrations of the order of 10^4 molecules/cm^3, must now be considered incorrect in view of Barth's experimental values.

The airglow bands used by Barth (1964) to determine NO concentrations have been studied in the laboratory by Young and Sharpless (1962a). They found that the β bands were formed by the reaction

$$N + O + M \rightarrow NO + M$$

the δ bands by

$$N + O \rightarrow NO$$

while the γ bands were due to a combination of both of these reactions.

Any complete theory of a nitrogen-oxygen atmosphere should take account of the formation of nitrous oxide, N_2O, although this gas is normally considered separately. N_2O is the most abundant of the nitrogen oxides with a total amount of 2.0 mm STP, and is uniformly distributed in the atmosphere according to Rank et al. (1962). Goldberg (1954), however, considers the N_2O vertical distribution to be exponential. Bates and Witherspoon (1952) have discussed the formation of N_2O in the atmosphere and have shown that it is possible that it is produced by soil micro-organisms. On the other hand Harteck and Dondes (1954) on the basis of a rather crude calculation claim that N_2O is formed photochemically in the atmosphere, and is principally resident in the mesosphere. Bates and Witherspoon (1952) have discussed the various chemical reactions which can produce N_2O and consider that only the following two, which were those used by Harteck and Dondes, are important

$$N_2 + O + M \rightarrow N_2O + M$$

and

$$N_2 + O_3 \rightarrow N_2O + O$$

Both of these reactions have high activation energies and therefore small rate constants, but since the concentrations of the gases are fairly high a small concentration of N_2O should result. The destruction of N_2O results principally by dissociation

$$N_2O + h\nu \rightarrow N_2 + O$$

and

$$N_2O + h\nu \rightarrow NO + N$$

and would be the controlling factor in determing the N_2O concentration in the atmosphere. The second dissociation process of N_2O is important as it provides the only source of free nitrogen in the atmosphere below 100 km in addition to the Herzberg-Herzberg mechanism. Doering and Mahan (1961) have studied the dissociation products of N_2O at 1236, 1470 and 1850Å and have shown that there is a probability of 1 in 5 that an N atom rather than an O atom will be ejected by dissociation. Although the N_2O concentration is expected to be low in the mesosphere it is possible that a production rate of free nitrogen comparable to that given by the Herzberg-Herzberg mechanism is not unlikely, as Barth (1961) has shown that only about 1 N atom cm^{-3} sec^{-1} is produced by this mechanism in the mesosphere and lower thermosphere.

Much more work is undoubtedly required on the nitrogen-oxygen atmosphere in order to obtain realistic profiles of the various gases, and estimates of the effects of diffusion and mixing in the atmosphere. An experimental determination of the N_2O vertical distribution would be of particular interest now that NO concentrations have been determined.

Finally it may be concluded that the exclusion of nitrogen reactions in photochemical ozone calculations in an oxygen atmosphere do not seem to be of great consequence as regards the derived O and O_3 concentrations judging by Barth's reaction scheme given above.

2.4 The hydrogen-oxygen atmosphere

The major difficulty with the hydrogen-oxygen atmosphere (cf. the nitrogen-oxygen atmosphere) is the problem of determining theoretically the atomic hydrogen concentration. Atomic hydrogen is produced in the atmosphere by dissociation of molecular hydrogen, water vapour and methane and also from the accretion of solar protons. The last source is of some interest and it has been pointed out by de Turville (1961) that solar protons could be accumulated by the earth's atmosphere at an appreciable rate, and he has emphasized that in geological time the oxidation of atomic hydrogen derived from these solar protons is capable of accounting for the present water content of this planet. The production of water vapour in the atmosphere by this process could help to explain some of the problems of the observed water vapour distribution as discussed by Newell (1963). The problem is also complicated by the upward diffusion and eventual escape of atomic hydrogen from the atmosphere. Kockarts and Nicolet (1962) give an escape rate of 2.5×10^7 atoms cm^{-2} sec^{-1} at 100 km.

Some experimental data is available on the H distribution in the atmosphere from a rocket experiment carried out by Purcell and Tousey (1961), who found that the total number of H atoms between 100 and 200km does not exceed 1.5×10^{12} cm^{-2} column. Nicolet (1962) suggests from these figures that the H concentration is of the order 10^8 atoms cm^{-3} at 85km and 10^7 atoms cm^{-3} at 100km (see Kockarts and Nicolet, 1962). Information on the water vapour mixing ratio in the mesosphere might help to determine the H concentration at mesospheric levels where data is greatly lacking.

The photochemistry of the hydrogen-oxygen atmosphere is rather complicated because of the many reactions which are possible. Bates and Nicolet (1950) present a comprehensive list of these reactions, but again only those reactions which are considered to be of major importance will be given here. The chemical reactions are

$$H + O_3 \rightarrow OH + O_2$$

$$OH + O \rightarrow O_2 + H$$

$$H + OH + M \rightarrow H_2O + M$$

$$H + O_2 + M \rightarrow HO_2 + M$$

$$H + HO_2 \rightarrow 2OH$$

$$OH + HO_2 \rightarrow H_2O + O_2$$

$$HO_2 + O \rightarrow OH + O_2$$

Most other reactions can be eliminated because of either low rate constants or low concentrations of the participants, but it must be mentioned that some of those omitted from the present discussion could be of marginal importance. Rate constants for most of the above reactions have been given by Kaufman (1964). In addition to the above reactions the following photodissociations need to be considered.

$$H_2O + h\nu \rightarrow OH + H$$

$$HO_2 + h\nu \rightarrow H + O_2$$

$$HO_2 + h\nu \rightarrow O + OH$$

$$OH + h\nu \rightarrow O + H$$

$$H_2 + h\nu \rightarrow 2H$$

Note, no reactions involving hydrogen peroxide, H_2O_2, have been included as it is generally considered (Bates and Nicolet, 1950) to have too low a concentration for it to be of importance in the atmosphere.

The first attempt to calculate vertical distributions for the various hydrogen compounds was made by Bates and Nicolet (1950), who defined a hydrogen profile by assuming that the fractional volume concentration of all hydrogen compounds amounted to 2.5×10^{-5} of that of N_2, this figure being roughly based on the specific humidity of the troposphere. They also assumed that equilibrium existed, but pointed out that sufficient time might not be available during the day for equilibrium concentrations to be achieved. Their results are presented in figure 13 from which it can be seen that they overestimated the H concentration obtaining values of about 5×10^9 and 5×10^8 atoms cm^{-3} at 85 and 100 km respectively compared to 10^8 and 10^7 quoted by Nicolet (1962). Now it has been shown by Schiff (1962), using recent data for rate constants, that the ratios HO_2/H and OH/H are approximately 10^{-3}, hence the values for the HO_2 and OH concentrations given in figure 13 will also need revision. The reduction in H concentration will also result in an increase in the O_3 and O concentrations and thus bring them into better agreement with those calculated from a pure oxygen atmosphere. The presence of H besides affecting the equilibrium O_3 and O concentrations also reduces the nocturnal ozone increase in the mesosphere. Venkateswaran (1963) has produced the curves given in figure 14 which illustrate the magnitude of these changes for various initial H concentrations. As can be seen from this figure an H concentration of 10^8 atoms cm^{-3} at 85 km reduces the O_3 concentration from a "pure oxygen value" of 10^{11} molecules cm^{-3} to 4×10^9 molecules cm^{-3} over a 12 hour period. It is apparent therefore that the exclusion of hydrogen reactions by the stipulation of an oxygen atmosphere is likely to result in a larger error than the exclusion of nitrogen reactions.

As discussed previously in section 1.7 the reaction

$$H + O_3 \rightarrow OH^* + O_2$$

is generally accepted as being responsible for the production of the hydroxyl airglow. Although Krassovsky has criticised this reaction and proposed various alternatives, Krassovsky (1963), an analysis of these propositions by Schiff (1962) has shown them to be less satisfactory than the original Bates-Nicolet reaction above. The only reaction proposed by Krassovsky which seems likely to produce vibrationally excited hydroxyl radicals is

$$HO_2 + O \rightarrow OH + O_2$$

and Schiff has indicated that at the most this reaction can produce only one quarter of the luminosity produced by the Bates - Nicolet reaction. It should also be noted that laboratory studies by McKinley et al. (1955) have shown that the reaction of H with O_3 produces OH radicals excited up to the 9th vibrational level as is observed in the atmosphere, while rocket measurements of the height of the airglow emission by Packer (1961) give the correct height

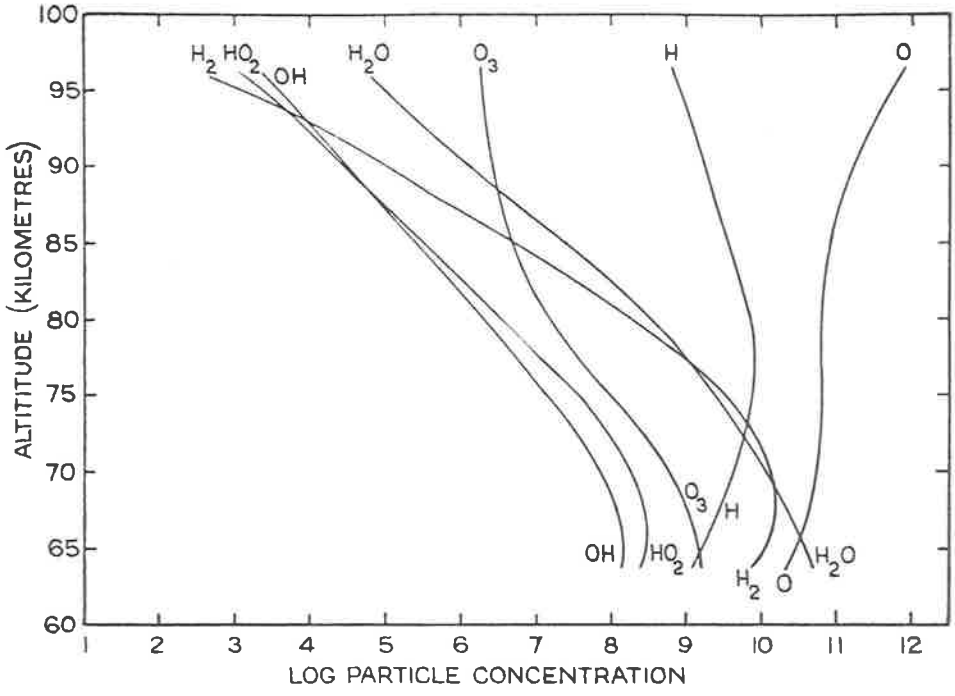

FIGURE 13. THE HYDROGEN - OXYGEN ATMOSPHERE
(AFTER BATES AND NICOLET, 1950)

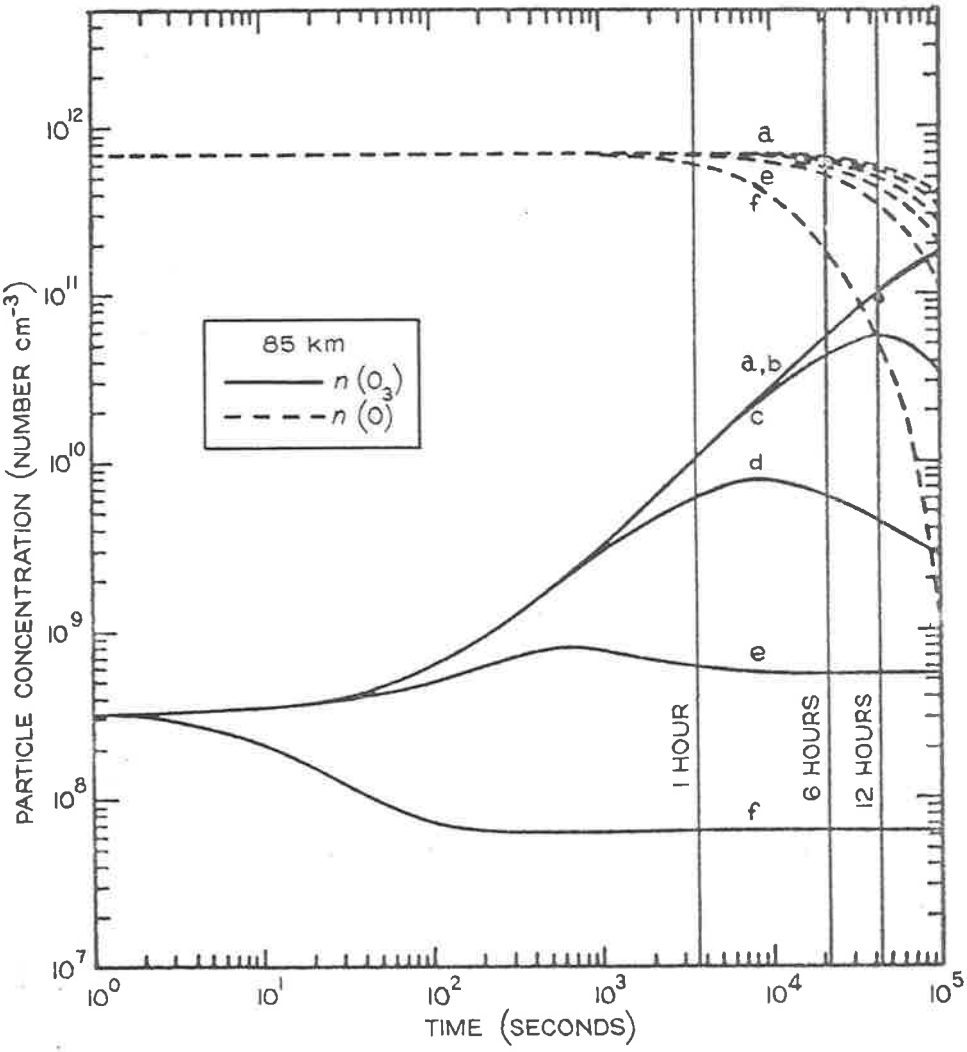

FIGURE 14. THE OZONE (O_3) AND ATOMIC OXYGEN (O) VARIATIONS AT 85KM AFTER SUNSET. THESE VARIATIONS ARE SHOWN FOR SIX (a to f) VALUES OF THE INITIAL H CONCENTRATION. THESE VALUES MAY BE TAKEN TO BE 0, 10^6, 10^7, 10^8, 10^9 AND 10^{10} ATOMS CM^{-3}, IF THE SPECIFIC RATE ASSOCIATED WITH THE OZONE-HYDROGEN REACTION IS 10^{-12} CM^3 SEC^{-1}. (AFTER VENKATESWARAN, 1963).

range. Schiff's analysis does not prove that the OH airglow is formed entirely by $H + O_3$ reaction, but it seems difficult to find a reaction scheme which is even partially as effective as this reaction scheme. Theoretical studies of the OH emission rate have been made by Wallace (1962) and Ballif and Venkateswaran (1963a). Wallace estimated that the night-time emission rate would be eight times greater than the day-time emission rate for the $H + O_3$ reaction, while the emission due to the $H + O_2^*$ reaction given in section 1.7 would remain essentially unchanged from day to night. Lytle and Hampson (1964) have emphasized the importance of these deductions by measuring the OH day glow intensity of the (1,0) band, which they found to be similar to that of the night glow. Hence the possibility arises that during the day some unknown reaction may be supplementing the $H + O_3$ reaction. More work is undoubtedly needed on the whole of the hydrogen - oxygen reaction scheme.

Finally it might be mentioned that the hydrogen - oxygen and nitrogen - oxygen atmospheres cannot be teated independently, as there are "cross coupling" reactions such as the fast reactions

$$H + NO + M \rightarrow HNO + M$$

and

$$H + HNO \rightarrow H_2 + NO$$

which need to be considered in any complete study of the atmosphere. A theoretical study of the combined oxygen - hydrogen - nitrogen atmosphere has yet to be made.

CHAPTER 3

AN INVESTIGATION OF THE ATMOSPHERIC EQUILIBRIUM PHOTOCHEMICAL OZONE PROFILE

3.1 Introduction

There have been many previous investigations of the photochemistry of ozone, of which those by Craig (1950), Dütsch (1956) and Paetzold (1953) in particular, have shown the basic features to be expected for photochemical ozone distributions in the atmosphere. The equations defining such an ozone distribution involve parameters such as the absorption coefficients of ozone and molecular oxygen, the spectral intensity of the sun's radiation, the atmospheric temperature distribution and other terms. Since the completion of the investigations mentioned above there has been a considerable improvement in our knowledge of the data required for photochemical ozone calculations, which, while still far from satisfactory, is the reason that the present work was undertaken. Despite the use of this improved data no essentially new results were expected, and it was therefore decided to investigate the effect of varying the parameters involved in the photochemical equations in order to determine the possible variations in the ozone profile due to various assumptions made for regions where the data were not sufficiently quantitative. This analysis would define the limits of the variations to be expected in photochemical ozone distributions and total ozone amounts, and, moreover, show where the effects of uncertainties in the data were important.

As mentioned previously in Sections 2.1 and 2.2 the restrictions of an oxygen atmosphere at rest have been imposed for the purposes of the present study. Bearing this in mind it must be emphasized that below about 35 km the derived O_3 profiles will not be representative of the actual atmosphere, since equilibrium does not exist at the lower levels in the atmosphere because of atmospheric mixing. Also above about 60 km the stipulation of an oxygen atmosphere results in higher O_3 and O concentrations than those to be expected in the actual atmosphere for reasons discussed in Section 2.4

3.2 The photochemical equations and their numerical solution

The five reactions R1 to R5 listed on p.15 were the only ones included in the O_3 reaction scheme. Other possible reactions in an oxygen atmosphere such as the following do not appear to be of importance.

The thermal decomposition of O_3 by the reverse of reaction R2

$$M + O_3 \rightarrow O + O_2 + M$$

or by the bimolecular reaction

$$2O_3 \rightarrow 3O_2$$

can be ignored for the atmospheric temperatures of interest 165° - 283°K) since they have activation energies greater than 20 000 cal.mole^{-1} (Benson and Axworthy, 1957).

Likewise the reactions

$$O_2 + O_2 \rightarrow O_3 + O$$

and

$$O_2 + O_2 \rightarrow 2O + O_2$$

can be completely ignored in atmospheric O_3 calculations as they have activation energies of approximately 100 000 cal.mole^{-1} (Benson and Axworthy, 1957).

Laboratory studies by McGrath and Norrish (1957) have shown that it is possible for vibrationally excited molecular oxygen produced by reaction R4 to partake in energy chains, thus producing an increased rate of O_3 destruction compared with that indicated by the assumed reaction scheme. Discussion of this phenomenon will however be delayed to Section 3.4.6. Also reactions involving electronically excited forms of oxygen will not be considered until Chapter 6. For the present, it will be assumed, as has always been done previously, that a completely adequate representation of the formation and destruction of O_3 in an oxygen atmosphere is given by reactions R2, R3 and R4.

Hence in order to obtain photochemical O_3 profiles it is necessary to solve equations E3 or E4 given on p.16. These equations are invariably solved numerically because of the complexity of the terms in the equations. This complexity arises because the absorption coefficients and the solar radiation intensity vary with wavelength, while the latter and the atmospheric density and temperature vary with height. The methods used in solving these equations followed very closely those given by Craig (1950), except that E3 was used whereas Craig dealt only with E4. The procedure adopted was to divide the wavelength and height ranges of interest into a number of small intervals in order to allow for the variations of the various terms in the equations. Then for a given height interval it is necessary to calculate the absorption terms $\alpha_2 q_2 [O_2]$ and $\alpha_3 q_3$. The former, which gives the absorption due to molecular oxygen, can be obtained exactly using the analytic expressions derived by Craig (1950). The term $\alpha_3 q_3$, associated with the O_3 absorption, is derived by assuming that the radiation is of constant intensity over the height interval of interest and taking the value of the incident radiation as the value for q_3. Since the absorption spectra of O_2 and O_3 overlap below 2424Å it

was assumed for convenience that the O_2 absorbed first. For a given height interval it is necessary to sum the contributions of the individual wavelength intervals in order to obtain the terms $\alpha_2 q_2[O_2]$ and $\alpha_3 q_3$. Hence, knowing the value of these terms, and evaluating the quantities associated with the collision reactions R2, R4 and R5 for conditions at the centre of the height interval, the value of $[O_3]$ can be calculated. Finally assuming that the O_3 concentration is constant throughout the height interval, we can derive the value of the transmitted radiation q_1 for a given value of the incident radiation q_0, for each wavelength interval, using

$$q_1 = q_0 \exp(-\alpha_3 [O_3] \Delta Z)$$

where ΔZ is the thickness of the height interval. The various q_1's are then used as the values of the incident radiation intensity for the succeeding, lower layer.

Because of the large number of wavelength intervals and atmospheric layers used in the calculations the effect of the approximations in this numerical approach are not likely to result in any large errors. For the height dependent variables 46 layers, varying in thickness from 2.5 km for the upper layers to 1 km for the layers below 40 km, were used for the height range from 80 to 11 km. 41 intervals were used to represent the variation of the wavelength dependent variables. The detailed calculations were made on an IBM 7090 computer.

3.3 The data used in the photochemical calculations

For the purpose of the present study it was necessary to have some criterion by which the effects on the ozone profile of changing the variables in equation E3 could be judged. A choice was made that one particular set of data should be designated as Case I, and that all the other cases considered should represent a variation of normally a single term from this standard data. Hence the data selected for Case I will be considered in some detail, while in the subsequent sections only the deviations in the data and the resulting effects on the photochemical ozone distribution will be discussed.

3.3.1 The oxygen absorption coefficients

For the purpose of the present photochemical ozone calculations a knowledge of α_2 was required for the wavelength range 1775Å to 2424Å, thirteen 50Å wide intervals being used to represent the variation of α_2 with wavelength in this region. The short wavelength limit of 1775Å was determined by the height at which these calculations were commenced. For the model atmosphere selected it was convenient to take this height as 80 km, moreover, previous calculations (Dütsch, 1956) and measurements (Johnson et al., 1952) have indicated that very little ozone is present above 80 km. Wavelengths greater

than the dissociation limit of 2424Å for the oxygen molecule need not be considered, since oxygen is such a weak absorber than its attenuation of the incident solar radiation can be neglected in comparison with that of ozone.

The oxygen absorption spectrum in the wavelength region responsible for the production of the ozonosphere consists of the Schumann-Runge absorption bands and the Herzberg continuum. Absorption at these wavelengths by molecular oxygen results in the production of two atoms of oxygen in their ground electronic states.

$$O_2 + h\nu \rightarrow O(^3P) + O(^3P) \text{ for } 1750\text{Å} < \lambda < 2424\text{Å}$$

The Schumann-Runge absorption bands shown in figure 15 consist of 21 bands commencing at 2024Å and converging at 1750Å (Watanabe et al., 1953), where they are followed by the intense Schumann-Runge continuum. There has been some doubt expressed as to whether absorption by oxygen in these bands results in dissociation. Thus Bates and Nicolet (1950) assumed that this absorption did not contribute to the formation of the ozonosphere in their photochemical calculations, while both Craig (1950) and Dütsch (1956) assumed that all absorption by oxygen in these bands produced dissociation. Since predissociation has been observed in these bands by Wilkinson and Mulliken (1957) and Carroll (1959), this assumption made by Craig and Dütsch was repeated for the purposes of Case I. In Section 3.4.1 various alternatives are considered. Measurements of α_2 for the wavelength region associated with the Schumann-Runge bands have been made by Ditchburn and Young (1962) and Watanabe et al. (1953). Neither set of measurements was sufficiently quantitative and an apparent pressure variation of the absorption coefficient was observed, in each case being attributed to poor instrumental resolution, although a possible real pressure effect was not excluded. It was assumed however, as previous authors have done, that Beer's law was obeyed for absorption by oxygen in these bands. The measurements of Watanabe et al. (1953) were preferred for the wavelengths from 1775Å to 1975Å, which include most of the Schumann-Runge bands, and the value of α_2 averaged over 50Å wide intervals was derived from their data.

The Herzberg continuum commences at 2424Å and extends to shorter wavelengths where, according to Ditchburn and Young (1962), it appears to underlie the Schumann-Runge bands. Although the absorption by molecular oxygen in this continuum is very weak it is, nevertheless, the primary cause of the ozonosphere as an "atmospheric window" near to 2100Å permits

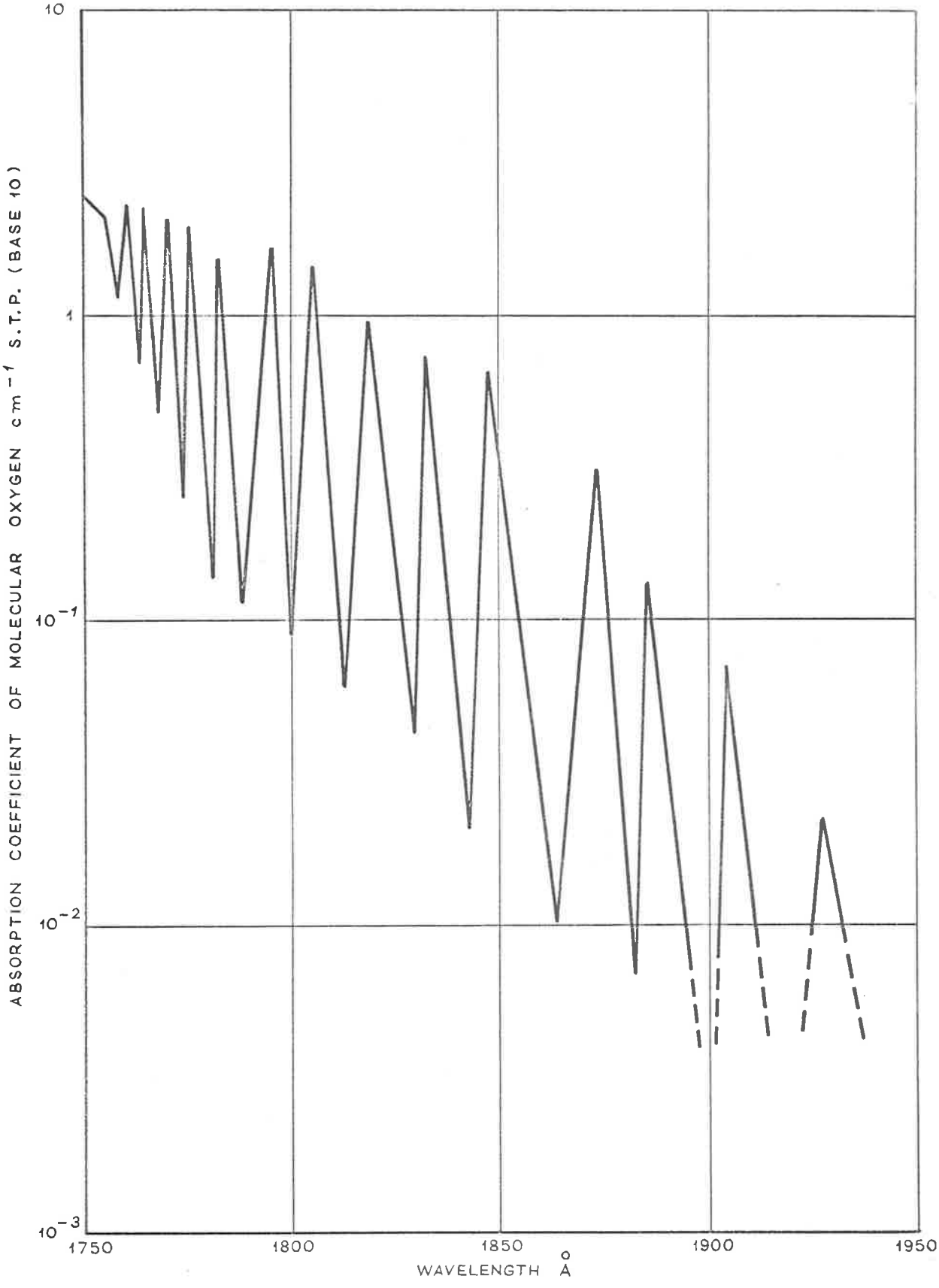

FIGURE 15. THE VARIATION OF THE OXYGEN ABSORPTION COEFFICIENT WITH WAVELENGTH FOR THE SCHUMANN - RUNGE BANDS

fairly intense solar radiation to penetrate to 20 to 25 km, where any atomic oxygen formed reacts easily to produce ozone because of the higher pressure. Owing to the failure of Beer's law the oxygen absorption coefficients show an apparent variation with pressure, which Ditchburn and Young consider may be due to absorption by ozonium, O_4. From their recent measurements in this wavelength region they give the pressure dependence of α_2 as:

$$\alpha_2(\lambda) = \alpha_o(\lambda) + \frac{p}{p_o} \cdot \Delta\alpha(\lambda) \qquad \text{E5}$$

where $\alpha_2(\lambda)$ is the value of the absorption coefficient at wavelength λ and pressure p, α_o being the value of α_2 extrapolated to zero pressure, while $\Delta\alpha$ is the increase in the value of α_2 due to a pressure p. p_o is a pressure of one atmosphere. Their results are illustrated in figure 16.

For Case I the term $\frac{p}{p_o} \cdot \Delta\alpha$ was taken to represent the absorption due to O_4 as this seemed to be the easiest and most satisfactory means of accounting for the Beer law violation. As such this absorption would, presumably, not result in any dissociation of oxygen, unlike the absorption of the α_o term. Hence, for Case I the value of α_2 used in equation E3 was taken to be that of α_o, while the attenuation of the incident radiation was calculated using the full expression for α_2, i.e. $\alpha_o + \frac{p}{p_o} \cdot \Delta\alpha$, where the value of p was that of the atmospheric pressure at the centre of the height interval under consideration.

For the region from 1975Å to 2424Å, which includes the Herzberg continuum and the first three of the Schumann-Runge bands, nine 50Å wide intervals were used to represent the variation of α_2 with wavelength. The values of α_o and $\Delta\alpha$ averaged over these intervals were derived from Ditchburn and Young's data (1962). In Section 3.4.2 other possible forms of equation E5 are considered.

No temperature dependence of the oxygen absorption coefficient has been reported.

The values of the oxygen absorption coefficients used are tabulated in table 1 in Appendix I.

3.3.2 The ozone absorption coefficients

The ozone absorption coefficients are now well-known for the three band systems occurring in the wavelength range of interest for photochemical ozone calculations. Commencing

at the short wavelength limit of 1775Å these band systems consist of the Hartley, Huggins and Chappuis bands, of which the Hartley bands are by far the strongest with an intense maximum at 2550Å. Near 3000Å the Hartley bands merge with the Huggins bands which extend to about 3500Å where the absorption by ozone becomes negligible, see figure 17. In the visible region of the spectrum ozone has a very weak absorption system due to the Chappuis bands, as shown in figure 18, which extend from about 4500Å to 7500Å with a maximum near 6000Å. Ozone has additional absorption bands in the infra-red but these are not of photochemical interest being beyond the dissociation limit of the ozone molecule. All absorption for the three band systems mentioned above is assumed to result in dissociation of ozone since absorption continua are known to underlie the bands (Inn and Tanaka, 1953). Measurements reported by Hearn (1961) supply additional justification for this assumption.

Thirty five 50Å wide intervals were used to represent the variation of α_3 with wavelength in the ultra-violet region of the spectrum. For the region below 2025Å the results of Tanaka et al., (1952) were selected. They consider that there is a maximum error of 10% in their measurements, but no information is given regarding the temperature and pressure dependence of the absorption coefficient, such an effect being unlikely in this wavelength region. Both Vigroux (1952) and Inn and Tanaka (1953) at about the same time published new values for the ozone absorption coefficients for the Chappius and Huggins bands, and for the Hartley bands above about 2000Å; for wavelengths greater than 2800Å the two sets of measurements are in close agreement. For the region from 2025Å to 3025Å Inn and Tanaka's data were selected, but from 3025Å to 3525Å Vigroux's data is considered to be more accurate and has in fact been recommended by Inn and Tanaka in preference to their own. The values of α_3 averaged over the 50Å wide intervals used in the present study were derived from the data presented in the above references.

The ozone absorption spectrum is simpler than that of oxygen as Beer's law appears to be obeyed. The values of the absorption coefficients reported by Inn and Tanaka for the spectral range 2000Å to 7500Å were the average of several values measured at different ozone pressures, the maximum deviation from the average being given as ±5%. In particular for the region from 2000Å to 3000Å they found that a change of 25-fold in the ozone pressure did not affect the observed

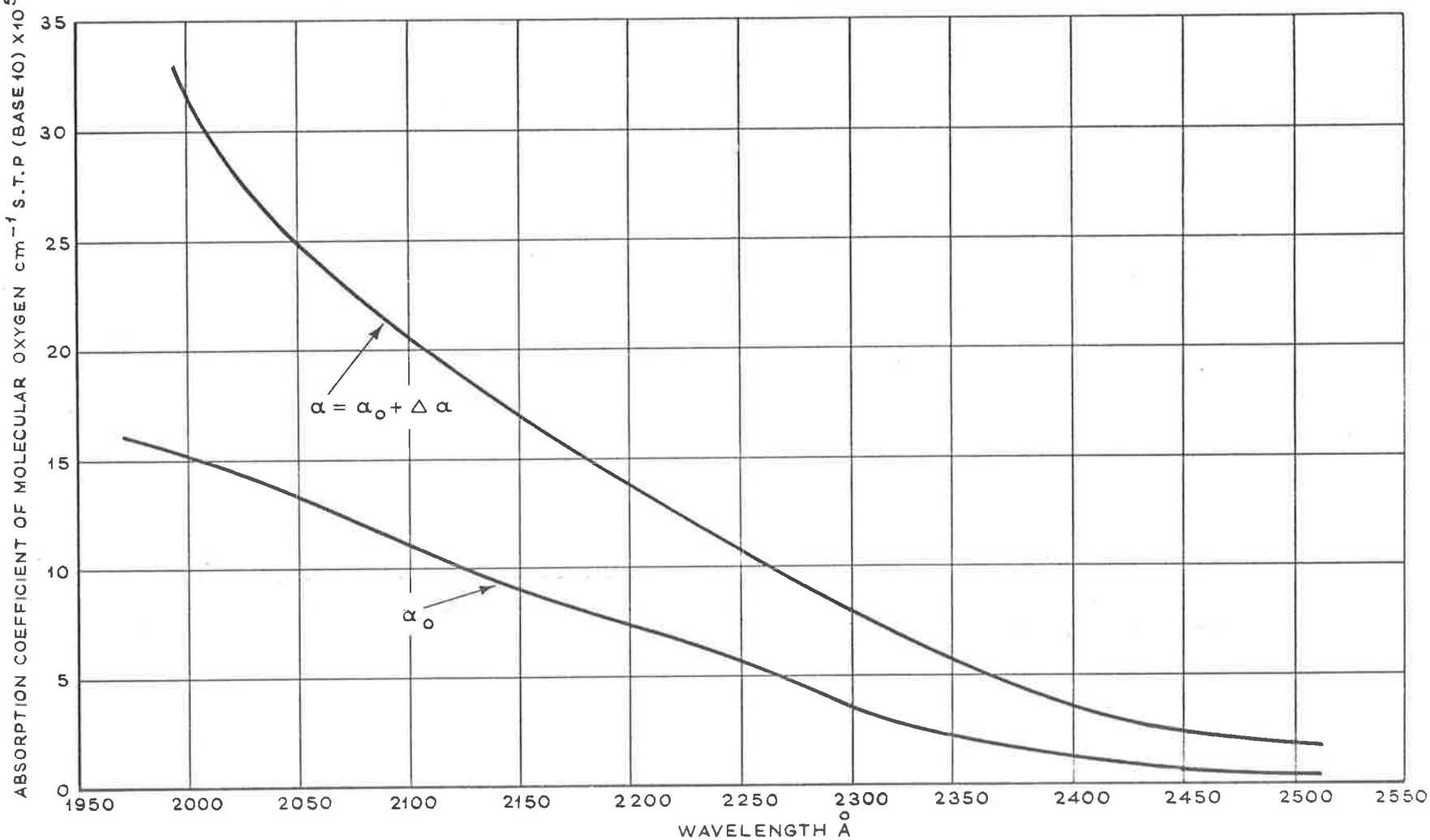

FIGURE 16. THE VARIATION OF THE OXYGEN ABSORPTION COEFFICIENT FOR THE HERZBERG CONTINUUM
(The upper curve gives the value of the absorption coefficient for a pressure of one atmosphere, the lower curve gives the value of the absorption coefficient extrapolated to zero pressure).

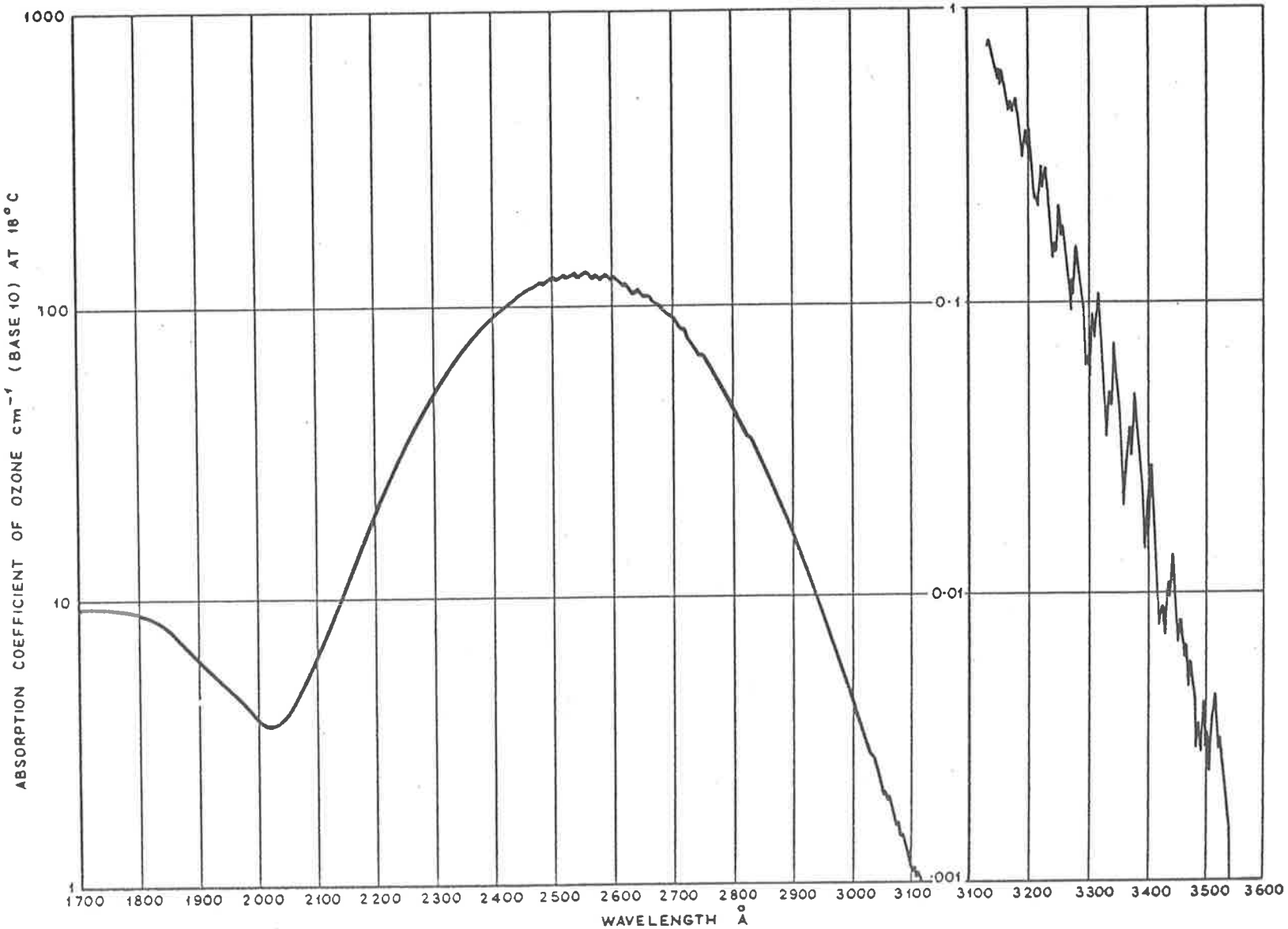

FIGURE 17. THE VARIATION OF THE OZONE ABSORPTION COEFFICIENT WITH WAVELENGTH FOR THE HARTLEY AND HUGGINS BANDS

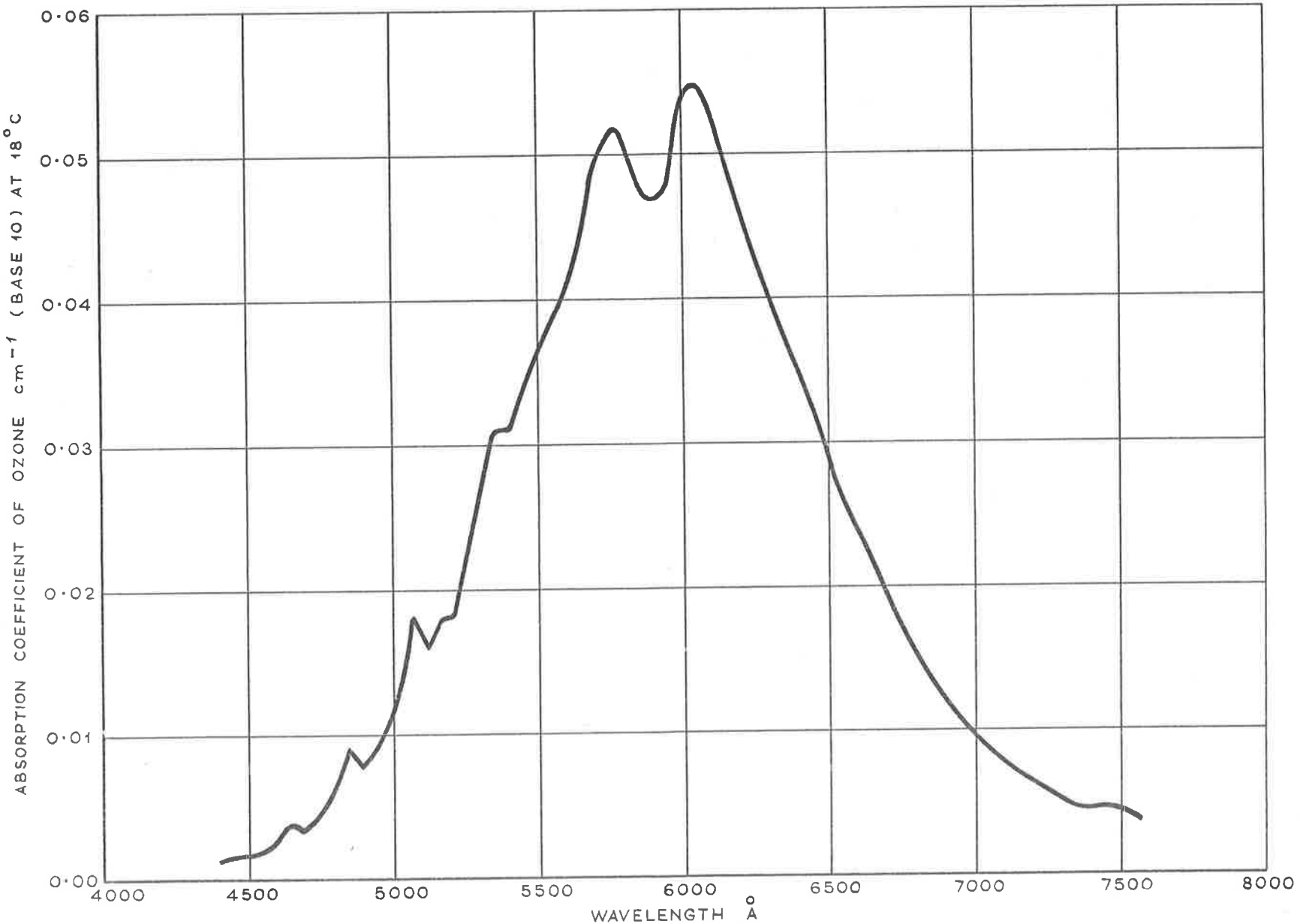

FIGURE 18. THE VARIATION OF THE OZONE ABSORPTION COEFFICIENT WITH WAVELENGTH FOR THE CHAPPUIS BANDS

absorption coefficient.

However, the ozone absorption coefficients are temperature dependent and a very careful study of the effect of temperature variations on these coefficients has been made by Vigroux (1952). Results are given for temperatures between 18°C and -92°C, which effectively covers the range of temperatures of interest in the atmosphere, i.e. 10°C to -102°C. The values of the absorption coefficients at the lower temperatures are all quoted with reference to their respective values at 18°C, the results given show a variation of between 0.98 and 0.46 depending on the wavelength and temperature considered. Below 2875Å the temperature correction was only 3 or 5 per cent and was therefore neglected. From 2875Å to 3025Å the temperature correction given by Vigroux was applied to the results of Inn and Tanaka: since the correction is a relative effect this procedure should be satisfactory. In this region the corrections were about 7 or 8 per cent and showed little variation with wavelength or temperature. From 3125Å to 3375Å there was a marked variation with wavelength and temperature. But, when the results for the various temperatures were averaged over the 50Å wide intervals used, it was found that for a given interval the correction was constant, or nearly so, for the various temperatures considered. Hence a single correction was applied for a given 50Å interval to allow for the variation of temperature in the atmosphere. This correction reduced the absorption coefficient by a maximum of 25% of its value at 18°C for this wavelength region. The corrections are listed in table 2, Appendix I. For the wavelength range 3375Å to 3525Å no data on temperature variations was available.

The measurements of Inn and Tanaka (1953) were selected for the Chappuis bands, the data being averaged over six 500Å wide intervals in the region from 4500Å to 7500Å since the absorption coefficients are small and do not vary too rapidly with wavelength. For these bands the few results given by Vigroux show that there is no temperature effect.

For Case I the temperature correction given in table 2 was applied to α_3, in Section 3.4.3 the minor importance of this temperature correction is discussed.

The values of the ozone absorption coefficients are tabulated in table 2 in Appendix I.

3.3.3 The spectral intensity of the sun

Nearly all previously published photochemical ozone distributions have required an extrapolation of the available data in order to obtain information on the sun's radiation output

below 2200Å. Recently, however, data from rocket measurements have become available thereby removing the need for such extrapolation.

Various wavelength ranges have been covered by different authors and the sources of the data for the individual ranges are given below. Detwiler et al. (1961) have published values for the radiation output of the sun for wavelengths from 825Å to 2625Å. Their results, which were used for the wavelength range 1775Å to 2625Å, are conveniently presented in the form required for use in the present calculations as the total radiation incident within a 50Å wide wavelength interval. The intensity of the solar radiation for the six 50Å wide intervals in the range from 2675Å to 2975Å was estimated from the high resolution curves published by Wilson et al. (1954) for this region. Above about 3000Å the solar radiation intensity can be obtained from measurements made at ground level, and, of the many measurements made, those of Dunkelman and Scolnik (1959) for the wavelength range from 3032Å to 6500Å were selected and used for the intervals from 3125Å to 3525Å and from 4500Å to 6500Å. From 6500Å to 7500Å and for the gaps in the data between the various sets of results the data tabulated by Johnson (1954) were used. Johnson's data actually cover all the wavelengths of interest in the ozone calculations down to 2200Å but Detwiler et al. (1961) state that his data, which are nearly the same as the most recent results to 2400Å, are low by nearly a factor of two at 2200Å. Despite the fact that several sources are used for the solar intensity data discussed here the various sets of data are self-consistent, since the absolute energy scale for the rocket measurements was established by adjusting the long wavelength end of the rocket results to make them agree with Dunkelman and Scolnik's data over the range from 3000Å to 3300Å where the rocket and ground observations overlap.

As the calculations for the photochemical ozone distribution were commenced at a height of 80 km, the assumption being made that there is no ozone above this altitude, it was therefore necessary to calculate the attenuation of the solar radiation above 80 km due to oxygen absorption. As stated previously it was found that no radiation below 1775Å could penetrate below 80 km, it was also found for the longer wavelengths that only radiation below about 2000Å was appreciably attenuated.

The variation of the solar radiation intensity with wave-

length is illustrated in figures 19 and 20 and the values used in the calculations are tabulated in table 3 in Appendix I.

3.3.4 The standard atmosphere

The standard atmosphere selected for Case I was the 1959 ARDC model atmosphere (1959) shown in figure 9. This atmosphere was convenient for use in the photochemical calculations as in the height range of interest, 10 to 80 km, it consists of two isothermal and two linear lapse temperature layers. In this model it is assumed that the atmospheric composition remains constant up to an altitude of 90 km, hence 21% of the air by volume can be taken to be molecular oxygen, while above 90 km an increasing percentage of the oxygen will be dissociated. The amount of molecular oxygen above 80 km is important since it determines how much radiation will penetrate to this altitude for wavelengths affected by oxygen absorption. However, because of the exponential decrease of density with altitude, most of the attenuation of the solar radiation above 80 km for the wavelengths of interest here, ($\lambda \geq 1775\text{Å}$), will occur between 80 and 90 km, hence uncertainties concerning the atmospheric composition above 90 km are not very important.

The effects of variations of the atmospheric temperature profile on the photochemical ozone distribution are discussed in Section 3.4.8.

3.3.5 The rate constants

3.3.5.1 k_5, the rate constant for recombination of atomic oxygen

In the last few years several values for k_5 have been reported based on widely differing experimental techniques. As might be expected there is considerable disagreement between these values and they range from 5×10^{-34} to 1×10^{-32} cm^6 $molecule^{-2}$ sec^{-1}. The value of k_5 selected for Case I was that reported by Reeves et al. (1960) of 2.7×10^{-33} cm^6 $molecule^{-2}$ sec^{-1}. This is in agreement with the recommendations of Kaufman and Kelso (1961) who have made a critical survey of the published measurements of k_5.

At the present time there is no experimental information available concerning the variation of k_5 with temperature for temperatures of interest in the atmosphere. Measurements made at high temperatures (Matthews 1959) suggest a temperature dependence approximately proportional to T^{-2} for temperatures in the range 3000° to 5000°K. The relevance of the value of k_5 in photochemical ozone calculations is

discussed in Section 3.4.5.1.

3.3.5.2 k_2, the rate constant for formation of ozone

There have been many measurements of the value of the rate constant k_2, but again the results vary considerably, ranging from 1×10^{-34} to 1.7×10^{-33} cm^6 $molecule^{-1}$ sec^{-1} at 300^oK. This rate constant is also known to be temperature dependent but relatively few experimental determinations of the activation energy of reaction R2 have been made. Kaufman and Kelso (1961) have also reviewed the published values of k_2 and suggest that its value is less than 2×10^{-34} cm^6 $molecule^{-2}$ sec^{-1}, at 300^oK. The value of k_2 and its temperature dependence chosen for Case I was that given by Zaslowsky (1962), i.e. $k_2 = 3.7 \times 10^{-34}$ $\exp(-300/RT)$ cm^6 $molecule^{-2}$ sec^{-1} for $M = O_2$. Because the activation energy is only 300 $cal.mole^{-1}$ the variation of the value of k_2 for the temperature range of interest is very slight.

The value of k_2 is also dependent on the gas which is used as the third body, M, in the reaction. In the atmosphere M will be mainly nitrogen, however, results given by Benson and Axworthy (1957) show that nitrogen is equally efficient as oxygen as a third body.

3.3.5.3 k_4, the rate constant for destruction of ozone

Relatively few values of the rate constant k_4 and its temperature dependence have been published so far, and the values which are available do not agree well as far as the temperature dependence is concerned. For Case I the results of Leighton et al. (see Harteck and Reeves, 1961) were selected, they give $k_4 = 6.45 \times 10^{-12} \exp(-3200/RT)$ cm^3 $molecule^{-1}$ sec^{-1}. In Section 3.4.5.3 the importance of the correct value of k_4 to photochemical ozone calculations is illustrated.

3.4 Presentation of results

3.4.1 The effect on the ozone distribution of different oxygen dissociating processes in the Schumann-Runge bands

In figure 21 Case I is compared with Cases II, III and IV, which differ from Case I only as regards the assumptions made concerning the quantum efficiency of the dissociation mechanism for absorption by oxygen in this wavelength region.

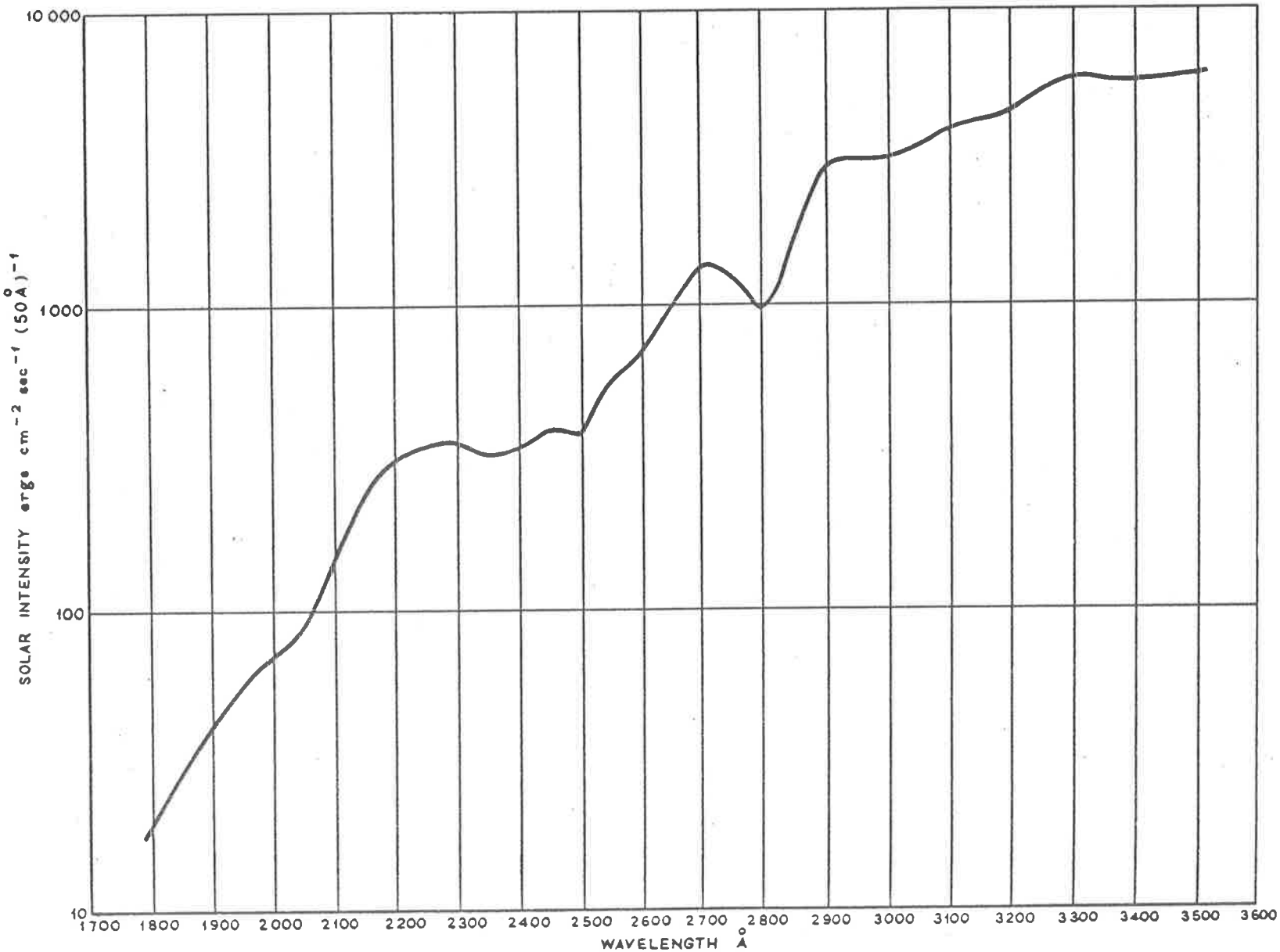

FIGURE 19. THE VARIATION OF THE SOLAR INTENSITY WITH WAVELENGTH OUTSIDE THE EARTH'S ATMOSPHERE IN THE NEAR ULTRA-VIOLET

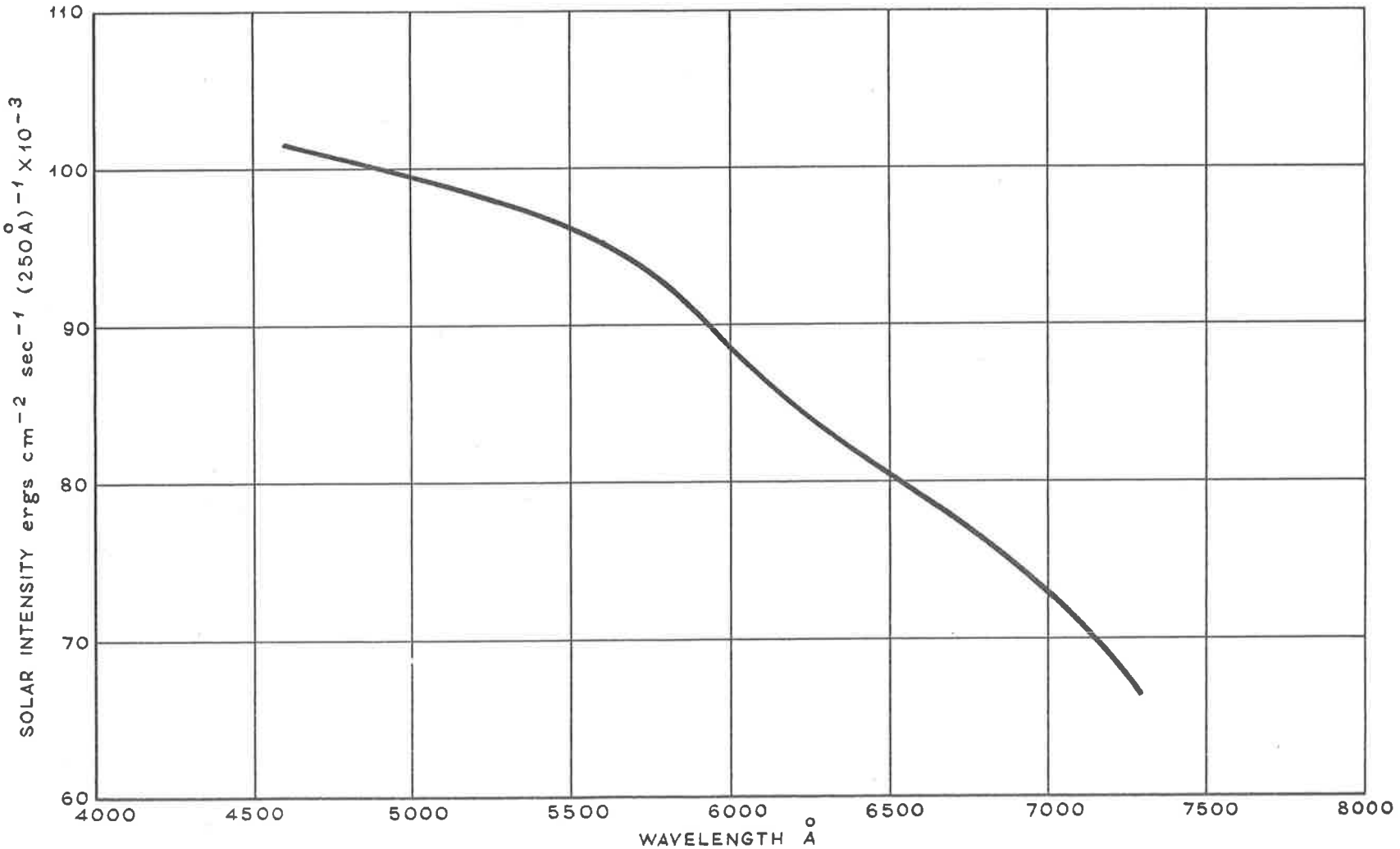

FIGURE 20. THE VARIATION IN THE VISIBLE OF THE SOLAR INTENSITY WITH WAVELENGTH OUTSIDE THE EARTH'S ATMOSPHERE

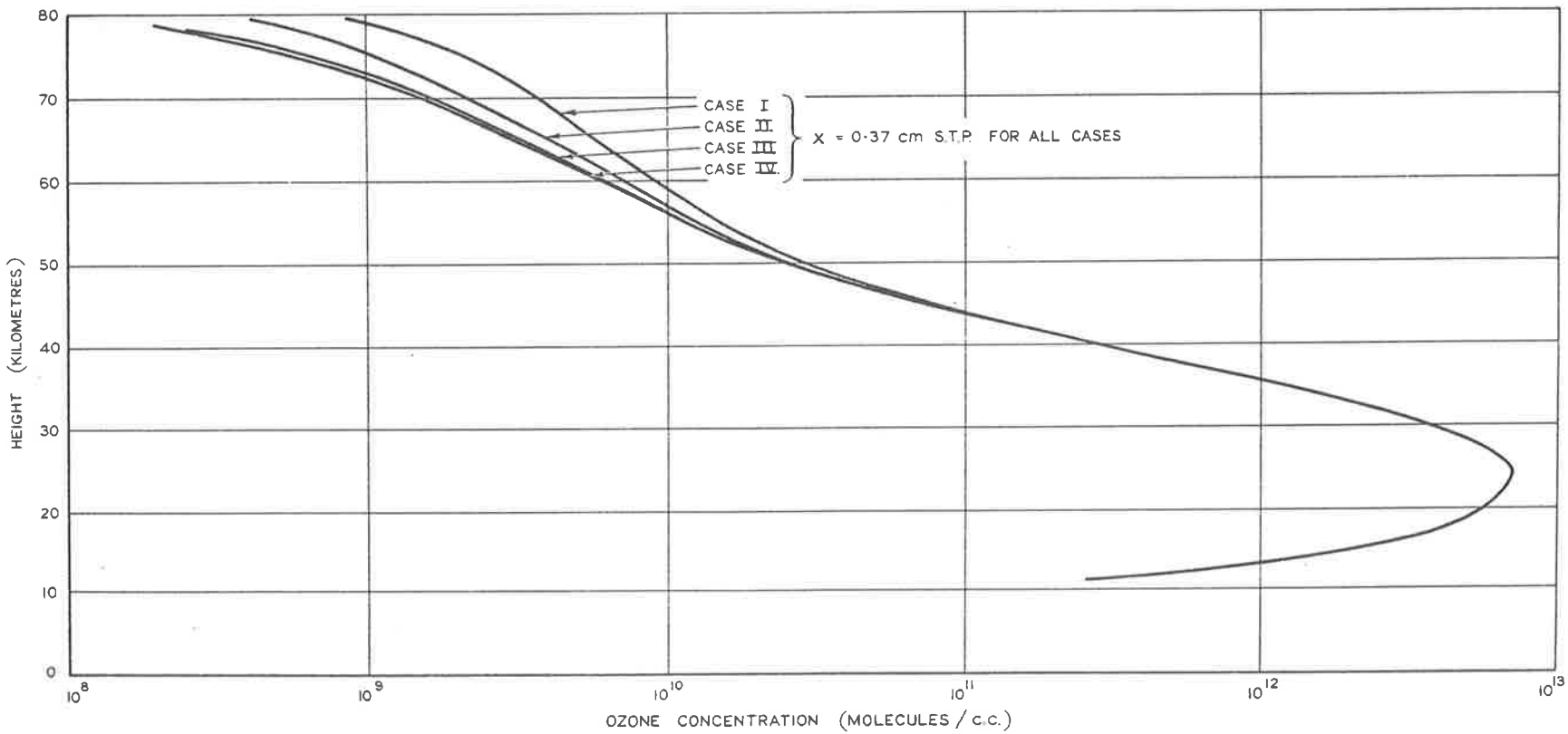

FIGURE 21. VARIATION PRODUCED IN THE OZONE DISTRIBUTION DUE TO POSSIBLE OXYGEN DISSOCIATION PROCESSES IN THE SCHUMANN-RUNGE BANDS

For Cases II and III the predissociation mechanism of Case I was disregarded and the dissociation was taken to be caused by continua underlying the Schumann-Runge bands. Wilkinson and Mulliken (1957) have found definite evidence for an underlying continuum below 1800Å which they suggest might be due to the following transition $^3\Pi_u \longleftarrow {}^3\Sigma_g^-$. Thus for Case II the values of α_2 for this wavelength region which were used in equation E3 were obtained by assuming that an absorption continuum lay immediately below the Schumann-Runge bands. Ditchburn and Young (1962) theoretically extrapolated their measurements for the Herzberg continuum and showed that the maximum was to be expected at about 1870Å, corresponding to the transition $^3\Sigma_u^+ \longleftarrow {}^3\Sigma_g^-$. The values of α_2 corresponding to this extrapolation, which are considerably less than those for the above "Π - continuum", were used in Case III. For Case IV it was assumed that no dissociation was caused by absorption in this wavelength region, thus Cases I and IV represent the extremes in the variation of the ozone distribution due to absorption in the Schumann-Runge bands. The attenuation of the incident radiation for all these cases was calculated using the same values of the absorption coefficients as for Case I.

As is apparent from figure 21 all four cases have virtually the same total ozone amount of 0.37 cm S.T.P., although there is a noticeable difference in the ozone profiles above about 50 km. The ozone distributions are however in the expected order, the case with the highest quantum efficiency for oxygen dissociation producing the highest ozone concentration. The relative unimportance of the Schumann-Runge bands results from the comparatively low intensity of the solar radiation in this wavelength region, only about 4% of the radiation reaching 80 km in the wavelength region from 1775Å to 2525Å is incident within the range from 1775Å to 1975Å. In spite of this it is nevertheless desirable to have more precise data for the oxygen absorption coefficients for this region.

It should be noted for all of these ozone distributions that the maximum ozone concentration occurs at 25 km and that there is a rapid and continuous fall in the ozone concentration on either side of the maximum. There is a change of nearly four orders of magnitude between the ozone concentration at the maximum and that at 80 km, the values varying from 7×10^{12} molecules/cm^3, (0.027 cm/km) to 10^9 molecules/cm^3 (4.0×10^{-6} cm/km) respectively for Case I.

The various cases considered in this Section and subsequent Sections are summarised in table 1 for convenience.

TABLE 1

LIST OF VARIOUS CASES CONSIDERED

Case number	Total ozone amount centimetre S.T.P.	Difference between this Case and Case I	Altitude range where differences occur
I	0.370	-	-
II	0.370	'Π' continuum underlying the Schumann-Runge bands.	50 - 80 km
III	0.370	Herzberg continuum underlying the Schumann-Runge bands.	50 - 80 km
IV	0.370	Assuming no contribution by absorption in the Schumann-Runge bands to the dissociation of oxygen.	50 - 80 km
V	0.373	The term $(\alpha_o + \Delta\alpha \cdot \frac{p}{p_o})$ used to represent the dissociation of oxygen in the Herzberg continuum instead of just the α_o term.	-
VI	0.270	$(\alpha_o + \Delta\alpha)$ term instead of α_o term, i.e. no pressure dependence of the oxygen absorption coefficient.	Whole altitude range.
VII	0.369	No temperature correction applied to the ozone absorption coefficients.	-
VIIIa	0.344	Ozone absorption coefficient increased by 10%	Very small differences over whole profile
VIIIb	0.373	Ozone absorption coefficient decreased by 10%	-
IXa	0.355	Oxygen absorption coefficient increased by 10%	Very small differences over whole profile
IXb	0.372	Oxygen absorption coefficient decreased by 10%	-
Xa	0.370	Solar radiation	-
Xb	0.370	given ± 10% variations	-

TABLE 1 (Continued)

Case number	Total ozone amount centimetre S.T.P.	Difference between this Case and Case I	Altitude range where differences occur
XI	0.370	Quadratic solution of photo-chemical equations	Above 70 km
XII	0.370	k_5 assumed to vary with temperature as $T^{\frac{1}{2}}$	Above 70 km
XIII	0.320	Using value of k_2 given by Zaslowsky et al. (1960)	Above 20 km
XIV	0.404	Using value of k_2 given by Benson and Axworthy (1957)	60 - 80 km and below 35 km
XV	0.640	Using values of k_2 and k_4 given by Eucken and Patat	Above 15 km
XVI	0.849	Using values of k_2 and k_4 given by Benson and Axworthy (1957)	Above 15 km
XVII	0.313	Quantum efficiency for the dissociation of ozone = 2 molecules per $h\nu$	Above 15 km
XVIII	0.246	Quantum efficiency for the dissociation of ozone = 5 molecules per $h\nu$	Above 15 km
XIX	0.240	Solar zenith angle $\theta = 45^{\circ}$	55 - 80 km and below 35 km
XX	0.154	$\theta = 60^{\circ}$	As above
XXI	0.370	Temperature distribution above 53 km increased so as to raise temperature at 80 km by 50°K	55 - 80 km

3.4.2 The pressure dependence of the oxygen absorption coefficients in the Herzberg continuum

As mentioned previously the variation of α_2 with pressure in this wavelength region was taken to be given by

$$\alpha_2 = \alpha_0 + \Delta\alpha \cdot \frac{p}{p_0}$$

In order to investigate the importance of this pressure dependence two alternatives to Case I were considered, Cases V and VI. Case V was similar to Case I in that it was assumed the attenuation of the incident radiation was due to an absorption coefficient of value $(\alpha_0 + \Delta\alpha \cdot \frac{p}{p_0})$, however, unlike Case I, this same value of the absorption coefficient was also taken to be responsible for the dissociation of the oxygen. For Case VI it was assumed that α_2 was independent of pressure and a constant value of $(\alpha_0 + \Delta\alpha)$ was used to calculate both the attenuation of the radiation and the dissociation of the oxygen for all heights. The resulting photochemical ozone distributions for Cases I and VI are shown in figure 22, that for Case V is not included as it was nearly identical with the distribution for Case I. The corresponding total ozone amounts for all three cases are given in figure 22 also.

The difference between the ozone distributions of Cases I and VI is due to the effect that absorption by oxygen has on the penetration of the solar radiation in this wavelength region. As the oxygen absorption coefficients for Case I are always smaller than those for Case VI, for the altitudes of interest here, there is less attenuation of the solar radiation initially, resulting in the formation of less ozone compared with Case VI because of the lower atomic oxygen concentration. Hence, the radiation reaching the lower levels will therefore be more intense for Case I, and, since the oxygen concentration is higher at these levels, correspondingly more oxygen will be dissociated, this being readily converted into ozone with the pressures at these altitudes. Although the total ozone amount for Case VI, 0.27 cm, is in better agreement with observation than that for Case I, 0.37 cm, Case VI is considered to be physically unrealistic and is only included to illustrate the effect of the pressure dependence of α_2 on the ozone distribution, and the errors which can occur by neglecting this effect.

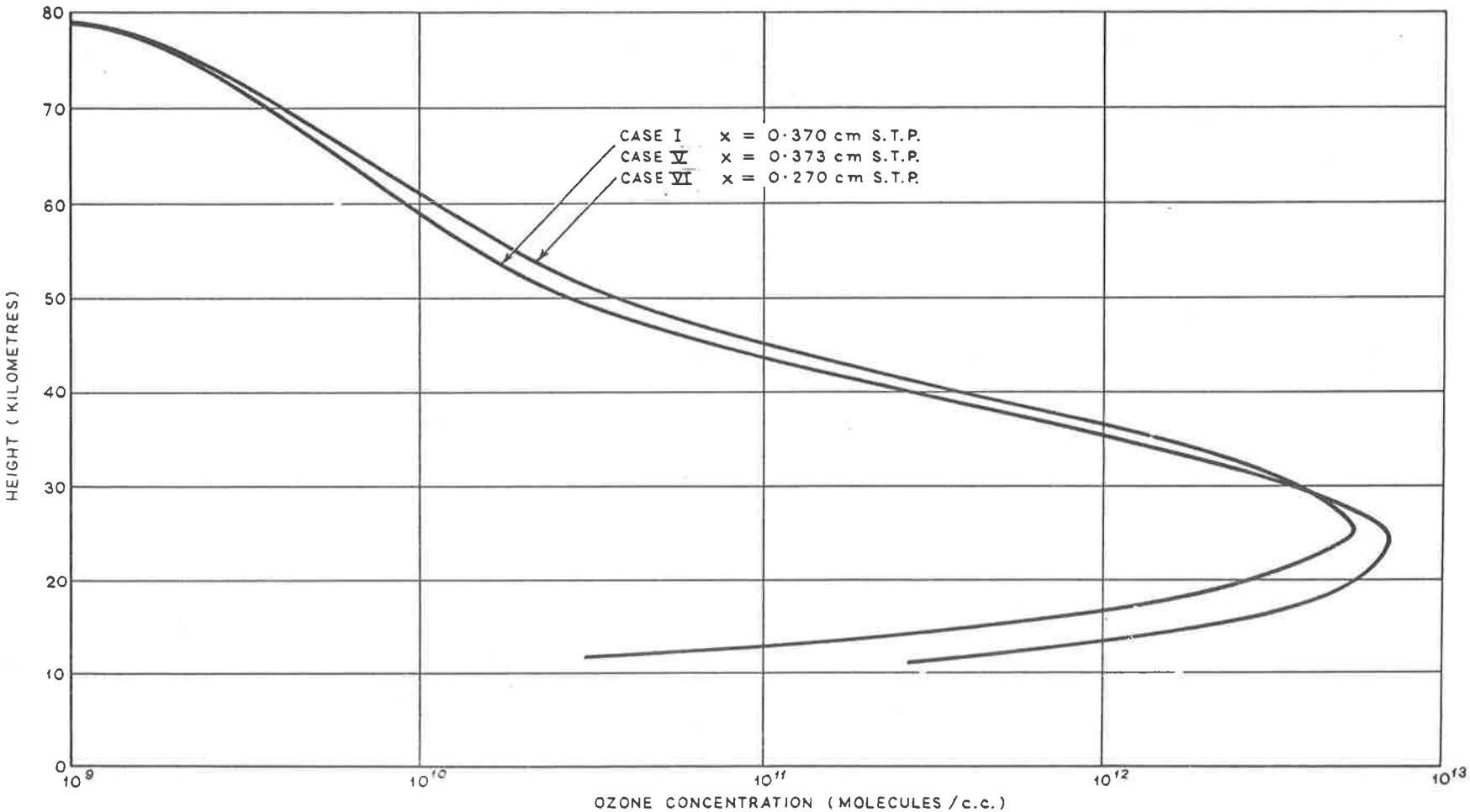

FIGURE 22. THE EFFECT OF THE PRESSURE DEPENDENCE OF α_2 IN THE HERZBERG CONTINUUM

The similarity between Cases I and V arises because the pressure term in α_2 is very small, p/p_o reaching approximately 0.2 at 11.5 km, which was the lowest level considered. The extra dissociation caused by using $(\alpha_o + \Delta\alpha \cdot p/p_o)$ instead of α_o can therefore be neglected for most of the height range, resulting in virtually identical ozone distributions.

3.4.3 The temperature dependence of the ozone absorption coefficients

Case VII differed from Case I in that no correction was made for the variation of α_3 with temperature. Although the temperature correction applied to Case I reduced the magnitude of α_3 for some of the wavelength intervals by up to 25%, only 11 of the 41 intervals were affected and these were in the region where ozone is a fairly weak absorber, the biggest corrections being made to the weak, long wavelength end of the Huggins bands. It is not surprising therefore that the ozone distributions for Cases I and VII are practically identical, the total ozone amounts being 0.370 and 0.369 cm respectively. It is apparent that the temperature dependence of the ozone absorption coefficients is not of importance in the photochemical theory of ozone.

3.4.4 The effect of experimental errors in the absorption coefficients and the solar intensity

Although the quoted experimental errors for some of the data are only ±5%, an investigation of the effect of ±10% variations in the values of the absorption coefficients and solar radiation intensity was made to determine the importance of such errors. Small changes in the total ozone amount were obtained for some of the cases corresponding to these variations, however, all of the ozone profiles were substantially the same as Case I and are therefore not shown graphically.

Cases VIIIa and VIIIb differed from Case I by ±10% variations given to the value of α_3, the total ozone amounts obtained being 0.344 cm and 0.373 cm respectively. The larger values of the absorption coefficients used in Case VIIIa apparently produced an increased rate of photolysis of ozone resulting in the smaller total ozone amount obtained. Reducing the value of the absorption coefficient caused only a small change in the total ozone amount, presumably because the radiation penetrating the atmosphere would be slightly more intense, thus producing a similar rate of ozone photolysis as that for Case I.

Very similar results were obtained for Cases IXa and IXb in which α_2 was changed by ±10% respectively. The variation of the total ozone from 0.355 cm to 0.372 cm for these cases is

in qualitative agreement with the results discussed in Section 3.4.2.

For Cases Xa and Xb, in which the intensity of the solar radiation incident on the earth's atmosphere was given a ±10% variation, no change whatsoever was produced in either the total ozone amount or the vertical ozone distribution compared with Case I. Owing to the eccentricity of the earth's orbit the intensity of the sun's radiation reaching the earth varies by ±3.5%; it is therefore obvious that no change in the photochemical ozone distribution will result from this effect.

3.4.5 The choice of rate constants

3.4.5.1 The rate constant k_5

As stated previously it was found that the three body recombination of atomic oxygen via reaction R5 was relatively unimportant in photochemical ozone calculations. In Case XI this reaction was completely ignored thus permitting equation E4 to be used to calculate the ozone distribution. The resulting distribution is not shown as it differed from Case I only above about 70 km, the ozone concentration at 80 km being 2.2×10^9 molecules/cm^3 for Case XI as opposed to 1.1×10^9 molecules/cm^3 for Case I. This difference would of course become more accentuated if the value of k_5 was, say, an order of magnitude greater, as reaction R5 would then proceed more rapidly.

A possible temperature dependence of k_5 was investigated in Case XII where the value of k_5 used for Case I was assumed to vary with temperature as $T^{\frac{1}{2}}$, which is the form given by elementary kinetic theory. This temperature dependence made virtually no difference to the ozone profile as the maximum difference between Case I and Case XII, which occurred at 80 km, was a rise from 1.1×10^9 to 1.2×10^9 molecules/cm^3.

3.4.5.2 The rate constant k_2

Two alternatives to Case I were investigated in Cases XIII and XIV. For Case XIII the value of $k_2 = 2.1 \times 10^{-34} \exp(-320/RT)$ cm^6 molecule^{-2} sec^{-1} given by Zaslowsky et al. (1960) was used, while for Case XIV the value of $k_2 = 6.9 \times 10^{-35} \exp(600/RT)$ cm^6 molecule^{-2} sec^{-1} was that given by Benson and Axworthy (1957). All three values of k_2 are fairly similar, and, what is more important, the various

activation energies quoted for reaction R2 probably cover the range in which the true activation energy is to be expected. The ozone profiles for Cases XIII and XIV are compared with that for Case I in figure 23. It is apparent that essentially the same ozone distribution is obtained for each case and that the maximum ozone concentration occurs at a height of 25 km, the agreement between Cases I and XIV in particular is very good, except above about 60 km. The difference between Cases I and XIII arises because the value of k_2 for Case I has been increased by a factor of 1.75 compared with Case XIII following the introduction of a new value of the equilibrium constant for reaction R2. The agreement between the total ozone amounts for these three cases is not so satisfactory as these range from 0.32 cm to 0.40 cm, and for this reason a more definitive value for k_2 is required. However, any change in the value of k_2 would not be expected to result in any substantial alterations to the photochemical ozone profile.

3.4.5.3 The rate constant k_4

The situation regarding the value of the rate constant k_4 is far from satisfactory at the present time as there is very poor agreement between the various quoted values, resulting in widely differing photochemical ozone profiles. Cases XV and XVI, which are compared with Case I in figure 24, illustrate the importance of the correct value of k_4 to photochemical ozone theory. For Case XV the much used data of Eucken and Patat (see Craig, 1950) were selected in order to provide a comparison with previous photochemical ozone calculations, as these have, almost without exception, been based on this data. Since Eucken and Patat only measured k_2/k_4 and not k_2 and k_4 explicitly equation E4 was used to calculate the ozone distribution for this case, hence the ozone concentration above about 60 km will be slightly high because of the neglect of reaction R5. There is, anyway, poor agreement between Cases I and XV both as regards the ozone distribution and the total ozone amount.

The data of Benson and Axworthy (1957) were selected for both k_2 and k_4 for Case XVI. The difference between the ozone distributions of Cases I and XVI is due principally to the value assigned to the activation energy of reaction R4, that given by Benson and Axworthy being 6000 cal. $mole^{-1}$ resulting in a value of $k_4 = 4.9 \times 10^{-11} \exp(-6000/RT)$ cm^3 $molecule^{-1}$ sec^{-1}, which is orders of magnitude less than the k_4 of Case I at atmospheric temperatures. The ozone concentrations and total ozone amount of 0.85 cm calculated for Case XVI are of course physically impossible in the atmosphere.

Since the value of k_4 selected for Case I was supported by measurements made by Phillips and Schiff (1962), and also produced a realistic ozone profile, it was thought at the time this work was carried out that the data of Leighton et al. used for k_4 in Case I was superior to that of Benson and Axworthy. Subsequent experimental work by Clyne et al. (1963) has suggested that this is not so, and the implications of this finding have therefore been investigated in Chapter 6. As the results shown in figure 24 indicate, the greatest uncertainty in photochemical ozone calculations at the present time is the value of the rate constant k_4.

3.4.6 The question of the quantum efficiency of the photochemical ozone reactions

It has been assumed in the results presented so far that each time a quantum of radiation is absorbed by an ozone molecule dissociation occurs, and that the mechanism governing the ozone reaction scheme in an oxygen atmosphere is given by reactions R2, R3 and R4. The maximum quantum efficiency of this reaction scheme is two, and would be obtained in the absence of any appreciable O_2 concentration and for $\lambda > 3100$ Å. In 1925 Kistiakowsky reported quantum efficiencies greater than 2 molecules/$h\nu$ when studying ozone decomposition due to a red - yellow radiation light source. For many years these results were the source of considerable controversy as regards the mechanism of ozone decomposition. These difficulties now appear to have been overcome by a new study of this particular reaction by Castellano and Schumacher (1962). Using the improved techniques now available they have shown that the results of Kistiakowsky were apparently in error, and that the reaction scheme of reactions R2, R3 and R4 is adequate to explain their results.

On the other hand McGrath and Norrish (1957) in experiments on the flash photolysis of ozone obtained high quantum efficiencies which they explained on the basis of the follow-

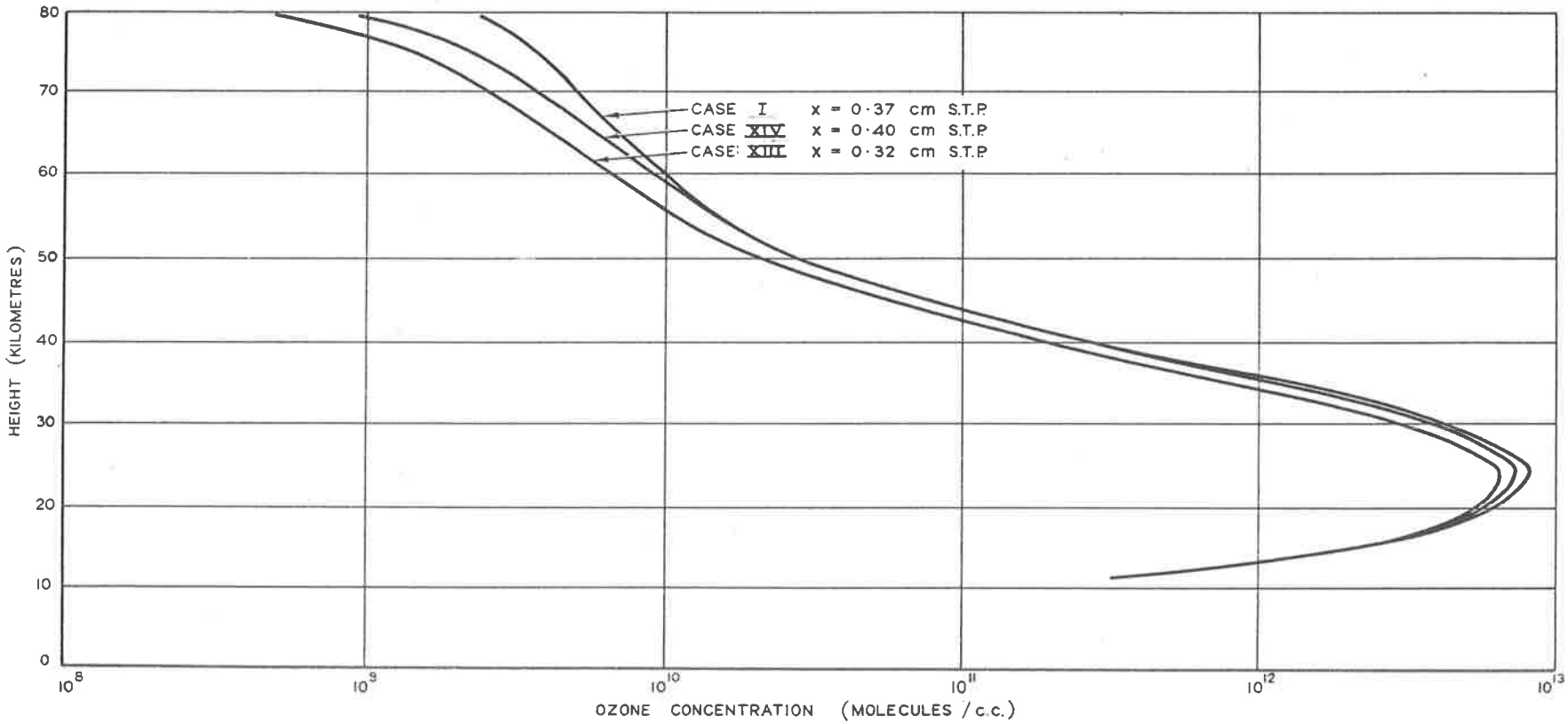

FIGURE 23. VARIATIONS IN THE VERTICAL OZONE DISTRIBUTION DUE TO THE USE OF DIFFERENT VALUES OF THE RATE CONSTANT, k_2

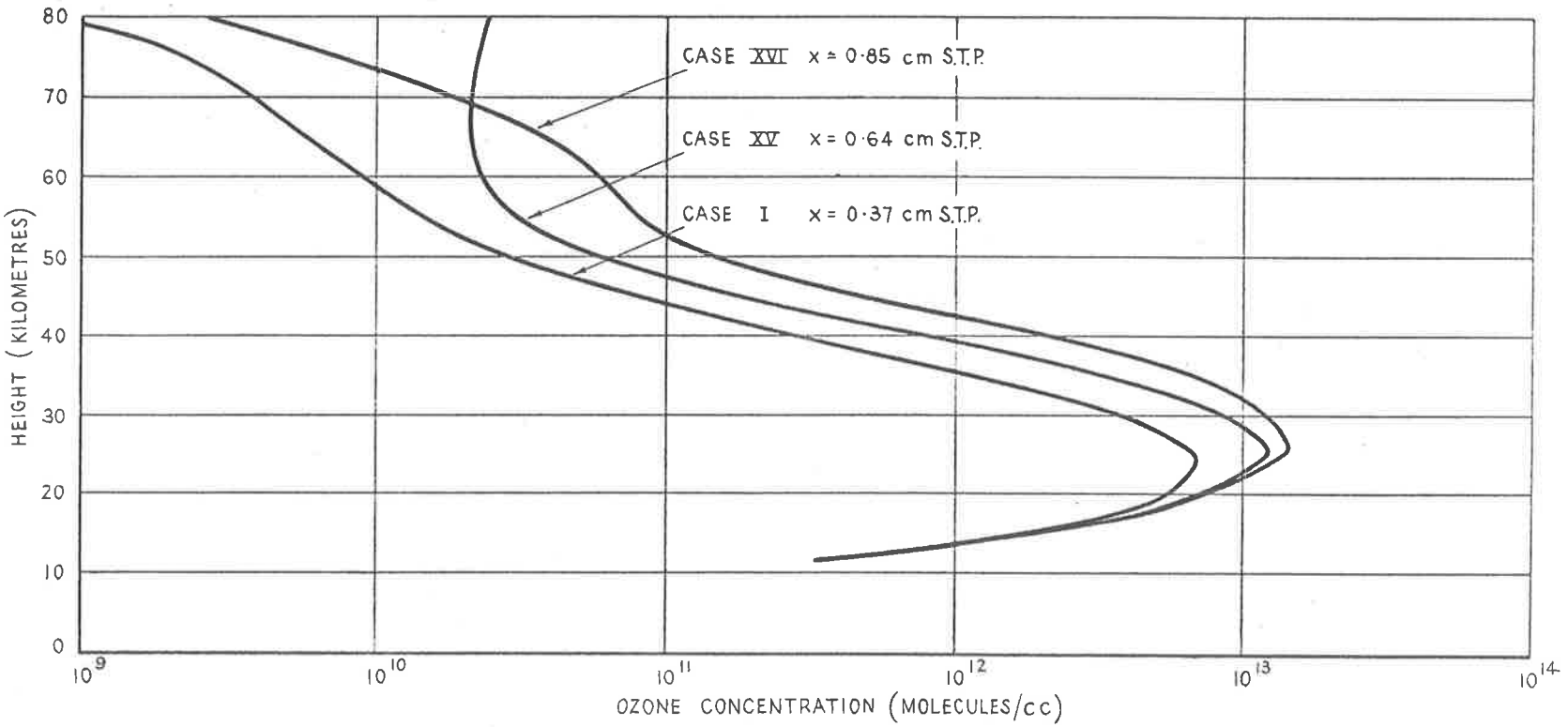

FIGURE 24. VARIATIONS IN THE VERTICAL OZONE DISTRIBUTION DUE TO THE USE OF DIFFERENT VALUES OF THE RATE CONSTANT k_4

ing atom-chain mechanism

$$O_3 + h\nu \rightarrow O_2 + O \qquad R3$$

$$O + O_3 \rightarrow O_2^* + O_2 \qquad R4a$$

and

$$O_2^* + O_3 \rightarrow 2O_2 + O \qquad R6$$

where O_2^* is a vibrationally excited oxygen molecule. The chain is maintained by the O atom produced by R6 partaking in R4a. Subsequent work by McGrath and Norrish (1960) indicated that the efficient propagation of this chain required the chain atom to be electronically excited to the ^1D state. Such excited atoms can be produced by the dissociation of ozone at wavelengths below 3100 Å, or possibly from reaction R6 when the vibrational excitation is above the 17th level.

The possibility that chain reactions can be produced in the atmosphere is discussed in Chapter 6, for the present only a crude investigation of the possible effects of quantum efficiency variations will be made to determine what influence these variations have on the photochemical ozone profile. Two alternatives were considered, Cases XVII and XVIII, which differed from Case I in that for each quantum of radiation absorbed in reaction R3 two and five molecules/$h\nu$ were assumed to be dissociated respectively. The resulting ozone profiles are compared with Case I in figure 25, from which it can be seen that for all altitudes there is a marked reduction in the ozone concentration for these two cases, and that this reduction increases with altitude because of the increasing intensity of the incident radiation. The total ozone amounts for these cases are in better agreement with observation than that for Case I, but for these cases the ozone concentration is reduced at the mid-altitude levels, which is the reverse of that desired in order to obtain good agreement with experimental ozone profiles. Nevertheless, it is apparent that quantum efficiency effects can be of importance in photochemical ozone studies.

The attractive possibility that the high ozone concentrations obtained in Case XVI, where Benson and Axworthy's data were used for k_2 and k_4, could be reduced to realistic values by assuming a simple quantum efficiency variation as in Cases XVII and XVIII does not appear to be tenable. It was found that a value of 25 molecules/$h\nu$ for reaction R3 reduced the total ozone amount for Case XVI only from 0.85 cm to 0.52 cm, and such a high quantum efficiency seems unlikely to result from the presence of excited molecules alone.

3.4.7 Variations of the solar zenith angle, θ

Case I was calculated assuming photochemical equilibrium and a zenith angle $\theta = 0^{\circ}$, implying that the sun is vertically overhead. For any one place there is a diurnal and seasonal variation of the sun's zenith angle, and it is of interest to estimate the effect of zenith angle variations on the photochemical ozone profile. The ozone distributions of Cases XIX and XX have therefore been calculated for zenith angles of 45° and 60° respectively, and these distributions are shown together with that for Case I in figure 26. It is apparent from this figure that above 35km the zenith angle of the sun does not substantially affect the ozone distribution, while for lower altitudes the maximum ozone concentration decreases with increasing zenith angle, although the height of the maximum concentration is not changed. The change in the ozone distribution with zenith angle results from the increased absorption of the solar radiation at the higher levels because of the longer atmospheric pathlengths, these slant pathlengths increasing as sec θ for $\theta < 70^{\circ}$.

The decrease in the total ozone amount with increasing zenith angle is not observed experimentally, and for latitudes where the maximum solar zenith angle is large there is more ozone than there is at the equator where the maximum zenith angle is always small. This disagreement between theory and observation arises because below 35km the atmosphere is not in photochemical equilibrium and ozone can therefore accumulate at the lower levels. The point to note from figure 26 is that, neglecting possible variations in the atmospheric temperature profile, one is led to conclude that essentially the same photochemical ozone distribution is to be expected at all latitudes and for all seasons for altitudes above 35km. In Section 3.4.8 the influence of variations in the atmospheric temperature profile is discussed. The small differences between the ozone distributions above 55km in figure 26 arise because the longer atmospheric pathlengths associated with the increase in the zenith angle result in increased absorption by oxygen above 80km, the wavelengths principally affected being those associated with the Schumann-Runge bands.

3.4.8 The effect of changes in the atmospheric temperature profile

It is obvious that the temperature profile will influence the ozone distribution in the atmosphere, not only because of its control over the atmospheric density, but also because of the temperature dependence of the rate constants. However, the aim of the present study was not to investigate in detail the effect of seasonal and latitudinal changes in the atmospheric temperature distribution, this having been done recently by London and Prabhakara (1962) in any case, and in fact only one variation from the ARDC 1959 temperature profile was considered. This variation, Case XXI, which consisted in increasing the temperature linearly between 53 and 80km so

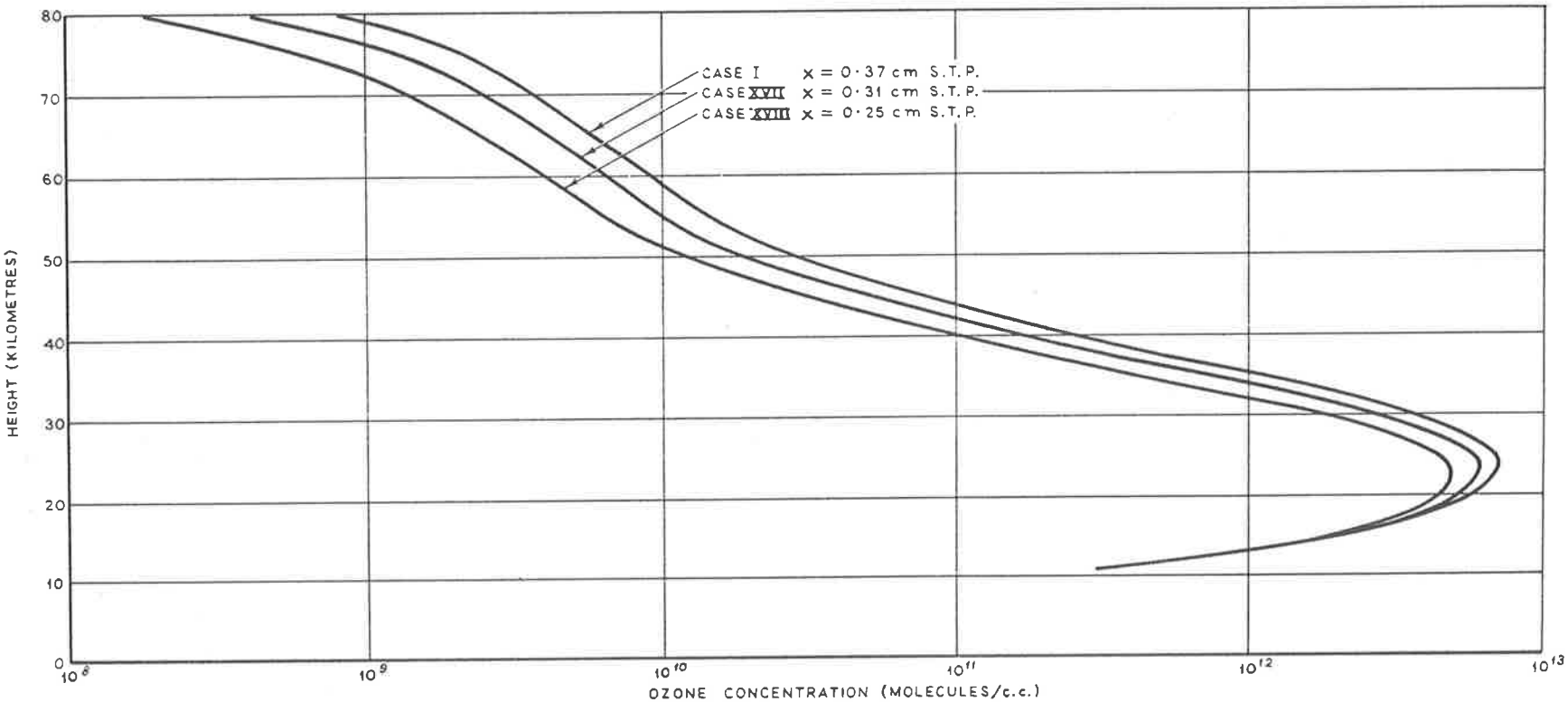

FIGURE 25. THE EFFECT OF VARIATIONS IN THE QUANTUM EFFICIENCY OF THE PHOTOCHEMICAL REACTIONS ON THE OZONE PROFILE

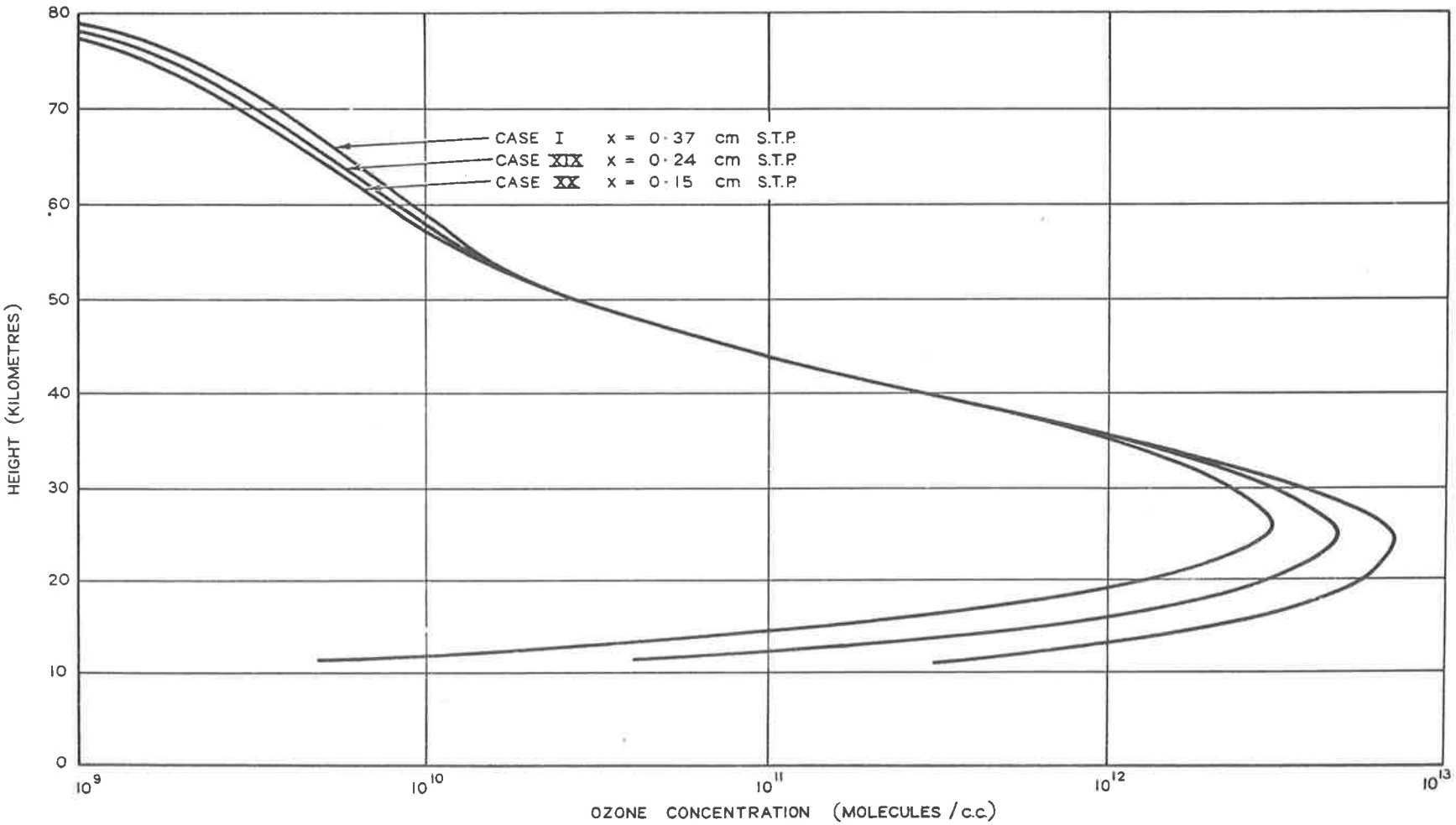

FIGURE 26. THE VERTICAL OZONE DISTRIBUTION FOR SOLAR ZENITH ANGLES $\theta = 0^{\circ}$, 45° AND 60°

that the temperature at 80 km was raised by 50°K to 216°K, was considered because most previous photochemical ozone calculations used model atmospheres with temperatures of the order of 220°K at 80 km. In addition atmospheric temperatures obtained by means of the rocket-grenade experiment by Stroud and Nordberg (1961) show that the largest temperature change occurs at 90 km where they observed a rise of 70°K from summer to winter at 70°N. The ozone distribution for Case XXI is compared with that for Case I in figure 27, from which it can be seen that only a minor change has occurred, the higher temperatures resulting in lower ozone concentrations. This change is due principally to the variation in the rate constants rather than that of the atmospheric density. The results of Stroud and Nordberg indicate that apart from high latitudes, i.e. greater than about 65° latitude, the effect of variations in the atmospheric temperature profile will produce only minor changes in the ozone profile so that theoretically essentially the same ozone concentrations are to be expected at all latitudes and seasons between about 35 and 60 km.

3.4.9 The relative concentrations of atomic oxygen, ozone and air

In figure 28 the equilibrium atomic oxygen and ozone distributions for Case I are compared. Although the atomic oxygen concentration is very much higher than the ozone concentration at the maximum altitude considered of 80 km, its concentration varies more rapidly with height, decreasing continuously with decreasing altitude, unlike that for ozone. The decrease in the atomic oxygen concentration in this height range follows from two reasons. One, the intensity of the radiation capable of forming atomic oxygen by dissociation of either molecular oxygen or of ozone is rapidly reduced for these lower levels; and two, because of the higher pressures at these levels, the probability of a three body reaction of atomic oxygen to form ozone is higher. Although the atomic oxygen concentration reaches 10^{12} atoms/cm^3 at 80 km this represents less than 1% dissociation of the molecular oxygen concentration at this altitude. Note that above 54 km the atomic oxygen concentration is greater than that for ozone.

The variation of the ratio of the number of molecules of ozone to the number of molecules of air is shown in figure 29. The maximum ozone to air ratio of 10^{-5} occurs at 29 km, which altitude is slightly above that for the maximum ozone concentration, viz. 25 km. Above about 50 km the ozone to air ratio ceases to decrease and even shows a slight increase with increasing altitude. The minimum ozone to air ratio in this altitude region is at 54 km, which also happens to be the height at which the atomic oxygen and ozone concentrations are equal.

The number ratio shown in figure 29 can be converted to a mass mixing ratio (microgram. of ozone to gram. of air) by multiplying by 1.66×10^6. It is therefore apparent that a

constant ozone mixing ratio is not obtained for an atmosphere in photochemical equilibrium, although above 50 km this condition appears to be approached. Experimental results given by Godson (1962), for ozone distributions obtained by means of the umkehr method, indicate that above about 30 km a constant mixing ratio does occur in the atmosphere.

3.5 Comparison of results

3.5.1 Comparison with previous photochemical ozone calculations

In figure 30 the ozone distribution for Case I is compared with photochemical ozone distributions calculated by Craig (1950), Dütsch (1956) and Paetzold (1953). All four distributions were calculated assuming the zenith angle of the sun was zero and that the "oxygen" atmosphere was in photochemical equilibrium. The agreement between the various profiles and total ozone amounts is quite satisfactory considering the uncertainties in the data and the assumptions made by the various authors. The data selected for Case I differed from those used previously mainly as regards the spectral intensity of the sun below 2400 Å, the pressure dependence of the oxygen absorption coefficients and the values of the rate constants k_2 and k_4. The agreement between Dütsch's results and Case I is particularly good between 30 and 50 km, but, due to the differences in the two sets of data, this agreement is considered to be fortuitous.

3.5.2 Comparison of Case I with experimental results

Very few direct measurements have been made of the vertical ozone distribution above 30 km. Ozone profiles have been obtained, however, from spectrographs carried by rockets launched from White Sands in America, latitude 32°N (Johnson et al., 1952); two such profiles are shown in figure 31 together with Case I. The experimental values are in accord above about 40 km, but only for the middle altitude range is the ozone concentration for Case I of the same order as the experimental values. Agreement would not be expected for altitudes below 35 km since the atmosphere in this region is not in photochemical equilibrium, and in addition Case I is representative of the photochemical ozone distribution which would be expected at the equator. For the upper layers the assumption that sufficient time has elapsed for photochemical equilibrium to be attained results in a higher ozone concentration than would actually be present in the atmosphere, as also does the limitation of an oxygen atmosphere. The experimental ozone concentration above 60 km is in fact considerably less than the theoretical concentration. However, due to the subsequent revision of the ozone absorption coefficients, the experimental ozone distributions may be in error, in addition the experimental accuracy is low for the high altitude range because of the small amount of ozone

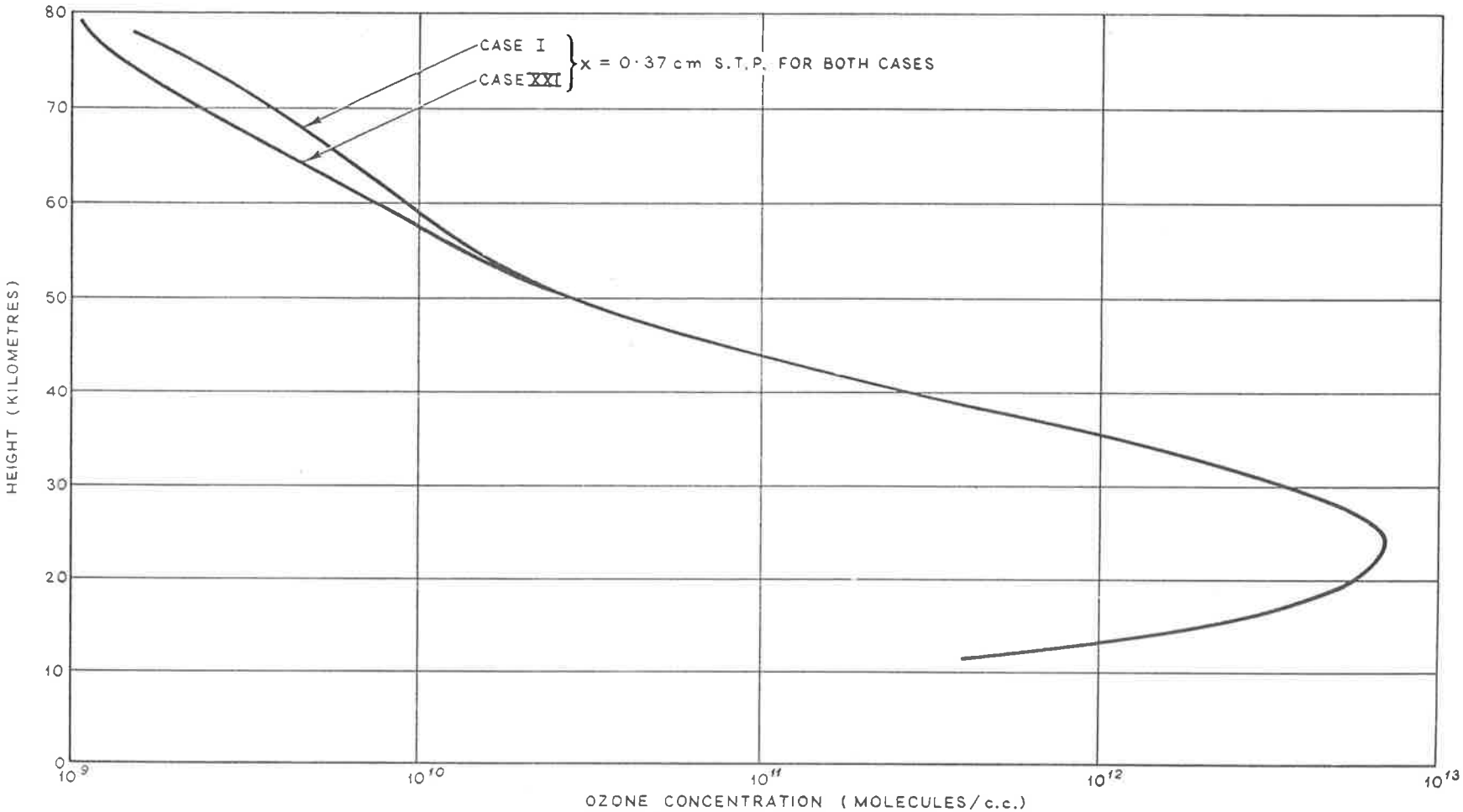

FIGURE 27. THE CHANGE IN THE OZONE PROFILE DUE TO CHANGES IN THE TEMPERATURE DISTRIBUTION ABOVE 53 KM

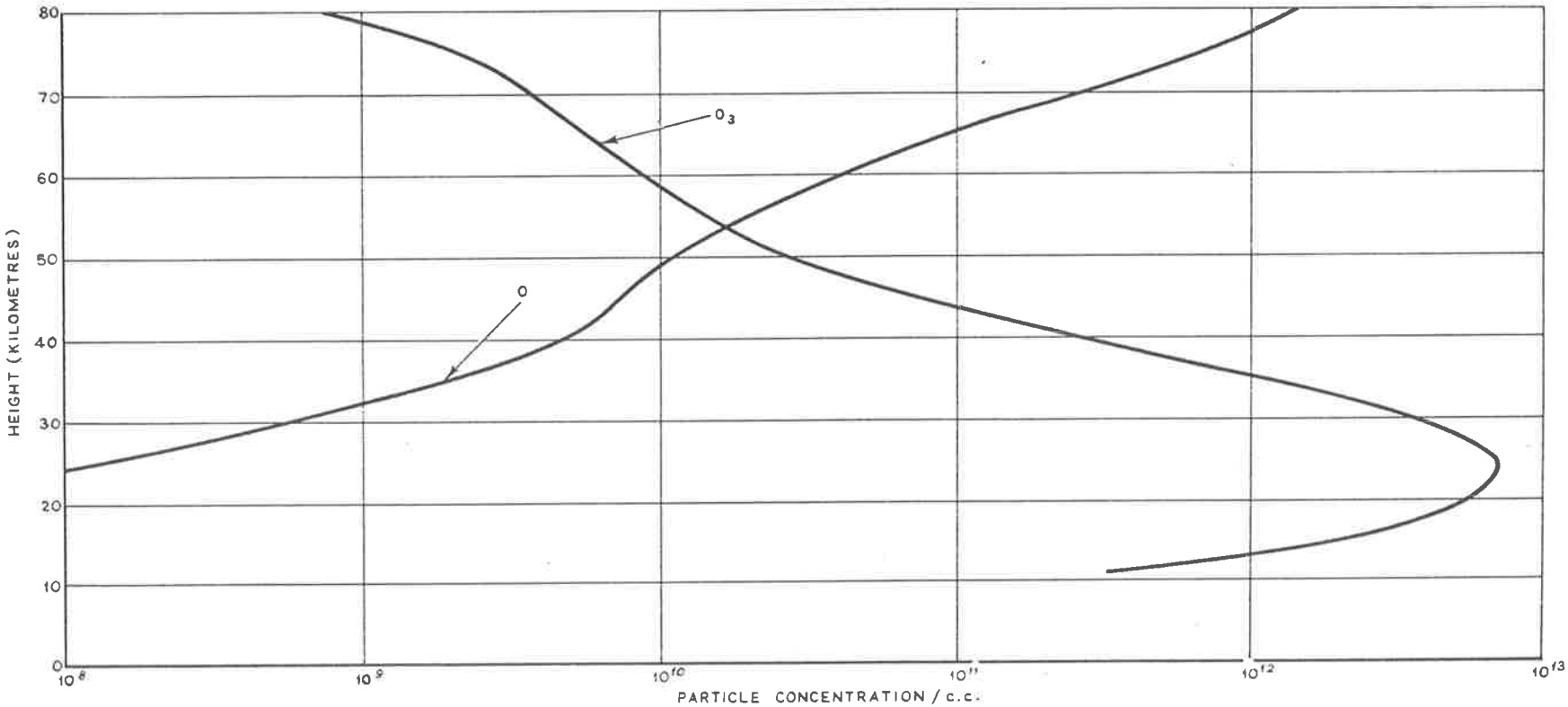

FIGURE 28. ATOMIC OXYGEN AND OZONE VERTICAL DISTRIBUTIONS FOR CASE I

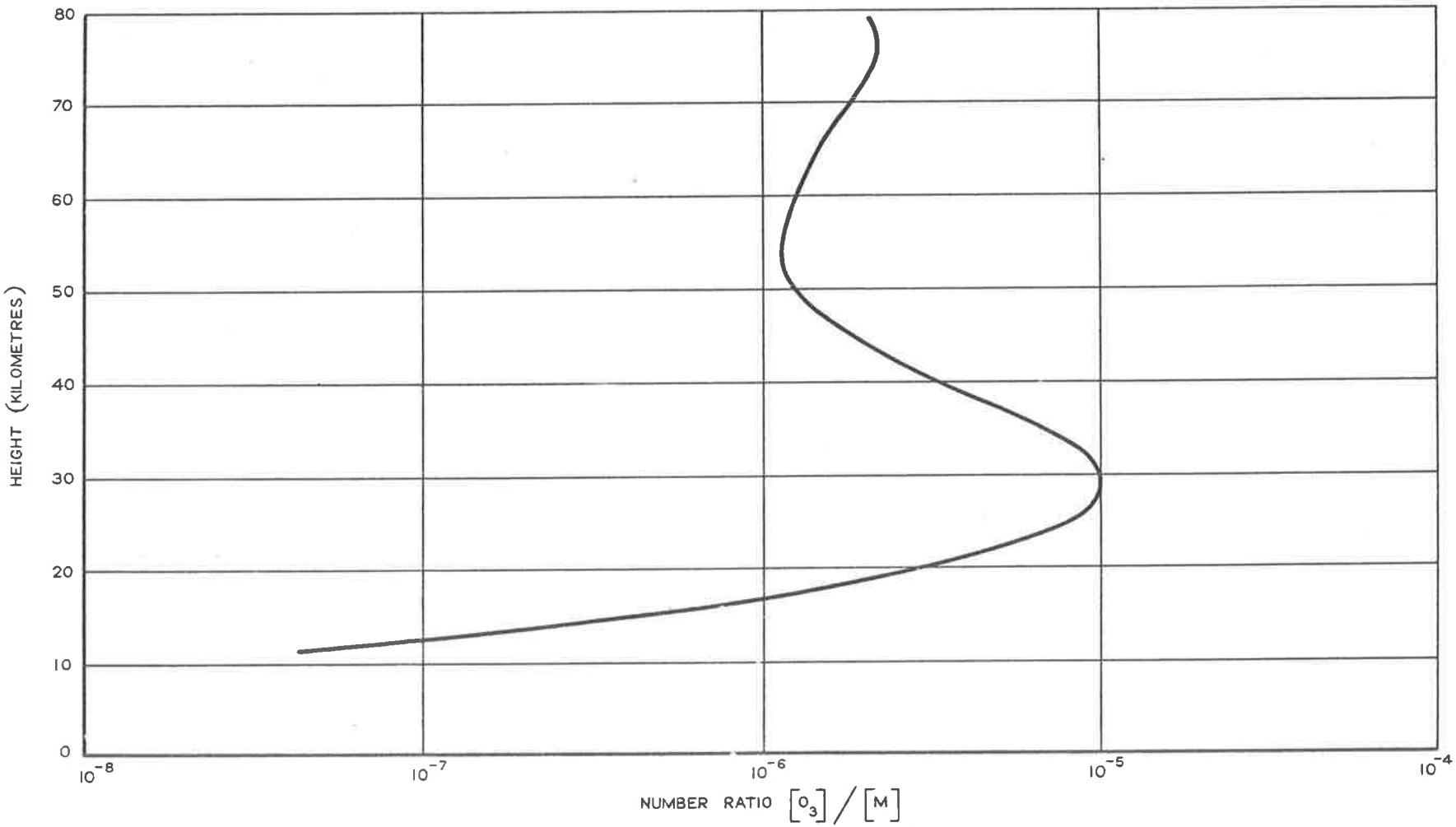

FIGURE 29. OZONE TO AIR RATIO

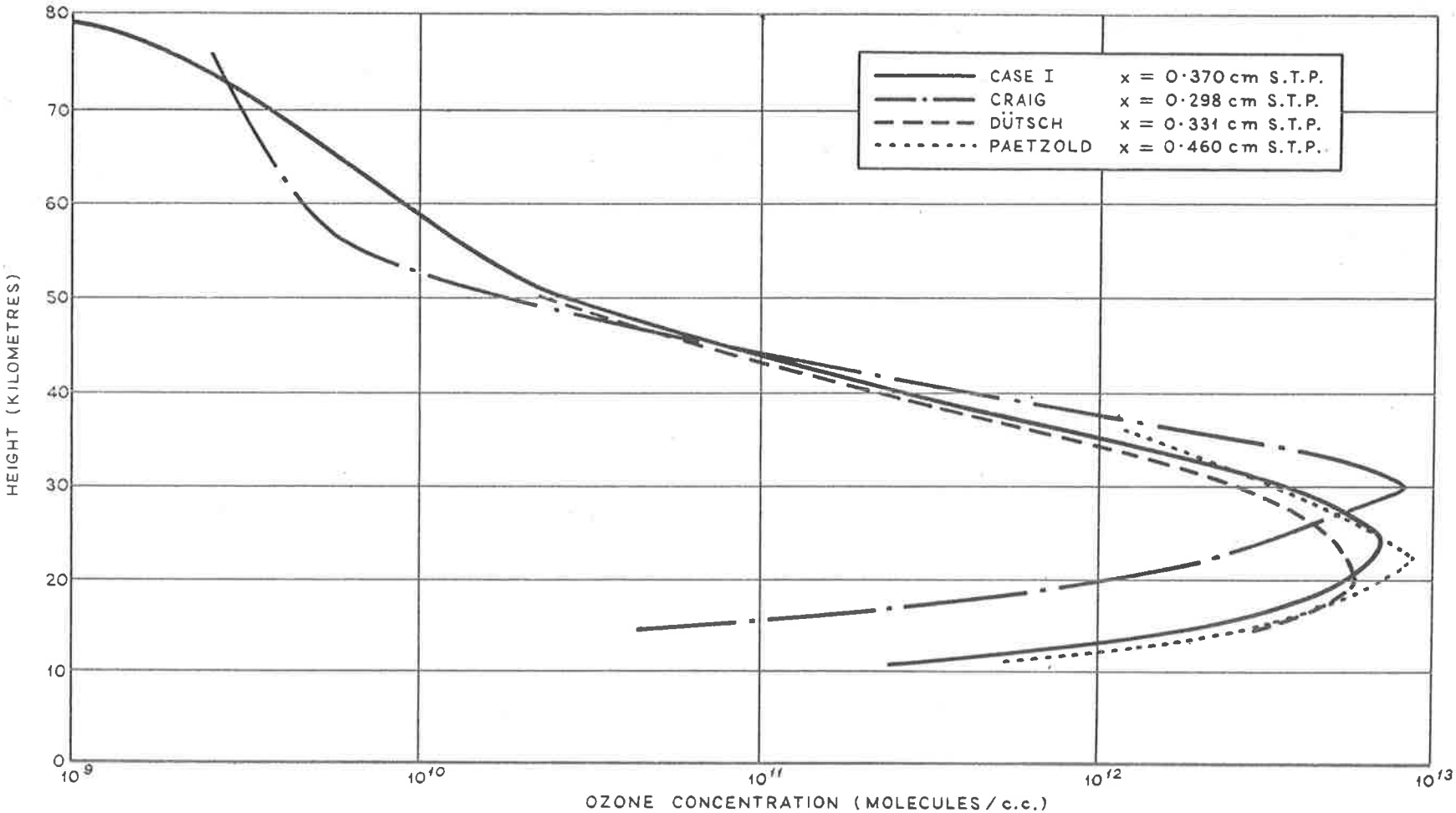

FIGURE 30. COMPARISON OF CASE I WITH OTHER PHOTOCHEMICAL OZONE DISTRIBUTIONS

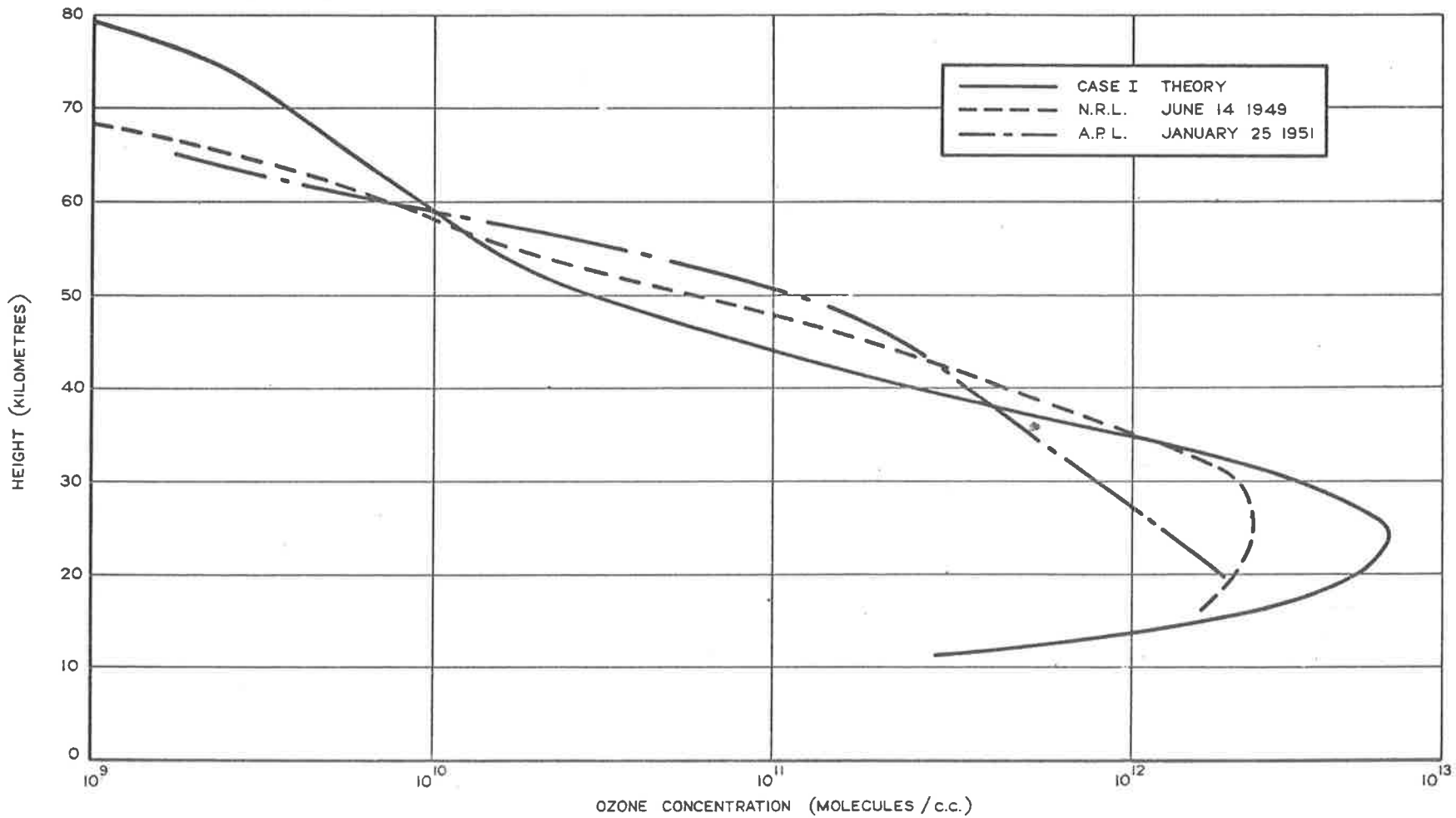

FIGURE 31. COMPARISON OF CASE I WITH VERTICAL OZONE DISTRIBUTIONS MEASURED FROM ROCKETS

between the rocket and the sun, hence the importance of the difference between the observed and the calculated ozone concentrations above 60 km cannot be fully assessed. The agreement between the rocket results and Case I is considered to be satisfactory having regard to the possible sources of error in the theoretical and experimental values.

The modification of the photochemical ozone distribution by atmospheric motions, which becomes important below 35 km, is illustrated in figure 32 where Case I is compared with an umkehr ozone distribution for the Belgian Congo, latitude $2^{o}S$, taken from results presented by Dütsch (1959). As can be seen photochemical theory indicates that there is less ozone above 30 km than is actually observed while below 30 km the theory predicts much more ozone, there is also a significant difference between the experimental total ozone amount of 0.23 cm and the theoretical value of 0.37 cm. The reason for the disagreement between theory and observation in this height range arises because the air in the equatorial region ascends and then moves polewards transporting ozone with it, thus producing the deficit noted in the ozone distribution below 30 km.

3.6 Conclusions

It is apparent from the discussion in the preceding sections that despite the improvements in recent years there is still some uncertainty about the values of some of the terms required for photochemical ozone calculations. There are probably minor errors in the photochemical ozone profiles because of the lack of sufficiently quantitative values for the oxygen absorption coefficients associated with the Schumann-Range bands, and the question of the quantum efficiency of dissociation of oxygen in this wavelength region. These uncertainties would affect the ozone concentrations above about 50 km only. The values of the ozone absorption coefficients and the spectral intensity of the sun would appear to be satisfactorily known at present for the wavelength region of interest, and no important changes in the photochemical ozone profile would be expected to result from a subsequent revision of these values.

The major sources of error in photochemical ozone calculations at present would appear to be in the rate constants k_2, k_4 and k_5. Of these k_5 is the least important as the results of Section 3.4.5.1 show, the ozone profile being influenced only above 70 km by reaction R5. In the case of k_2, although there is a wide range of reported values, it seems from the discussion of Kaufman and Kelso (1961) that the actual value of k_2 lies near to that used here. Since the temperature dependence of k_2 is not of great importance it seems probable that the essential features of the photochemical ozone profile are adequately represented by the value of k_2 used in the present calculations. Undoubtedly the major uncertainty concerns the value of k_4 and its temperature dependence, and a definitive value of k_4 is of vital importance as regards the

photochemistry of atmospheric ozone. Not only is the value of k_4 of great consequence in calculating the ozone concentration, but perhaps of more importance are the implications the value of k_4 can have to the theory of the photochemistry of ozone. This topic is developed in detail in Chapter 6.

For the present it will be assumed that an adequate representation of the photochemical ozone distribution in the atmosphere is given by Case I, and the data selected for this case will be used in Chapters 4 and 5. Since there is reasonable agreement between Case I and experimental results this assumption would appear to permit realistic studies to be made.

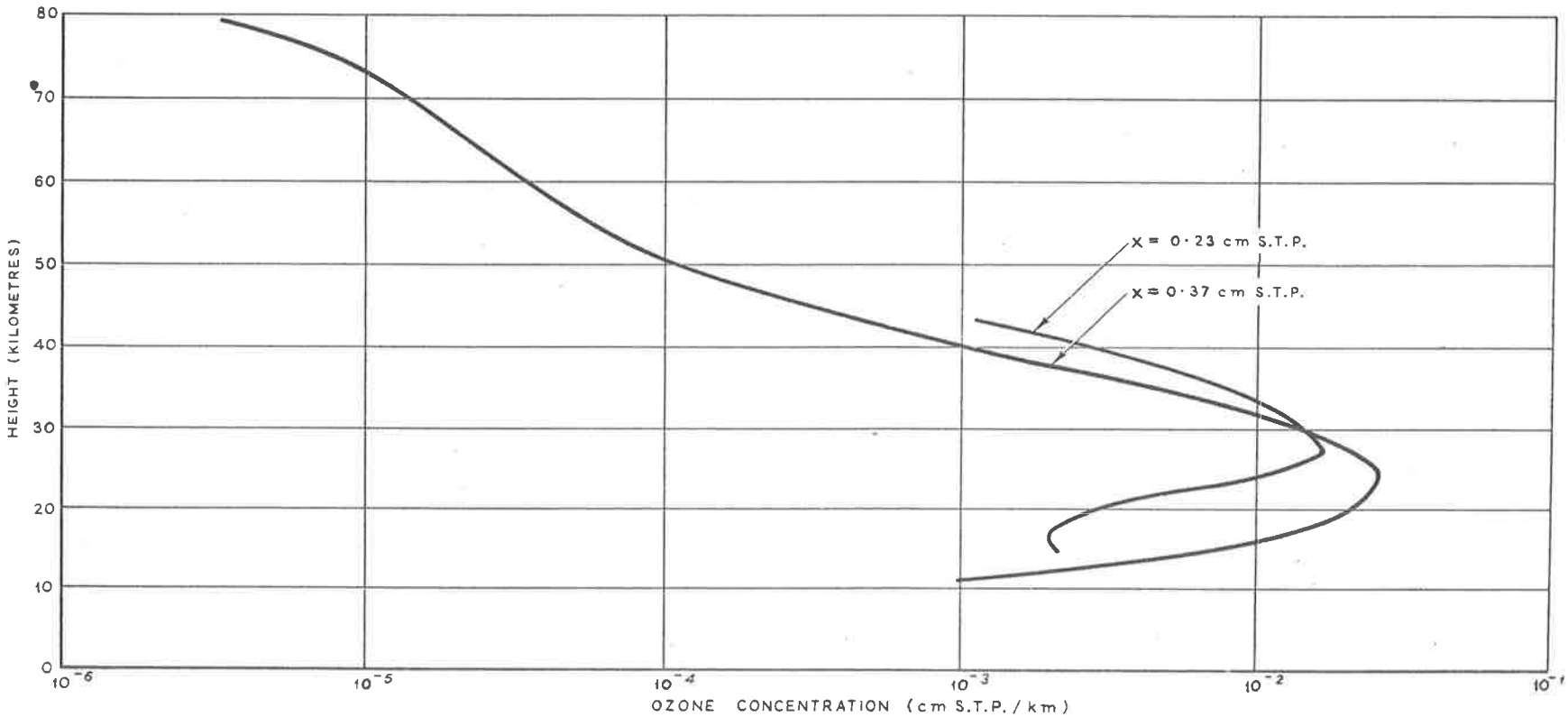

FIGURE 32. COMPARISON OF CASE I WITH UMKEHR OZONE DISTRIBUTION FOR THE BELGIAN CONGO, LATITUDE 2° S

CHAPTER 4

A NON-EQUILIBRIUM INVESTIGATION INTO THE DIURNAL PHOTOCHEMICAL ATOMIC OXYGEN AND OZONE VARIATIONS IN THE MESOSPHERE

4.1 Introduction

In the previous chapter the results have been presented of an investigation into the variations of the photochemical O_3 distribution for an oxygen atmosphere at rest, for conditions under which it was assumed that equilibrium had been attained. It is therefore of interest to investigate the diurnal variation of O_3 in the atmosphere, due to photochemical effects, and to determine whether the equilibrium state assumed above is actually attained.

Although O_3 is formed by photochemical reactions at all altitudes in the range 10 to 100 km, only the O_3 at the higher levels, above about 35 km, is affected by the solar radiation under normal circumstances. The O_3 at the lower levels, where it is principally stored, is protected from the intense short wavelength solar radiation, and as a result is independent of the diurnal variation in the solar radiation. The O_3 above 35 km does however respond to changes which alter its concentration from that which is in a steady state with the atomic oxygen concentration and the incident radiation at a particular altitude. This response is faster at higher altitudes where the solar radiation is more intense, and, because of this, one might expect the ozone at these altitudes to show a diurnal variation following the variations in the solar radiation. The resulting change in the total ozone concentration in a column of the atmosphere would be very small, and hence extremely difficult to detect experimentally. This is due to the low ozone concentration at the higher altitudes, the ozone amount above 40 km being less than 1% of the total. The observation of diurnal ozone changes is also complicated by the fact that the standard instrument, the Dobson spectrophotometer, is calibrated by assuming that there is no diurnal ozone change. Nevertheless, by means of a statistical analysis, Dütsch (1956) has reported that a small ozone change occurs during the sunlit hours, also, Khalek and Vassy (1952) have noted that a reduction in the total ozone amount can occur around noon. The biggest increase in the diurnal ozone variation takes place after sunset when the ozone concentration increases at the expense of the atomic oxygen concentration. These increases in the total ozone amount have been observed by using the moon as a light source, although the results are apparently subject to some speculation (Ramanathan et al, 1961).

Theoretical studies of these effects are of interest as they provide information on a region of the atmosphere which is still relatively unexplored, and it is possible to relate atomic oxygen

and ozone concentrations in the mesosphere and above with atmospheric motions as shown by Young and Epstein (1962). Calculations of the ozone increase at night have been made by Barth (1961), Dütsch (1961) and Paetzold (1961). Dütsch (1956) has also attempted an investigation of the diurnal photochemical ozone change, but assumptions he had to make in the derivation of his equations and also concerning the values of rate constants limited the results he obtained. Very recently Leovy (1964) has also made a study of the diurnal ozone variation and the departure from equilibrium in the mesosphere, and obtained results fairly similar to some of those given here independently. He was however primarily interested in the radiative properties of the mesosphere in his study rather than the properties of the ozonosphere as reported here.

The present work is an attempt to improve on previous calculations by using a more realistic mathematical treatment and the best data available. The principal difference between the treatment given here and those used previously is that the equations defining the atomic oxygen and ozone concentrations are maintained in their complete differential form and simultaneously integrated numerically on a computer. This permits a completely non-equilibrium approach to be used and avoids making the usual assumption that photochemical equilibrium prevails at some time in the atmosphere. The differential equations have been integrated to permit a study of the variations in the ozone and atomic oxygen concentrations for a period extending from noon one day to noon on the succeeding day.

4.2 The photochemical reactions and equations

The limitations of an oxygen atmosphere at rest were again imposed for the present study, and the same reaction scheme as before, reactions R1-R5 only, was considered. The time rates of change of the O and O_3 concentrations due to these reactions are then given by equations E1 and E2 (p.16). When considering the radiation free time at night the above two equations reduce to

$$\frac{d[O_3]}{dt} = k_2 [O][O_2][M] - k_4 [O][O_3] \qquad E6$$

$$\frac{d[O]}{dt} = -k_2 [O][O_2][M] - k_4 [O][O_3]$$

$$- 2k_5 [O]^2 [M] \qquad E7$$

By integrating these pairs of simultaneous equations numerically it is possible to investigate the diurnal variation of O and O_3 in the atmosphere.

The data selected for this study was the same as that used for Case I in Chapter 3, as this was considered to give a fairly realistic representation of the actual conditions in the atmosphere. The equilibrium concentrations of O and O_3 for Case I were those used as the preliminary initial values for the diurnal integration routine. Since in the diurnal investigation one is concerned only with the upper layers of the ozonosphere, it is possible to ignore the pressure dependence of the O_2 absorption coefficient in the Schumann-Runge bands, as given by equation E5 on p.29, and put $\alpha_2 = \alpha_o$. The neglect of the $\Delta\alpha \frac{p}{p_o}$ term is justified for the altitude range under consideration as the maximum value of this term amounted to less than 0.1% of α_o.

In the equilibrium study of Chapter 3 the O_3 concentration above 80km was neglected, but, for the diurnal investigation the atmospheric pathlengths at dawn and sunset are very large, and the absorption by the O_3 above 80km can produce a noticeable attenuation. For this reason a value of 5×10^{13} molecules/cm^2 column was taken for the total O_3 amount above 80km, while an estimate of 4.6×10^{19} molecules/cm^2 column was made of the total O_2 amount above 80km.

It was assumed for the purposes of the diurnal investigation that there was no diurnal variation of temperature in the atmosphere, for the altitude range of interest (48 to 80km) indications are that any such variation would be of minor importance. The effect of variations in the atmospheric temperature profile is discussed in Section 4.5.4.

The "day" used for the diurnal investigation was taken as that of the equinox at the equator, the zenith angle at noon therefore being zero. The sun was then given a 1^o rotation every 4 minutes so that the relative times of night, day, dawn and sunset were as for the actual atmosphere.

4.3 The characteristic times for atomic oxygen and ozone in the atmosphere

Before discussing the numerical methods used in the present work it is as well to consider the characteristic times (half restoration times) for O and O_3, these being the times taken for disturbances $\Delta[O]$ or $\Delta[O_3]$ from the equilibrium values $[O]_o$ and $[O_3]_o$ to be reduced to e^{-1} of their initial values. Dütsch (1956) has derived an expression for the characteristic time for O_3 in the atmosphere from a consideration of equations E1 and E2, neglecting the term involving atomic oxygen recombination, which is of minor importance for the altitude range under consideration. Assuming that $[O]$ is equal to its equilibrium value and therefore $d[O]/dt = 0$ enables $[O]$ to be eliminated from E1, hence

$$\frac{d[O_3]}{dt} = \frac{2\alpha_2 q_2 k_2 [O_2]^2 [M] - 2\alpha_2 q_2 k_4 [O_2][O_3] - 2\alpha_3 q_3 k_4 [O_3]^2}{k_2[O_2][M] + k_4[O_3]} \qquad \text{E8}$$

If $[O_3]$ is not in equilibrium but is given by $[O_3] = [O_3]_o + \Delta[O_3]$ then substituting for $[O_3]$ in E8 and remembering that $d[O_3]_o/dt = 0$. the following expression is obtained

$$\frac{d\Delta[O_3]}{dt} = \frac{-2\alpha_2 q_2 k_4 [O_2]\Delta[O_3] - 4\alpha_3 q_3 k_4 \Delta[O_3][O_3]_o - 2\alpha_3 q_3 k_4 \Delta[O_3]^2}{k_2[O_2][M] + k_4([O_3]_o + \Delta[O_3])}$$

By considering the relative importance of the various terms in this equation Dütsch was able to integrate it, and obtained a rather lengthy expression from which the characteristic time, τ_3, for O_3 is given by,

$$\tau_3 = \sqrt{\frac{k_2[M]}{16\ k_4\alpha_2\alpha_3 q_2 q_3}} = \frac{k_2[O_2][M]}{4\alpha_3 q_3 k_4 [O_3]_o} \qquad \text{E9}$$

Similarly, by considering $[O_3]$ to be in equilibrium instead of $[O]$ one can use Dütsch's method to obtain the characteristic time, τ_1, for O,

$$\tau_1 = \frac{\alpha_3 q_3}{2\alpha_2 q_2 k_4 [O_2] - 4k_2 k_4 [O_2][M][O]_o} \qquad \text{E10}$$

In calculating values for τ_3 and τ_1 from E9 and E10 the values used for the various terms in these equations were the same as those used for Case I in the previous equilibrium calculation. The variation of τ_1 and τ_3 with height for an overhead sun is given in figure 33.

The significance of figure 33 is that it readily permits the height ranges to be determined for which either O or O_3 would not be expected to be in equilibrium. Of the 8.64×10^4 seconds in a day only about 10^4 seconds are available in which the atmosphere will be able to attain equilibrium with the incident solar radiation, hence altitudes for which the characteristic time is much greater than 10^4 seconds will probably not be in equilibrium because of mixing in the actual atmosphere. In addition if there is a variation in the concentration of an atmospheric constituent due to reactions taking place at night, it will not reach its equilibrium concentration during the day if its characteristic time is greater than about 10^4 seconds, regardless of any mixing in the atmosphere. From figure 33 it can be seen that above about 65 km O, and below about 35 km O_3, will probably not be in photochemical equilibrium

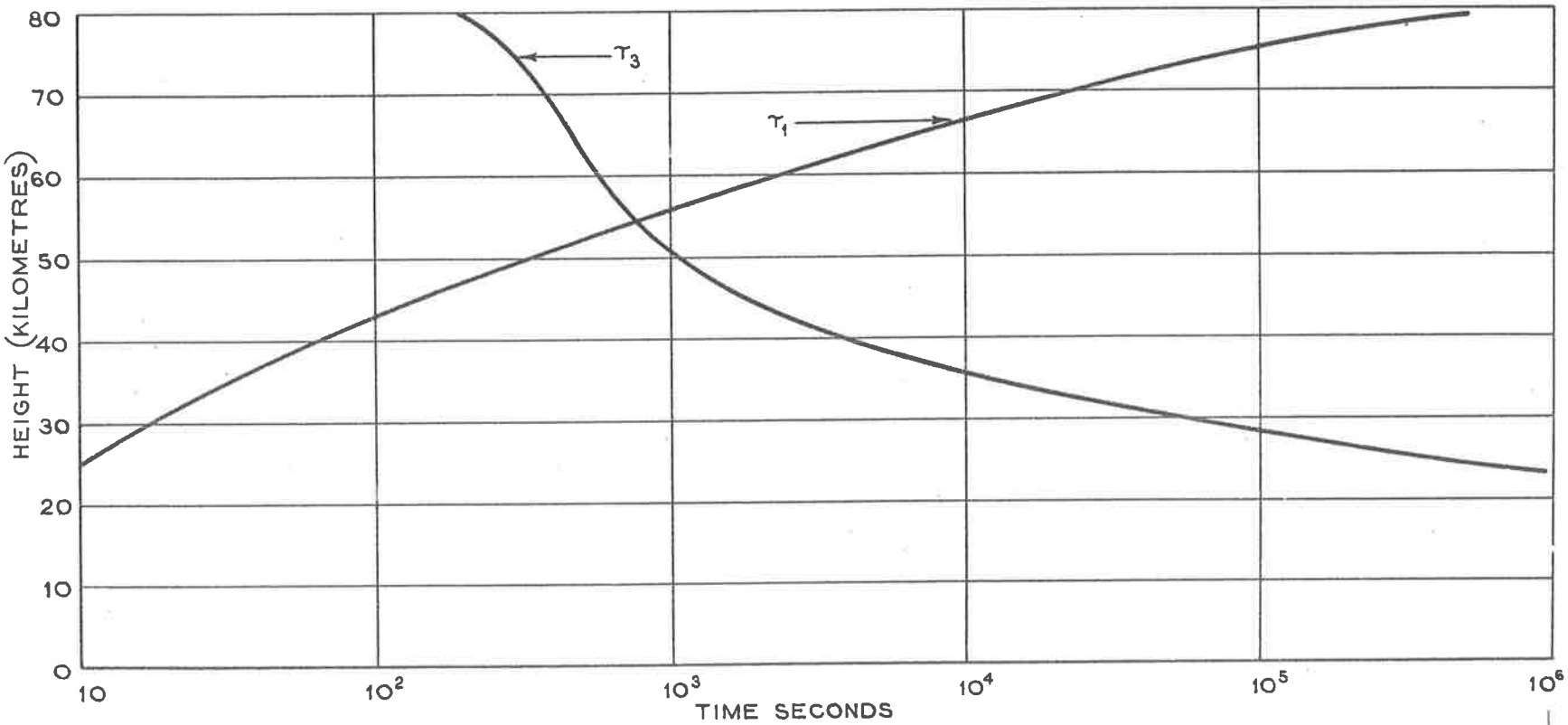

FIGURE 33. THE CHARACTERISTIC TIMES FOR OZONE, τ_3, AND ATOMIC OXYGEN, τ_1.

in the atmosphere. In fact from a study of τ_1, Wallace (1962) has estimated that the daytime value for the O concentration might be less than the equilibrium value by at least one order of magnitude in the altitude range from 85 to below 60 km. Subsequent results will show that this is partially correct.

As is well known, the high value of τ_3 below 30 km is the reason that relatively large amounts of O_3, in some cases many times the equilibrium value, are to be found in the atmosphere, since it is in this region (10 to 30 km) that the atmosphere "stores" its ozone supply. Similarly the high value of τ_1 above 70 km results in non-equilibrium amounts of O being formed, and such non-equilibrium values will also cause the O_3 in this region to be in non-equilibrium. This follows because the O_3 concentration is closely related to the O concentration at these altitudes and cannot attain its equilibrium concentration independently, despite its small characteristic time.

4.4 Numerical methods

A four point Runge-Kutta integration routine was used to integrate simultaneously equations E1 and E2 for daytime conditions, and equations E6 and E7 for the radiation free time at night on an IBM 7090 computer. Because of the variation with height of the gas concentrations and the radiation intensity it was necessary to divide the atmosphere into a number of height intervals. Fourteen intervals in the height range 80 to 47 km were used, these being 2.5 km thick down to 55 km and 2 km thick from 55 to 47 km. The upper height limit was selected because this was the limit set in the previous equilibrium calculations, while the lower limit arises from the fact that the time step for the integration routine starts to become prohibitively small at the lower altitudes; also below this altitude this study is not of interest because photochemical equilibrium exists.

In the radiation free time the various layers are completely independent of each other and can be treated separately if desired. However, during the day the layers are interconnected by the radiation terms, the intensity of the radiation incident on a given layer being that transmitted from the layer above. As a result of this it is desirable to use a common time interval for the integration routine for the whole altitude range under investigation in order to reduce complications arising in the calculation of the solar intensity. This intensity varies continuously because the variation in the sun's zenith angle with time of day results in changing atmospheric pathlengths, and hence in the corresponding atmospheric absorption. The time intervals determined for the integration step were sufficiently short to be able to assume that the solar intensity was constant over the step length, and its value was calculated for the time corresponding to the centre of the time interval.

The solar intensity, q_h, reaching a layer at height, h, is related in general to the solar intensity incident on the earth's atmosphere, q_o, by

$$q_h = q_o \exp(-\alpha N \sec\theta)$$

where α is the absorption coefficient, N is the number of absorbing particles in a vertical column above the height h, and θ is the solar zenith angle. For $\theta < 70^\circ$ the atmospheric path-length was taken to vary as sec θ, while for $\theta > 70^\circ$ sec θ was replaced by the Chapman function, Ch (X,θ), which allows for the sphericity of the earth's atmosphere (Chapman, 1931). For $\theta > 99^\circ$ no radiation can reach any of the layers of the atmosphere considered here as they lie in the earth's shadow. The value of θ at which this cut-off occurs varies from 99° to 97° for the altitude range 80 to 47 km. In any case by this time the intensity of the radiation is very weak and the radiation terms in the equation are of minor importance. The evaluation of Ch (X,θ) was performed by the computer as required using a five point Gaussian quadrature.

In an integration routine of the Runge-Kutta type it is necessary to determine the time step with some care in order to avoid inaccuracies or round-off errors. It can be shown (Nicholls, 1962) that the time step, Δt, is related to the eigen values, λ, of the matrix defining the pairs of simultaneous equations E1 and E2 or E6 and E7. For computational stability the largest negative eigen value must be retained, an additional requirement for stability is that $|\lambda \Delta t| < 2.8$, while for good accuracy $|\lambda \Delta t| < 1.0$. The variation of Δt with altitude corresponding to $|\lambda \Delta t| = 1.0$ is given in figure 34 for daytime conditions. A different variation is obtained of course for the radiation free time at night.

It will be seen that below 50 km the time step becomes critically small for a 24 hour interation. Figure 34 only defines the upper limit to Δt corresponding to $|\lambda \Delta t| = 1.0$, and it is necessary to determine the lower limit empirically. For the present investigation a time step of 30 sec was used for the period from dawn to sunset, while for the night two time steps were used, one of 240 sec for 80 to 60 km and one of 40 sec for 60 to 53 km. The lowest three layers were not considered at night since by the end of sunset, $\theta = 99^\circ$, there was insufficient O left to produce any change in the O_3 concentration.

The actual details of the calculations can now be discussed. For each time step during the day it was necessary to calculate the radiation terms $\alpha_2 q_2[O_2]$ and $\alpha_3 q_3[O_3]$, where the $\alpha_i q_i$ were the sums taken over all the wavelength intervals of interest. The O_2 absorption term was dealt with as before using the analytic method given by Craig (1950). In the case of the O_3 absorption the term $\alpha_3 q_3[O_3]$ involved the variable $[O_3]$ which was being integrated,

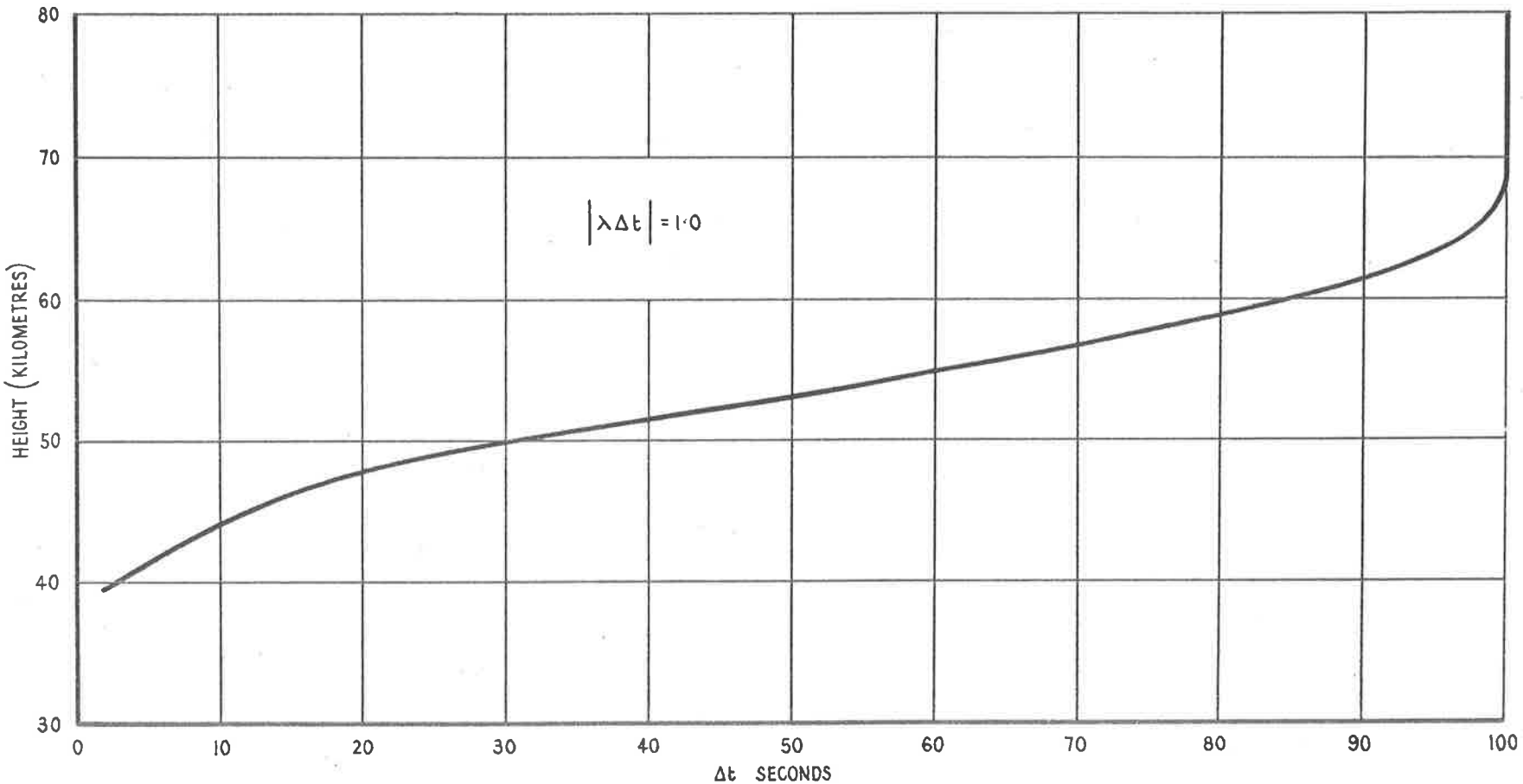

FIGURE 34. THE VARIATION OF THE INTEGRATION TIME STEP WITH ALTITUDE.

hence strictly the whole term should be evaluated at each of the four points used in the Runge-Kutta routine. In practice this involved excessive computing time and also it was not necessary as neither $[O_3]$ nor q_3 varied noticeably during an integration step. The value of $\alpha_3 q_3$ was maintained constant for a given step, and was calculated using the value of $[O_3]$ at the beginning of the step with the value of q_3 corresponding to the zenith angle at the centre of the step as stated above. This procedure was found to be completely satisfactory in practice since $[O_3]$ only changed significantly at dawn or sunset when the collision terms predominated over the radiation terms. The collision terms were calculated for conditions at the centre of each layer, as the $[O_2]$ and $[M]$ vary with height and the rate constants k_2 and k_4 are temperature dependent.

Once the required time step for the Runge-Kutta routine was determined no trouble was experienced with the integration procedure, good stability being obtained at all times and uniform smooth variations in the $[O]$ and $[O_3]$ from one time step to the next. Integration began at noon and proceeded until after 24 hours noon was again reached. As was expected the initial equilibrium values of $[O]$ and $[O_3]$ were not obtained, and it was necessary to repeat the integration using the new values until a stable state was reached in which the values of $[O]$ and $[O_3]$ for a given time one day were the same as those for the same time on the preceeding day. It was found that the lower layers rapidly stabilized while the top layers required several 24 hour iterations to attain a steady state.

4.5 Presentation and discussion of results

4.5.1 The departure from photochemical equilibrium in the mesosphere

The principal result obtained from the present investigation was that photochemical equilibrium concentrations are not obtained for vertical O and O_3 distributions in the atmosphere above 60 km, in agreement with Leovy (1964). The extent of the departure of the O and O_3 concentrations from their equilibrium values, which is due to photochemical effects alone, is shown in figure 35 where equilibrium and non-equilibrium values are compared for conditions at noon, $\theta = 0^0$. Complete photochemical distributions are given for the altitude range 10 to 80 km in figure 35 and subsequent figures in order to indicate fully the extent of the variations in the concentrations, regardless of the known departure from equilibrium below about 35 km due to atmospheric effects. From figure 35 it is apparent that above 60 km the atmosphere does not have sufficient time after dawn to achieve equilibrium concentrations by noon, and that the departure

from equilibrium increases with altitude, reaching nearly one order of magnitude for both the O and O_3 concentrations at 80 km. It should be noticed that there is a secondary maximum in the O distribution around 70 km arising from the breakdown at dawn of the secondary O_3 maximum which is formed at this altitude during the night. Later in the afternoon this secondary O maximum virtually disappears and the more "normal" monotonic O increase with altitude is observed.

The departure of the O and O_3 concentrations from equilibrium results from the effects that the rates of reactions R2, R4 and R5 have on these concentrations in the radiation free time at night. When equilibrium concentrations are used as the initial values for these reactions the reaction rates are about an order of magnitude greater than those for non-equilibrium concentrations above 70 km. Now reactions R4 and R5 both lead to the disappearance of two "odd" forms of oxygen (O or O_3), and the initial equilibrium concentrations are sufficiently high to permit these reactions to proceed at such a rate that the number of odd forms of oxygen which are consumed cannot be made up during the daylight hours. The only reaction which leads to additional odd forms of oxygen is the dissociation of O_2, reaction R1, and this proceeds too slowly (10^{-8} sec^{-1} per unit concentration at 80 km) to be able to make up the deficiency above 60 km in the time available. Below 60 km the situation is slightly different as the O concentration is too low to permit any significant reduction in the number of odd forms of oxygen overnight. The extent of the consumption of these odd forms of oxygen for the various altitudes is shown in figure 36 for non-equilibrium conditions. The numbers of odd forms of oxygen are plotted for conditions existing for $\theta = 90^{\circ}$ in the afternoon, just before the night O_3 increase commences, and for $\theta = -99^{\circ}$ in the morning, just before the dawn breakdown of the O_3 concentration. The figure indicates the number of odd forms of oxygen which have to be produced during the day at the various levels so that the given values at sunset will be attained. This value is a maximum around 75 km, as this is the altitude at which the sum of the rates of reactions R4 and R5 is a maximum when integrated over the whole night. Below 75 km the rapid reduction in the O concentration causes this combined rate to diminish with decreasing height. Above 75 km the combined rate falls off because of the smaller O_3 concentration, and also because the lower pressure reduces the rate of the three body reactions. Only above 75 km is reaction R5 more important than R4 and this is true only for the initial period of the night, before the O concentration undergoes any appreciable reduction.

The importance of the characteristic time, τ_1, for O can

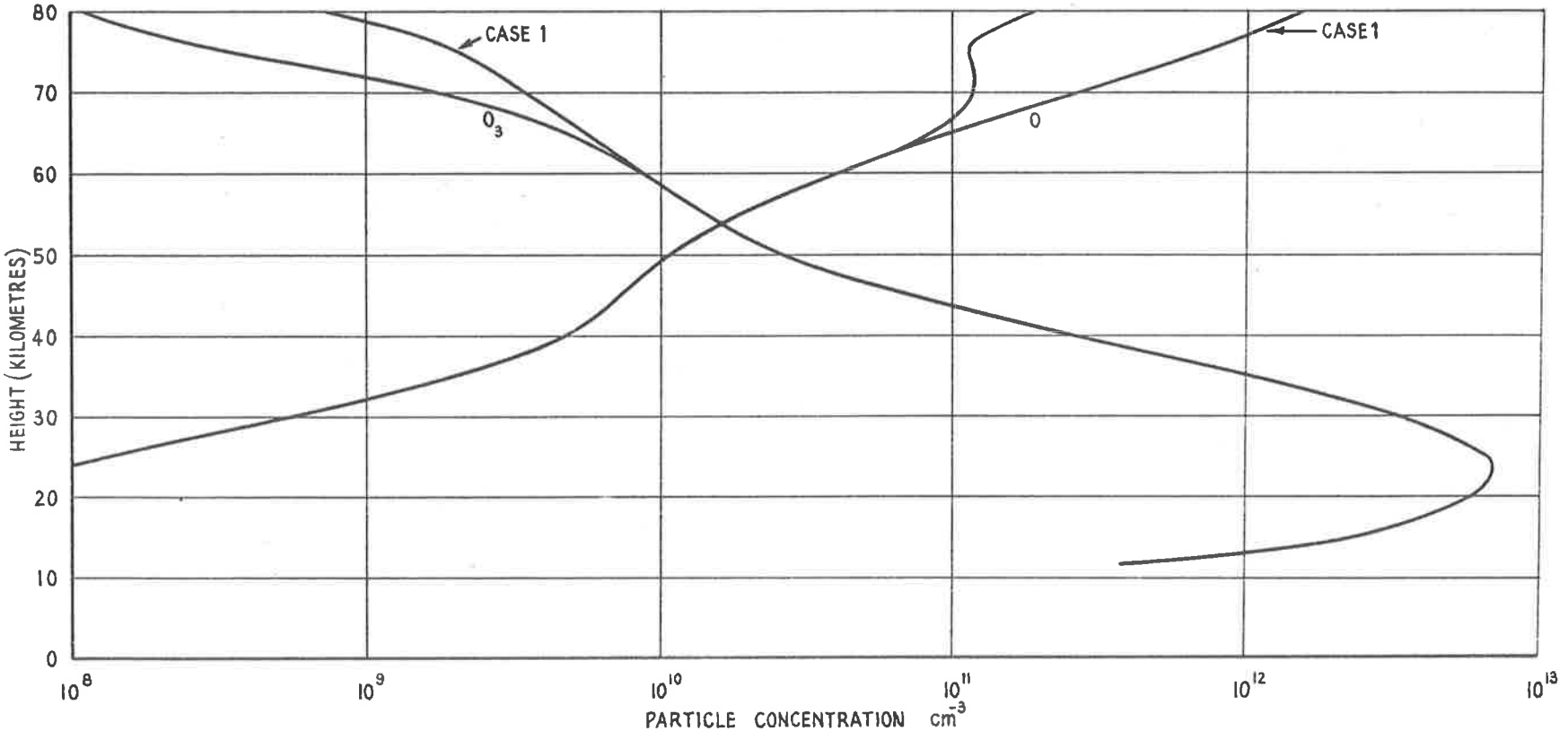

FIGURE 35. COMPARISON OF EQUILIBRIUM, CASE I, AND NON-EQUILIBRIUM OZONE AND ATOMIC OXYGEN CONCENTRATIONS AT NOON.

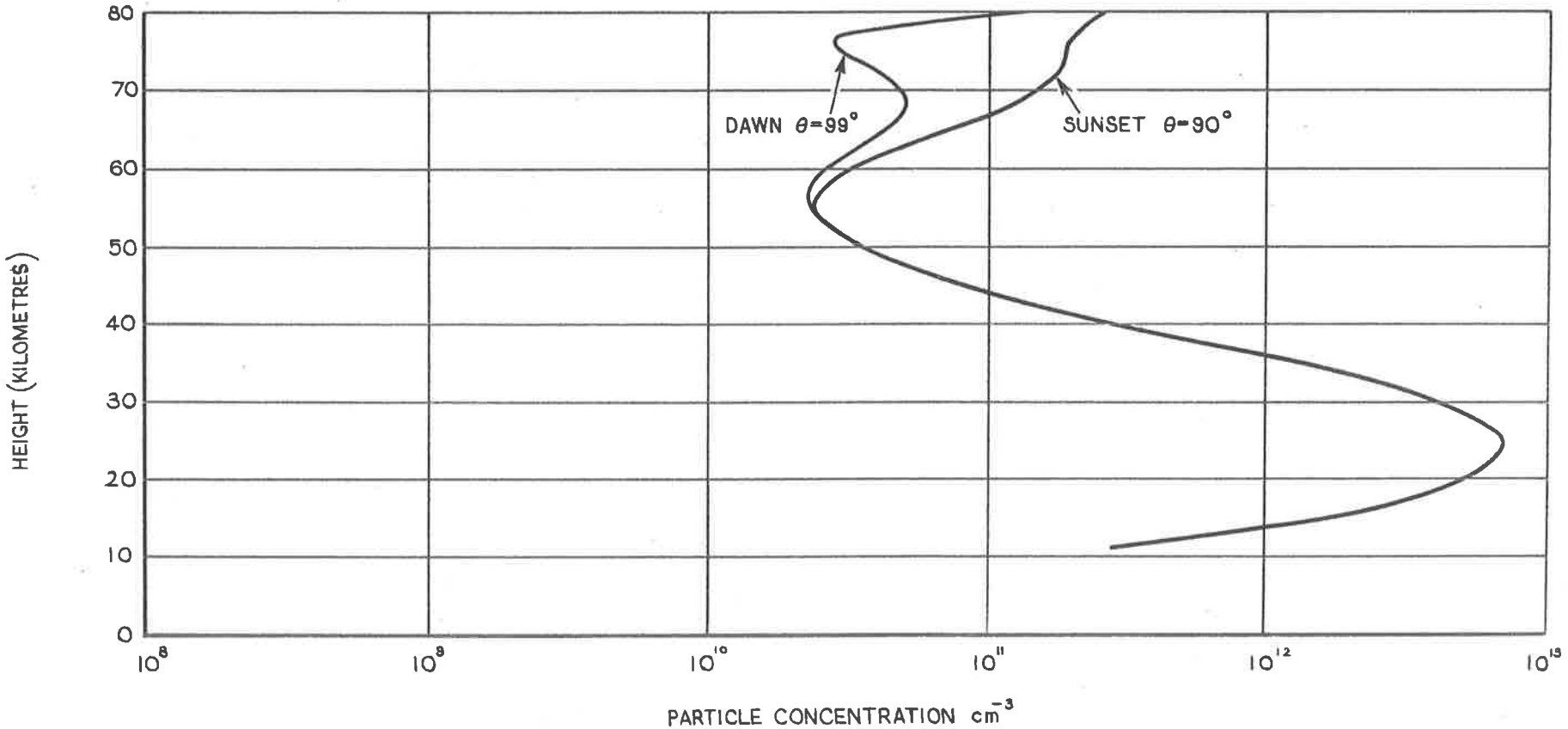

FIGURE 36. THE DECREASE IN THE TOTAL NUMBER OF ODD FORMS OF OXYGEN ($O + O_3$) BETWEEN SUNSET AND DAWN.

now be more fully understood following the above discussion. The departure from photochemical equilibrium arises simply because τ_1 is of the order 10^5 sec at 80 km and therefore there is insufficient time for the O to recover its equilibrium concentration following the losses suffered during the night. This low O concentration in turn results in a low O_3 concentration, as the rate of formation of O_3 is directly proportional to the O concentration.

Another consequence of the large value of τ_1 in the mesosphere and above is that atmospheric motions can also result in non-equilibrium concentrations. Nicolet and Mange (1954) have shown that O concentrations greater than those predicted by photochemical equilibrium theory are to be expected above 70 km in the atmosphere because of mixing and downward diffusion. However, for the purposes of the present study it was assumed that the atmosphere was at rest and that no transport mechanisms were operating.

4.5.2 The diurnal variation of atomic oxygen and ozone in the mesosphere

The diurnal variation of O and O_3 for several heights in the atmosphere is shown in figure 37, while profiles of O and O_3 are given in figure 38 for dawn, noon and sunset. For the purposes of the present discussion dawn is defined as the time solar radiation first reaches the top layer under consideration (77.5-80 km), and sunset as the time this radiation is first cut-off from the top layer; these times are respectively 36 minutes before and after these events occur at the surface. At dawn the O_3 concentration is a maximum throughout the height range while the O concentration is a minimum, below 70 km it is in fact zero. With the onset of solar radiation, which is capable of dissociating O_3 only for about the first 20 minutes after dawn (the shorter wavelengths are still completely absorbed) very rapid changes take place in the O and O_3 concentrations. These changes of course occur first for the upper layers, as can be seen from figure 37, the most marked effect being a reduction of over two orders of magnitude in the O_3 concentration in the top layer in 30 minutes. The changes at the lower levels become progressively smaller so that for a height of 48 km only a minor effect is discernible. The dissociation of the O_3 at dawn completely destroys the build up which has taken place in the preceding 24 hours, and results in the minimum O_3 concentration for the day. The dissociation of the O_3 causes very little change in the number of "odd" forms of oxygen ($O + O_3$) at any level, see figure 37, as except for the upper layers, no appreciable quantity of these odd forms of oxygen is consumed by the collision reactions R4 and R5.

After the marked dawn variations there follows a steady build up in both the O and O_3 concentrations for all levels until noon, as is apparent from figure 37. Below 60 km this build up ceases at noon as equilibrium values are attained, see figure 35. The intensity of the solar radiation reaching the layers under consideration starts to decrease after noon because of the increased absorption through the longer atmospheric path-lengths. Below 60 km a corresponding reduction is observed in the O and O_3 concentrations following the decrease in the rate of dissociation of O_2, but above 60 km the O and O_3 values continue to increase because they are below their equilibrium values. In fact for the top layer considered the O concentration continues to increase until sunset when the O_3 build up commences. The sunset value shows an increase of a factor of 4 over the dawn value, indicating that the O concentration above about 75 km persists essentially unchanged during the night.

At sunset large changes occur in the concentrations of both gases as shown in figure 37, the O_3 concentration increasing at the expense of the O concentration once the sun's dissociating radiation is absent. The order of the changes are very nearly the same as those at dawn although they are not quite so rapid. At the lower levels the O is almost completely converted to O_3 and a steady state is attained in about an hour. The O and O_3 concentrations at sunset are shown in figure 38 from which it can be seen that a secondary ozone maximum has appeared at 65 km. This secondary maximum appears at this level because the net rate of formation of O_3 is a maximum in this region during the sunset period, as the intensity of the sun's radiation is much less than that for the upper layers, and also the rate of reaction R2 is faster due the higher pressure. However, because of the higher pressure at the lower levels, the higher rate of reaction R2 soon leads to depletion of the O supply and therefore to the attainment of a steady state at these levels. The secondary O_3 maximum appears ultimately at about 70 km because of the larger O supply. It cannot occur at higher levels because the rates of reaction R2 and R4 become of the same order soon after sunset so that the net rate of O_3 formation is very low. Although above 70 km the O_3 build up continues throughout the night it is essentially complete even for the top layer within an hour of sunset. The final O and O_3 profiles at dawn are given in figure 38 from which it should be noted that above 78 km the O concentration is still larger than the O_3 concentration. The cycle then repeats itself for the next 24 hours.

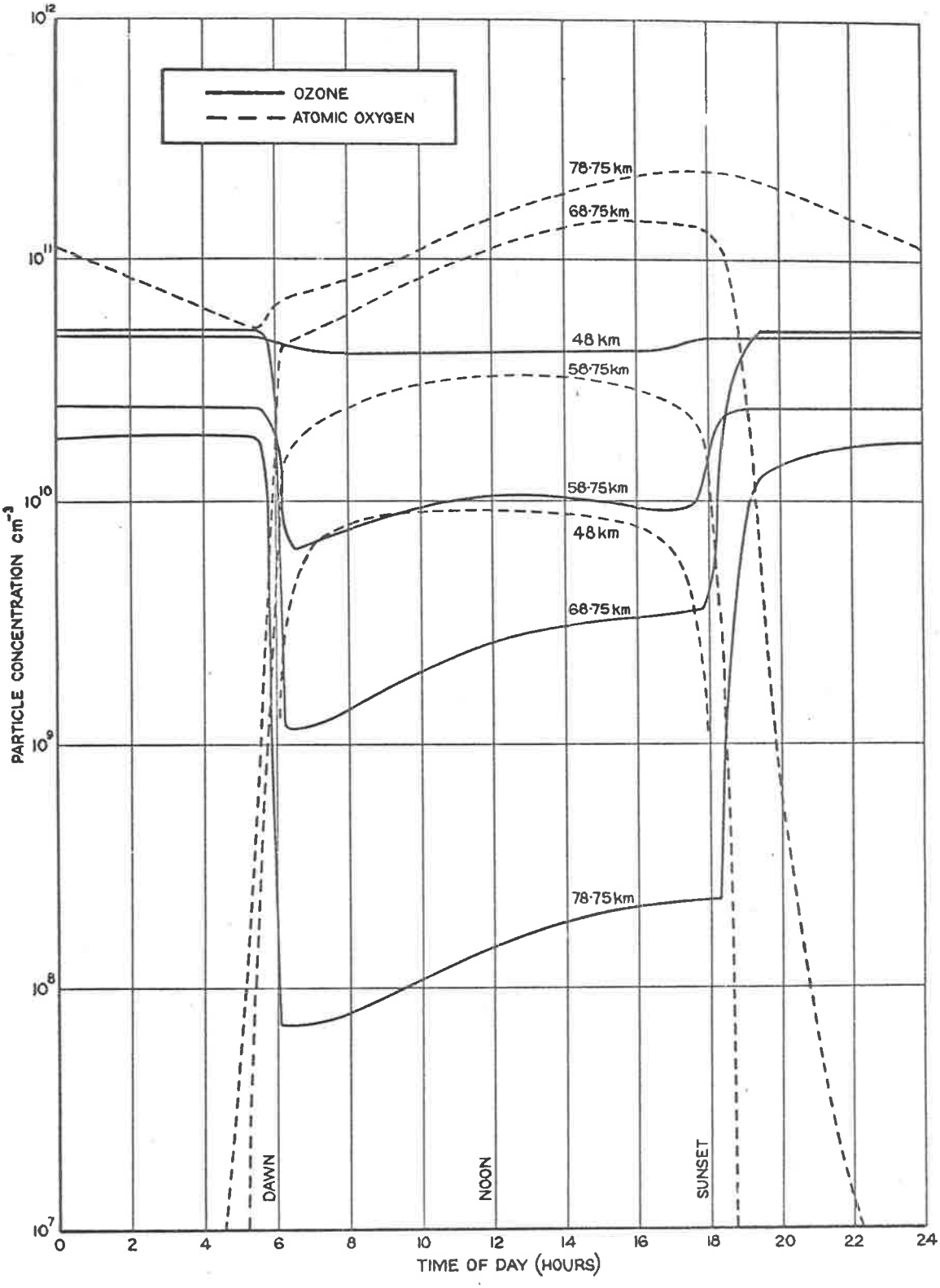

FIGURE 37. THE DIURNAL VARIATION OF ATOMIC OXYGEN AND OZONE AT DIFFERENT LEVELS IN THE ATMOSPHERE

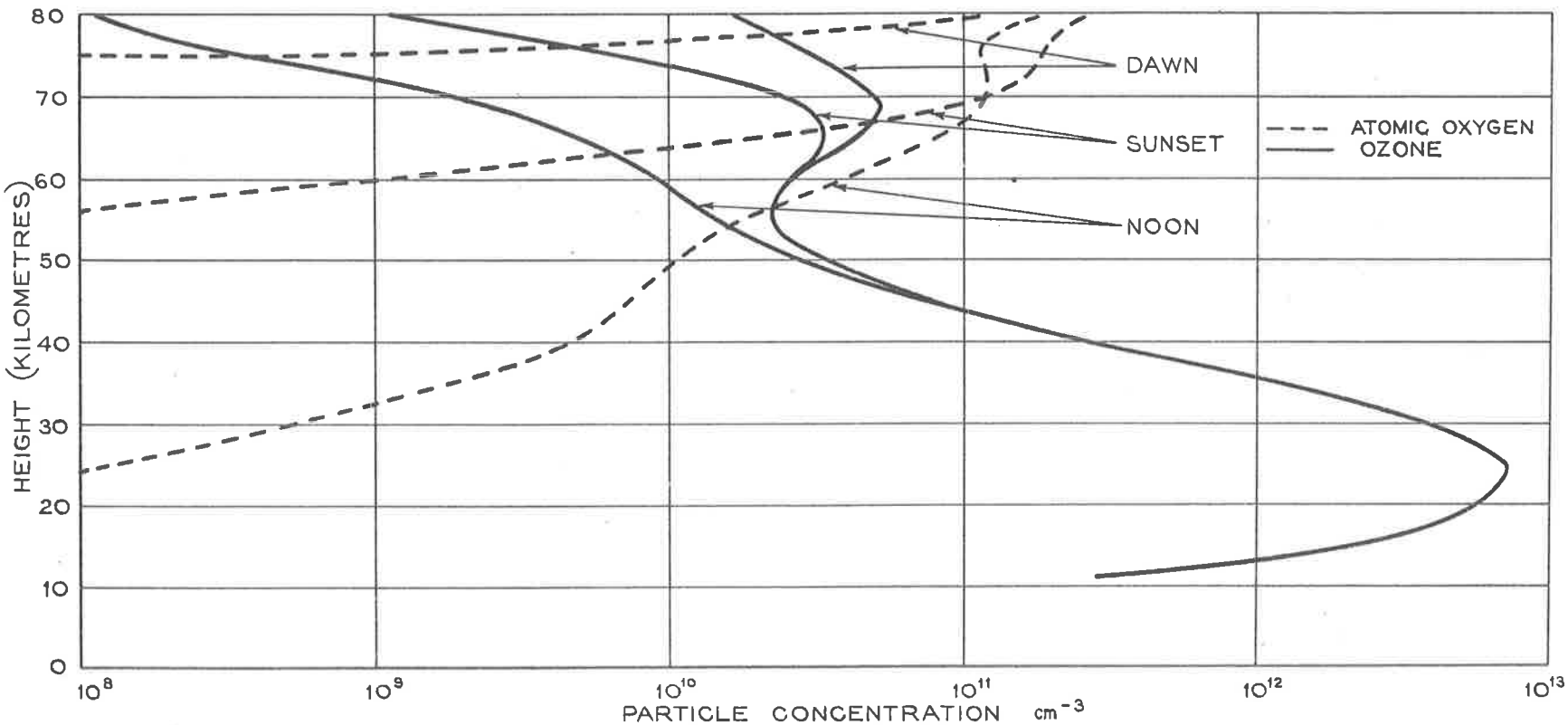

FIGURE 38. ATOMIC OXYGEN AND OZONE PROFILES AT DAWN, NOON AND SUNSET.

4.5.3 The diurnal photochemical total ozone variation

It is apparent from the previous discussion that there will be a variation in the total O_3 amount of the atmosphere due to the photochemical effects, regardless of any variation due to meteorological factors. The diurnal photochemical O_3 change is shown in figure 39 from which it can be seen that a decrease of 0.0031 cm S.T.P. occurs in the total O_3 amount at dawn which is followed by an increase of 0.0002 cm S.T.P. during the day, and a sudden increase of 0.0028 cm S.T.P. at sunset. The minimum total O_3 amount occurs just after dawn at the surface and the maximum at about midnight.

Since the range of the total O_3 change due to photochemical effects is only 0.0031 cm S.T.P. it seems unlikely that it could be observed from the surface, even at the equator where it would represent the biggest percentage variation of the total O_3 amount. Taking a total O_3 amount of 0.25 cm S.T.P. as being representative of the atmospheric O_3 content at the equator, it is seen that the photochemical variation represents a departure of only 1.2% from the total amount, while the quoted accuracy for the standard measuring instrument, the Dobson spectro-photometer, is only 2% (Dobson, 1957). Since the results presented here are for an oxygen atmosphere it is likely that they represent an upper limit for the variation of the total O_3 amount, hence in practice a departure of less than 1.2% may be expected. Night-time total O_3 measurements using the moon as a light source (Ramanathan et al., 1961), indicate total O_3 increases of between 0.015 cm and 0.069 cm S.T.P. depending on the wavelengths used for the observations. However, when the difference method (Dobson, 1957) was used it was found that there was no significant systematic increase of O_3 during the night. Such a result is predictable from figure 39 where it is apparent that within about 30 minutes of sunset at the surface no significant increase in the total O_3 amount will occur, and all one can expect to observe is the day to night change. It is conceded however that the inclusion of reactions involving atomic hydrogen would be expected to effect the results reported here, in particular the magnitude of the night-time photochemical total O_3 increase might be reduced. In spite of this it is concluded that no measurable change in the total O_3 amount should be observable during the day due to photochemical reactions, and that the day to night O_3 change can probably only be determined on a statistical basis.

There appears to be no support, as far as photochemical effects are concerned, for a reduction in the total O_3 amount around noon as observed by Khalek and Vassy (1952).

4.5.4 Latitudinal and seasonal effects

The results discussed in the previous sections are valid for the equator at the time of the equinox, and it is of interest to consider the effect of seasonal and latitudinal variations on these results. The height range under consideration is still limited to that of 48 to 80 km.

Now, for any one station, there are two effects to consider, one, the variation of the temperature profile of the atmosphere, and, two, the variation of the solar zenith angle. The effect of varying the atmospheric temperature profile has been discussed previously in Section 3.4.8, where it was concluded that apart from high latitudes essentially the same photochemical O_3 profiles could be expected for all latitudes and seasons between about 35 and 60 km. For latitudes within 35° of the equator the measurements of Nordberg and Stroud (1961) have shown that there are temperature variations from the mean temperature profile which reach a maximum at 80 km of ± 30°K, although these variations do not show any systematic pattern. Since the results presented in Section 3.4.8 indicate that a 50°K rise in the 1959 ARDC atmosphere at 80 km produces very minor changes in the O_3 and O concentrations, it follows that temperature variations of the order reported by Nordberg and Stroud will have a negligible effect on the results presented here for latitudes within 35° of the equator.

At high latitudes (65°) Nordberg and Stroud found that the mesospheric temperatures are higher in winter than summer by about 70°K at 80 km. The effect of the higher temperatures in the winter will be to reduce the O and O_3 concentrations compared to the summer because of the increase in the rate of reaction R4; the formation of O_3 will also be slower due to the reduced pressure at these levels in the winter. The faster rate of reaction R4 in the winter will lead to an increase in the number of odd forms of oxygen which are consumed during the night, and therefore to a more marked departure from photochemical equilibrium. This should also lead to a slightly smaller diurnal variation of the total O_3. Hence it would appear that variations in the mesospheric temperatures at high latitudes, unlike those at low latitudes, will have an effect on the results of Sections 4.5.1 to 4.5.3. Nordberg and Stroud (1961) have also found that a diurnal temperature variation of 5-10°K at 50 km exists at high latitudes, but such a variation is unimportant as far as the diurnal variation of the O_3 and O is concerned.

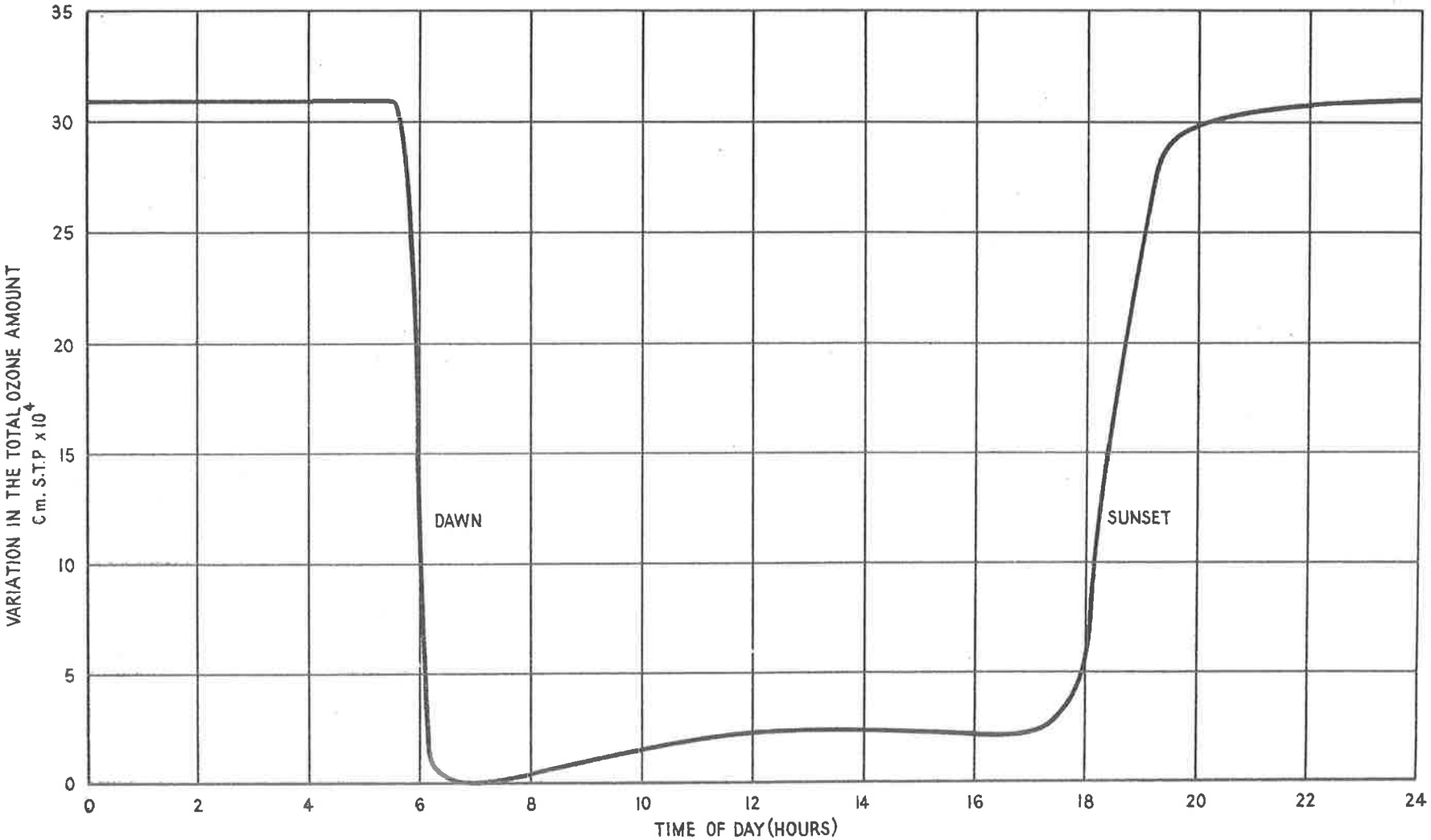

FIGURE 39. THE VARIATION IN THE TOTAL OZONE AMOUNT DUE TO PHOTOCHEMICAL EFFECTS.

Seasonal and latitudinal variations of the solar zenith angle would however be expected to be more important than temperature variations, particularly for the polar regions. One important effect is that the departure from equilibrium will be more marked in the upper layers for high latitudes due to the change in the relative lengths of day and night. This will occur since at night more time is available in the winter for the collision reactions, and a closer approach to complete exhaustion of the O supply above 75 km would be expected. As less time will also be available during the day for equilibrium to be approached, and the intensity of the solar radiation will be more attenuated because of the larger zenith angles, this will result in the departure from photochemical equilibrium being accentuated. The limit is set by the complete exhaustion of the O supply in the mesosphere, and, as Wallace (1962) has observed, it is difficult to see how any O could remain in the mesosphere during the polar night as far as photochemical considerations are concerned. During the polar day it should be possible for the O and O_3 in the mesosphere to approach equilibrium concentrations. It therefore appears that for latitudes within 35^{o} of the equator the results presented here will be essentially unchanged, while for higher latitudes more marked departures from photochemical equilibrium in the mesosphere are to be expected, with the extreme effects occurring in the polar regions as would be expected. However, in the actual atmosphere there are reasons to suggest that transport of O into the mesosphere occurs during the polar night by means of meridional circulations (Young and Epstein, 1962), so that the photochemically predicted state will not be achieved in practice.

4.6 Conclusions

The investigation presented in this chapter has demonstrated that the widely held and much used assumption that photochemical equilibrium O_3 and O concentrations are attained above 35 km in the atmosphere is not valid. Although the departure from equilibrium is only appreciable above about 70 km it is nevertheless an effect which needs to be taken into account, for example in atmospheric heating calculations and also airglow studies involving O_3. It appears fairly conclusive that ground based observations of the nocturnal O_3 increase are unlikely to be feasible, but rocket measurements of the O_3 profile in the mesosphere at night should be more rewarding, and would be of great value in determining the influence of atomic hydrogen on the O_3 concentration at these levels. It must be emphasized that the incorporation of reactions involving H and the additional reactions discussed in Chapter 6 are likely to alter the overall order of magnitude of the O_3 and O

changes given here, but the essential form of the diurnal variation should be unaffected.

The study of the O_3 and O changes by means of numerical integration of the governing differential equations provides a technique of considerable use in the atmospheric studies. Thus Leovy (1964) has used such a method to derive atmospheric temperature profiles for circulation studies. Another example of the use of this technique is presented in Chapter 5 where the effects of a solar eclipse on the ozonosphere are studied. In the future 24 hour integrations of differential equations governing the variations of atmospheric constituents will undoubtedly provide much interesting information.

CHAPTER 5

A THEORETICAL STUDY OF THE CHANGES OCCURRING IN THE OZONOSPHERE DURING A TOTAL ECLIPSE OF THE SUN

5.1 Introduction

It is well known that an eclipse of the sun results in marked changes in the state of the upper atmosphere, particularly in the ionosphere where the changes can be studied easily by means of radio waves. At lower heights a solar eclipse also affects the ozonosphere, where it is found that an increase occurs in the total ozone content in a vertical column of the atmosphere. There have been several reported studies of this effect, the most recent and best documented of which are the observations of Stranz (1961). Stranz, working from the Belgian Congo latitude 2°S, measured an increase of about 4% in the total ozone amount shortly after the maximum phase of an eclipse, in which only about 80% of totality was reached. Qualitatively it can be seen, from a knowledge of the diurnal photochemical atmospheric ozone variation and a study of the equations controlling the ozone concentration in the atmosphere, that an increase in the ozone concentration should occur above about 40 km as a result of a solar eclipse. However only about 1% of the total ozone amount is present above 40 km in the atmosphere, hence the experimental results indicate that a four-fold increase takes place in the total ozone content above 40 km during a solar eclipse. Such an increase can be easily shown to be physically impossible and the question therefore arises as to what actually happens to the ozone concentration during an eclipse, and what is the cause of the apparent ozone increase observed experimentally. For these reasons it was thought that a theoretical study of the ozone variation during a solar eclipse might help to resolve these paradoxes, especially as no such study appears to have been made previously. The present investigation shows that theoretically an ozone increase of only about 1% is to be expected during a solar eclipse, and reasons are advanced to explain the difference between theory and experiment.

5.2 Numerical methods

5.2.1 General details

The same reaction scheme, R1 to R5, and the same data as for Chapter 4 were used in the present study. Since only daytime conditions were of interest only equations E1 and E2 (p. 16) were considered. The details of the actual numerical procedures were identical to those developed for the diurnal study, except that the radiation terms had to be modified to allow for the variation of the intensity of the solar radiation reaching the atmosphere caused by the occultation of the sun by the moon during the eclipse. The initial

values of the O and O_3 concentrations required for the integration routine were also taken from the diurnal study, and corresponded to the non-equilibrium concentrations attained at noon at the equator for an overhead sun.

The time of the eclipse from first contact to fourth contact was taken as 9000 seconds, and at the instant of totality at 4500 seconds it was assumed that no solar radiation reached the earth. This is not strictly true in practice because of the existence of the corona around the sun, but since the intensity of the corona at the sun's limb is only 10^{-6} of the intensity at the sun's centre its presence was completely ignored throughout the investigation. For convenience the eclipse was considered to start at noon and during its course allowance was made for the variation of the zenith angle of the sun. After the completion of the eclipse the integration was continued in order to determine how long the atmosphere required to attain its normal O_3 and O concentrations. The time step for the integration routine was taken as 30 seconds, the same as that for the diurnal study, and was maintained constant with height, an empirical check being made to determine if truncation errors or other inaccuracies were present.

Two cases were considered in this study, a preliminary investigation in which no allowance was made for limb darkening of the sun, and the more realistic case in which allowance was made for limb darkening. Since the methods used to represent the variations in the solar intensity reaching the earth's atmosphere were basically different they will be discussed separately for convenience in the following sections.

5.2.2 The variation of the radiation term assuming no limb darkening

When the limb darkening of the sun is neglected the variation of the intensity of the sun's radiation reaching the earth is then directly proportional to the unocculted area of the sun, and can be defined in terms of the angle θ in figure 40.

Taking the apparent radii of the sun and moon equal to R we see that the occulted area, A_c, is given by

$$A_c = R^2 [\theta^c - \sin \theta]$$

and if $$A_o = \pi R^2$$

then $$A_\theta = A_o - A_c = R^2 [\pi - \theta^c + \sin \theta]$$

where A_θ is the unocculted area of the sun.

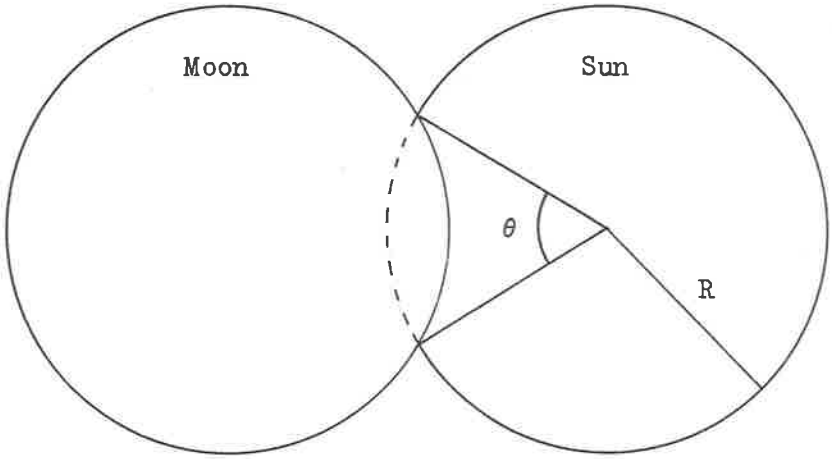

FIGURE 40. THE AREA REPRESENTATION OF THE SUN DURING AN ECLIPSE

If q_o is the radiation output of the sun corresponding to the area A_o then the radiation output q_θ is

$$q_\theta = q_o \frac{A_\theta}{A_o}$$

$$= q_o \left[\frac{\pi - \theta^c + \sin\theta}{\pi} \right] \qquad \text{E11}$$

Hence, by evaluating the coefficient of q_o in E11, the effective radiation output of the sun can be determined for any value of θ. It is necessary to relate θ to the integration time step Δt used with equations E1 and E2 in order to obtain the value of θ corresponding to a given time step. Taking $\theta = \theta_1$ at the beginning of the time step and $\theta = \theta_2$ at the end we can show that

$$\Delta t = 4500 \left[\cos\frac{\theta_1}{2} - \cos\frac{\theta_2}{2} \right] \text{ for } \theta_2 \leq \pi$$

where the value of θ required for equation E11 is given by $\theta = \frac{\theta_1 + \theta_2}{2}$. θ_2 attains its maximum value of π at 2nd contact. By putting $\theta_1 = \theta_2$ the new value of θ_2 at the end of the succeeding time step may be evaluated. In this manner, for the case with no limb darkening, the variation of the sun's effective radiation output during the eclipse was determined, and incorporated into equations E1 and E2 in order to determine the changes occurring in the O_3 and O concentrations during an eclipse.

5.2.3 The variation of the radiation term allowing for limb darkening

Limb darkening of the sun results from the effective radiation temperature of the sun decreasing towards the limb where the radiation is emitted from the cooler, outer layers of the sun. The radiation intensity for a given position on the sun is conventionally defined by the angle ψ as shown in figure 41. Hence we require to know the value of the radiation intensity $I(\psi)$ in order to allow for limb darkening. Values of $I(\psi)/I(0)$, where $I(0)$ is the intensity at the centre of the sun, have been given by Mitchell (1959) and Peyturaux (1955) for $\cos\psi$ values from 0.2 to 1.0 and for

various wavelengths down to about 3000Å. Their data, which are plotted in figure 42, have been extrapolated as indicated since wavelength data are required to 1800Å for the present study.

For a given wavelength Pierce and Waddell (1961) have shown that it is possible to represent the variation of $I(\psi)/I(0)$ with $\cos\psi$ by the following equation

$$\frac{I(\psi)}{I(0)} = a_\lambda + b_\lambda \mu + c_\lambda \left[1 - \mu \ln (1 + \mu^{-1}) \right] \qquad \text{E12}$$

where $\mu = \cos\psi$ and the coefficients a, b, c are functions of wavelength as indicated. This equation was convenient to use since it readily permitted the ratio $I(\psi)/I(0)$ to be calculated for the various values of ψ occurring in the representation of the eclipse. The values of the coefficients a, b, c were determined, for each of the 41 intervals used to represent the variation of the solar intensity with wavelength, by solving equation E12 for three different values of μ using data for $I(\psi)/I(0)$ taken from figure 42; the results are given in table 2. A check which was made for subsidiary values of μ revealed that this procedure gave results accurate to within 3 to 4%, which was considered to be satisfactory, the largest errors occurring for the shortest wavelengths.

It is necessary to relate the value of $I(0)$, the intensity at the centre of the sun, to that of F, the mean value of the intensity over the sun, as in the absence of any occultation of the sun the amount of radiation reaching the atmosphere for a given wavelength interval is given by F. The ratio $I(0)/F$ is plotted against wavelength in figure 43 from data given by Pierce (1959), below 3200Å it was again necessary to extrapolate the data as indicated. Because of the incorporation of limb darkening in the radiation terms in equations E1 and E2 the area representation given by equation E11 is no longer adequate and it is necessary to consider the surface area of the sun to consist of a number of annuli. The area of the sun was divided into 75 annuli corresponding to the time step of 30 seconds, which meant that an additional annulus had to be considered or neglected, depending on the extent of occultation, in each integration interval. For a given integration step the value of φ given in figure 44 was evaluated for each of the annuli which were occulted, the area of occultation being given by $\varphi\, r\, dr$.

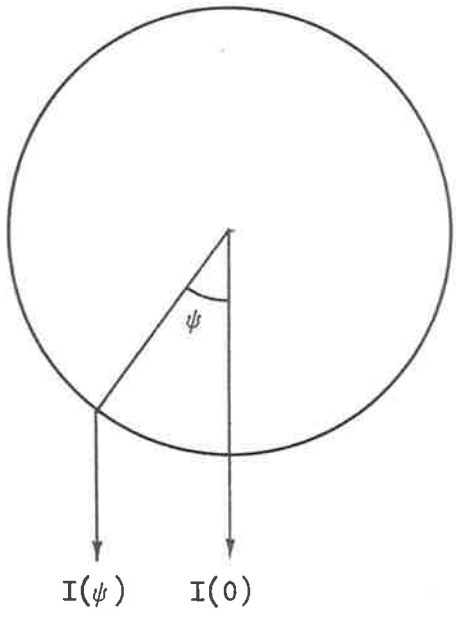

FIGURE 41. THE DEFINITION OF A POINT ON THE SUN'S SURFACE

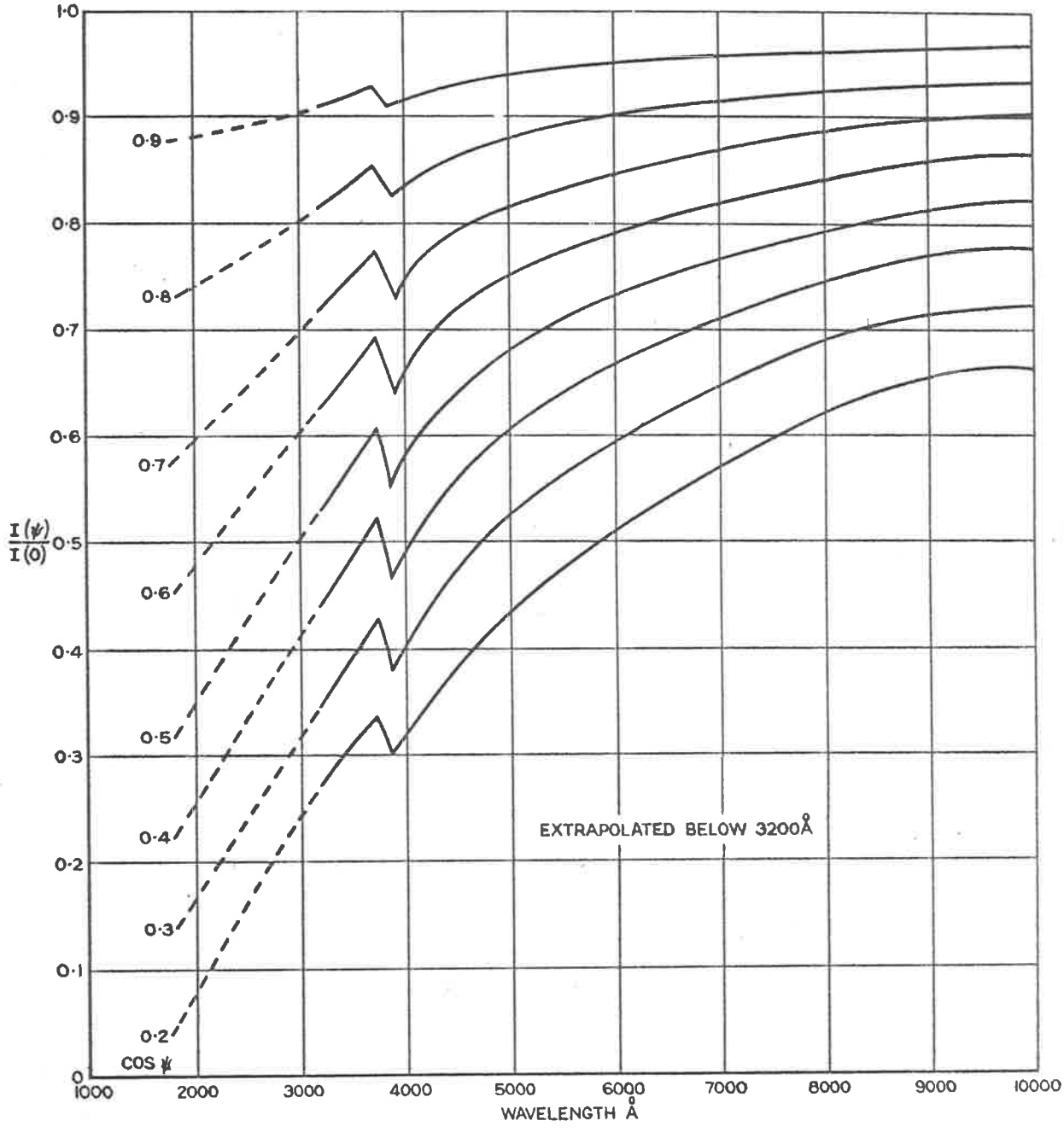

FIGURE 42. THE VARIATION OF $I(\psi)/I(0)$ WITH WAVELENGTH FOR DIFFERENT POSITIONS ON THE LIMB OF THE SUN

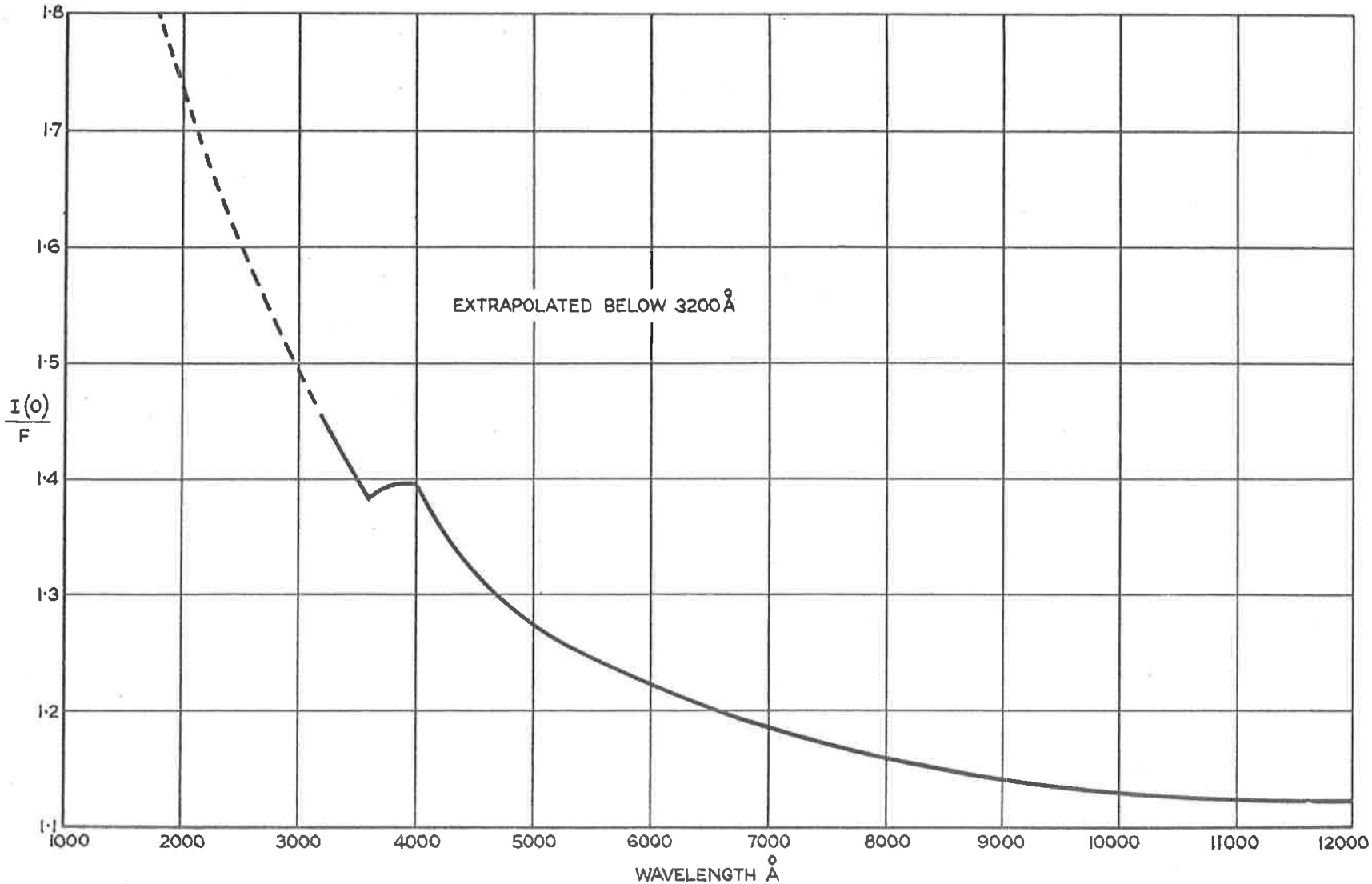

FIGURE 43. RATIO OF THE INTENSITY AT THE CENTRE OF THE SUN TO THE MEAN INTENSITY FOR VARIOUS WAVELENGTHS

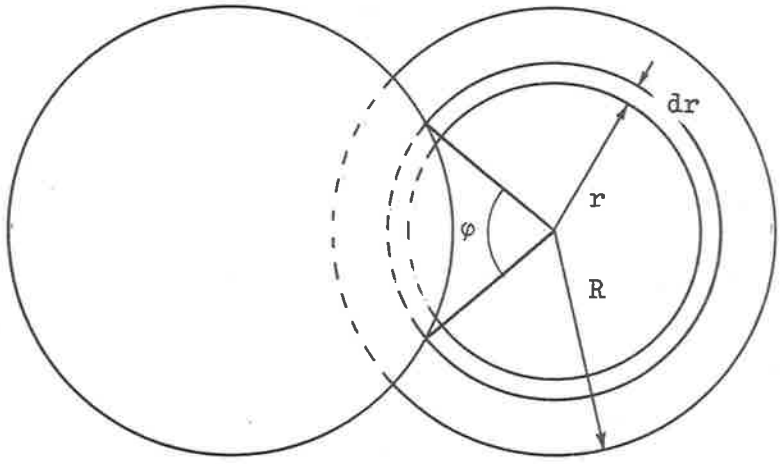

FIGURE 44. THE AREA REPRESENTATION OF THE SUN ALLOWING FOR LIMB DARKENING

TABLE 2

THE LIMB DARKENING COEFFICIENTS

a, b, c

λ	a	b	c
1800	-0.999	1.661	1.102
1850	-0.987	1.647	1.102
1900	-0.953	1.624	1.071
1950	-0.883	1.581	0.984
2000	-0.862	1.565	0.969
2050	-0.824	1.536	0.937
2100	-0.775	1.504	0.882
2150	-0.754	1.488	0.866
2200	-0.741	1.475	0.866
2250	-0.694	1.443	0.819
2300	-0.666	1.442	0.795
2350	-0.679	1.420	0.845
2400	-0.660	1.403	0.838
2450	-0.584	1.357	0.739
2500	-0.542	1.331	0.687
2550	-0.490	1.298	0.627
2600	-0.496	1.295	0.655
2650	-0.463	1.276	0.609
2700	-0.394	1.231	0.532
2750	-0.335	1.194	0.458
2800	-0.315	1.177	0.451
2850	-0.264	1.145	0.387
2900	-0.197	1.105	0.299
2950	-0.162	1.081	0.264
3000	-0.152	1.070	0.268
3050	-0.076	1.023	0.173
3100	-0.041	1.000	0.134
3150	0.011	0.968	0.070
3200	0.045	0.943	-0.039
3250	0.121	0.897	-0.060
3300	0.139	0.882	-0.070
3350	0.166	0.863	-0.095
3400	0.193	0.844	-0.120
3450	0.244	0.812	-0.183
3500	0.294	0.780	-0.242
4750	0.660	0.512	-0.560
5250	0.713	0.455	-0.546
5750	0.729	0.422	-0.493
6250	0.802	0.364	-0.542
6750	0.818	0.338	-0.507
7250	0.832	0.314	-0.475

The proportion of the mean value of the intensity, F, emitted by the occulted part of the annulus is then given by

$$I_c = \frac{\varphi \, r dr . I(\psi)}{\pi R^2 F}$$

where $$\frac{I(\psi)}{F} = \frac{I(\psi)}{I(0)} \cdot \frac{I(0)}{F}$$

The value of I_c was calculated for the radial centre of the annulus, r+dr/2, corresponding to conditions in the middle of the integration time step. Then, by summing I_c, for a given wavelength interval, over all the annuli occulted for the given time step the reduction in the radiation intensity for that wavelength interval was obtained. The net radiation intensity was that which was used in the integration of equations E1 and E2 in order to determine the changes in the O_3 and O concentrations for the time step. For the succeeding time step the number of annuli to be considered changed by one, all the values of φ altered and new values for I_c had to be calculated. By repeating this procedure the variation of the solar radiation intensity reaching the atmosphere during an eclipse was followed in time.

The numerical calculations were programmed for an IBM 7090 computer, the integration procedure used for equations E1 and E2, a four point Runge-Kutta routine, giving good stability and accuracy throughout the investigation.

5.3 Presentation and discussion of results

Only the results for the case in which limb darkening of the sun was considered will be presented here. The results were qualitatively very similar whether limb darkening was allowed for or neglected, but the magnitudes of the changes in the O_3 concentrations were slightly greater for the limb darkening case. The reasons for the similarity of the results will be discussed later.

5.3.1 The variation in the atomic oxygen and ozone profiles due to the eclipse

The increase in the concentration of O_3 and the corresponding decrease in that of O due to the eclipse are indicated in figure 45, where the concentrations existing just after totality are compared with the "normal" concentrations for the same time of day. The profiles are plotted for the time just after totality at which the increase in the total O_3 amount is a maximum, a very slight increase occurs in the

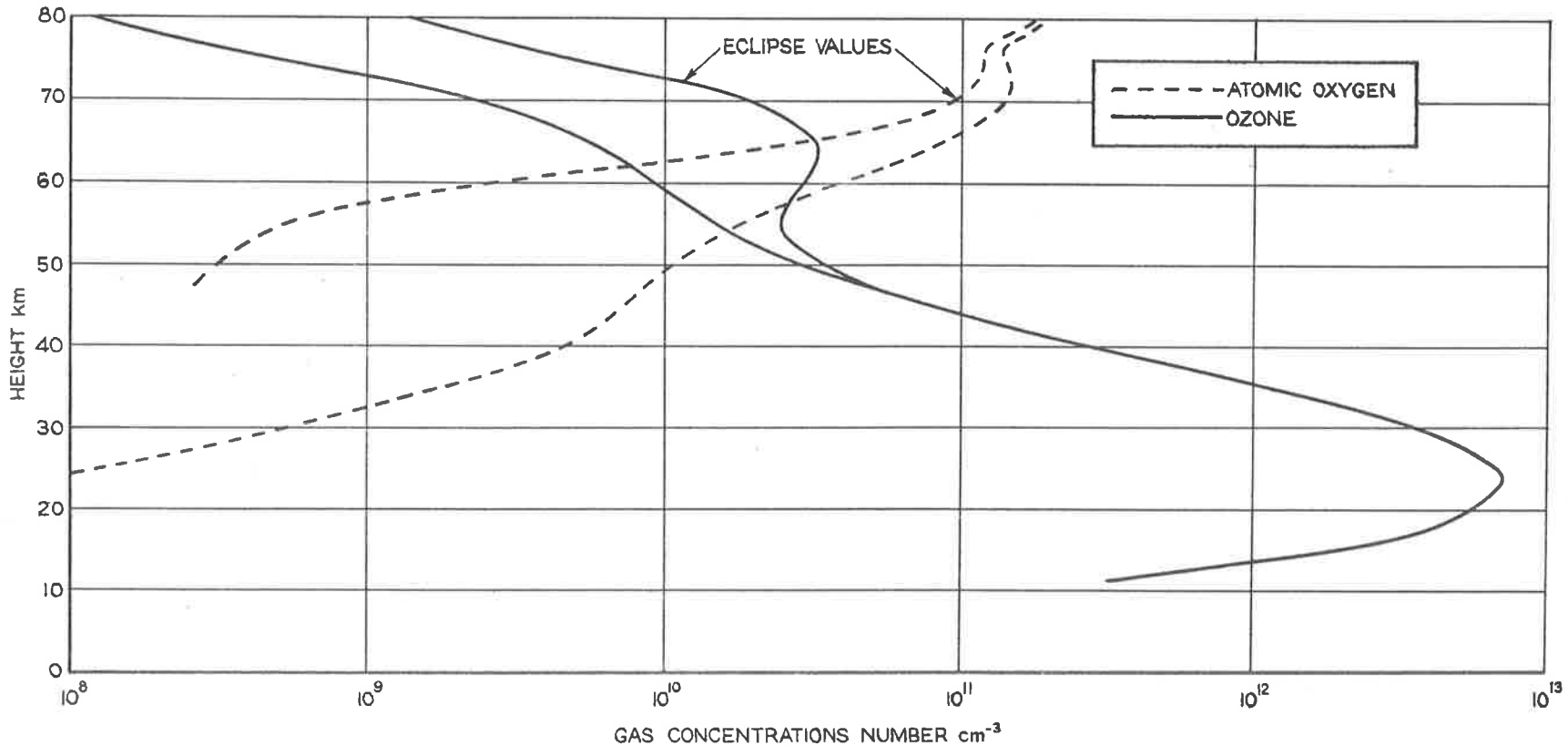

FIGURE 45. COMPARISON OF THE ATOMIC OXYGEN AND OZONE CONCENTRATIONS JUST AFTER TOTALITY OF THE ECLIPSE WITH THEIR NORMAL CONCENTRATIONS

O_3 concentration in the top two or three layers after this time with the maximum being attained three minutes later. Complete photochemical profiles are given in figure 45 in order to indicate more fully the extent of the changes occurring during the eclipse and their relative insignificance. There is a maximum increase of about one order of magnitude in the O_3 concentration above 70 km during the eclipse, but this increase falls off very rapidly with decreasing altitude, and below 45 km no change in the O_3 concentration can be expected. The variation of the O_3 concentration with time during the eclipse for several heights is shown in figure 46. The figure indicates the marked effect height has on the variation of the O_3 concentration and clearly shows the minor change which is obtained at 48 km. It should also be noted that the response of the ozonosphere to an eclipse varies with height, as might be expected, and that the maximum O_3 concentrations are obtained at different times for the various heights.

The increase in the O_3 concentration must obviously take place at the expense of the O concentration, and it can be seen from figure 45 that at all heights there is a reduction in its concentration which reaches over an order of magnitude at 60 km, and is even more accentuated at lower altitudes. Below 50 km the O concentration is much less than the O_3 concentration under normal conditions, hence even if all the O at these heights is converted to O_3 the percentage change in its concentration will be very small, and will rapidly approach zero with decreasing altitude. This is the reason why below 45 km the O_3 profile is not affected by the eclipse. At higher altitudes, above about 55 km, the concentration of O is greater than that of O_3 during the day, and relatively larger percentage changes can be expected in the O_3 concentration. However, at these heights the magnitude of the increase in the O_3 concentration is controlled by the losses caused by reaction R4 and not just by the rate of formation given by reaction R2. The O_3 concentration therefore does not attain the values which would be possible in the absence of reaction R4, and the resulting profile is that given by the net rate of O_3 formation. Above about 70 km, the O concentration remains essentially unchanged by the eclipse in spite of the large O_3 increase, since a very small change in the O concentration at these levels can produce a large change in the O_3 concentration because of the three orders of magnitude difference in their relative concentrations. The reason an increase occurs in the O_3 concentration during an eclipse is of course due to the reduction in the intensity

of the solar radiation reaching the atmosphere, which reduces the rate of dissociation of both O_2 and O_3 very markedly and allows the collision reactions to predominate as discussed above. In this respect the changes produced in the ozonosphere by an eclipse of the sun have many similarities to those produced by sunset where the same qualitative changes occur.

5.3.2 The variation of the total ozone amount during an eclipse

The theoretical increase in the total O_3 amount in a column of the atmosphere during an eclipse is perhaps the most interesting result of the present investigation, since experimental data are available for comparison. The calculated change in the total O_3 amount with time is given in figure 47, from which it can be seen that the maximum increase of 0.0016 cm S.T.P. is attained 4 830 seconds after the start of the eclipse, or 330 seconds after totality. The maximum occurs after totality rather than at totality, since the radiation intensity reaching the atmosphere takes several minutes to reach any significant level after third contact, and during this time the collision reactions continue to predominate. The rise in the O_3 content is very slow initially during the eclipse but increases as the percentage of the exposed area of the sun is reduced, after the maximum is attained there is a much more rapid decrease, the O_3 increase being reduced to zero in only 2 000 seconds compared with a build up time of 4 800 seconds. An interesting point is that the decrease in the O_3 content continues after the "normal" O_3 value for the corresponding time of day is reached, and a minimum occurs at about 8 500 seconds, or 500 seconds before fourth contact, when there is a "negative" value of 0.0002 cm S.T.P. The O_3 content then shows a small, steady increase back to the "normal" value, the restoration time being greater than two hours.

If we take a total O_3 value of 0.25 cm S.T.P. as being representative of the O_3 content at the equator, then the maximum percentage increase in the total O_3 amount during an eclipse will be 0.6%, using the data given in figure 47. This is considered to be significantly different from the value of 4% reported by Stranz (1961) for a similar total O_3 amount. Eclipse observations made by Fournier d'Albe and Rasool (1956) at the experimentally difficult time near sunset failed to reveal any noticeable change in the total O_3 amount, and they obtained only irregular and minor variations. Two eclipse observations have also been reported by Bezberkhny et al (1956) who appear to have recorded O_3 increases of between three and four times the

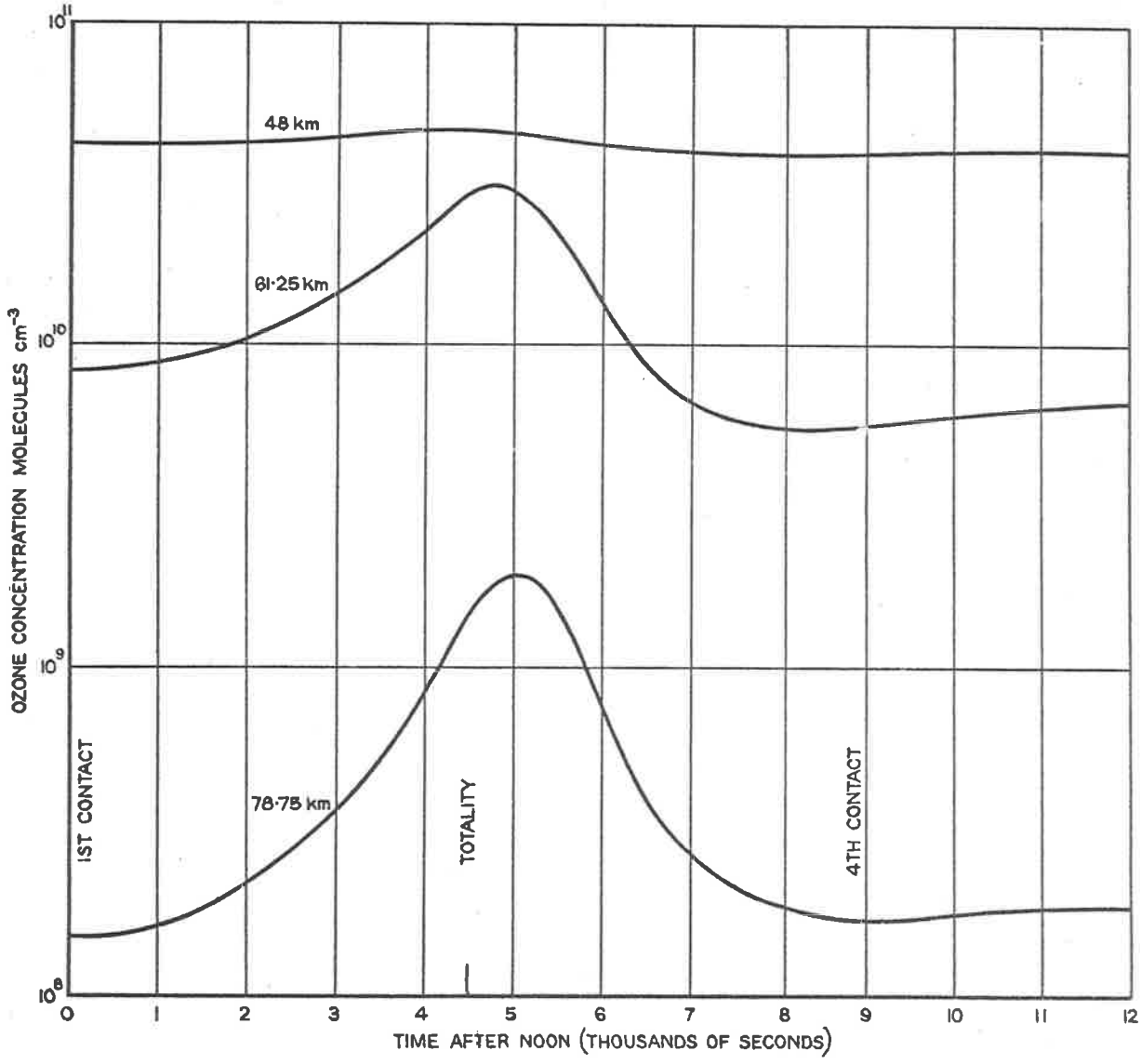

FIGURE 46. THE VARIATION OF THE OZONE CONCENTRATION AT VARIOUS ALTITUDES DURING AN ECLIPSE

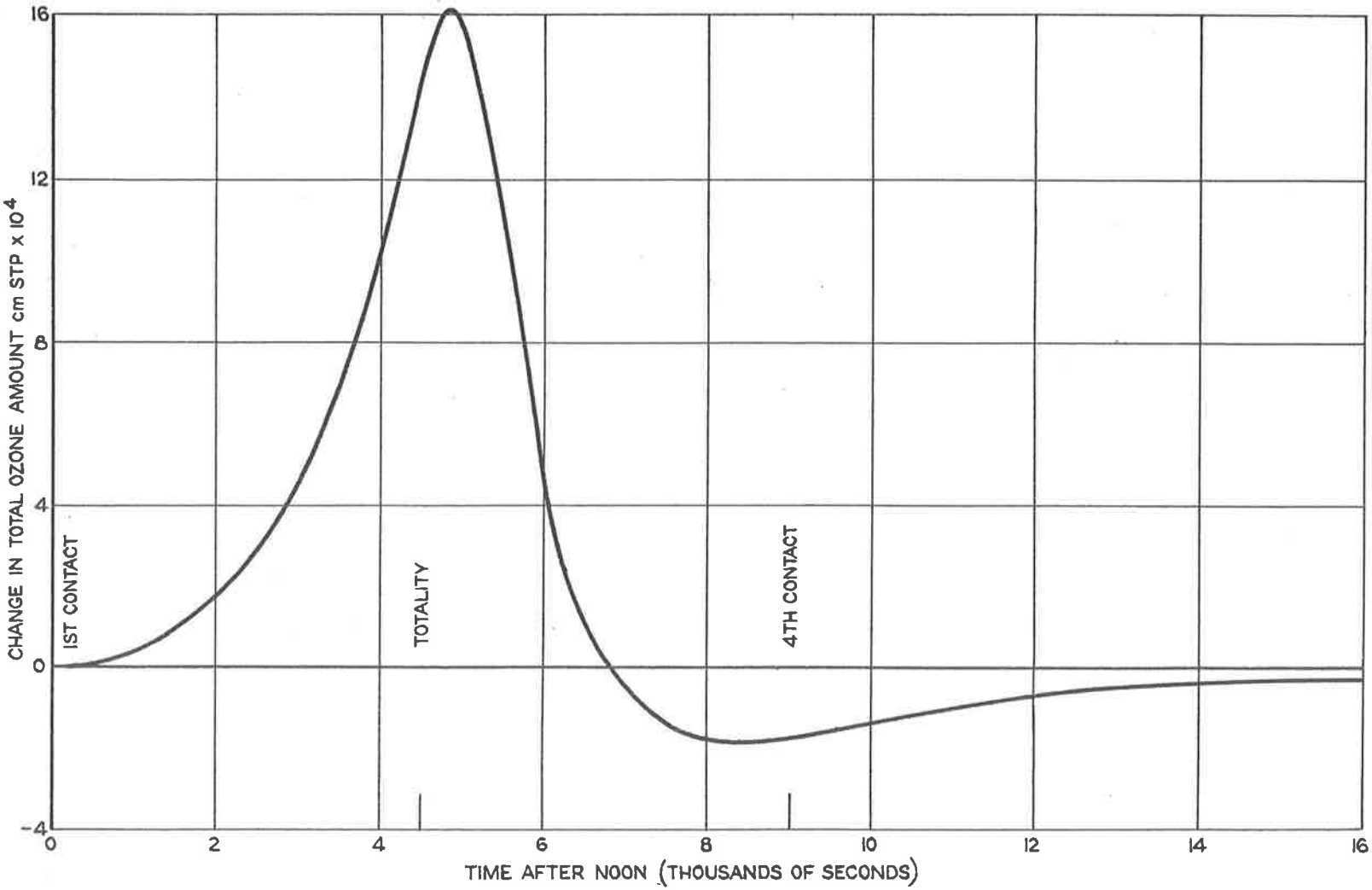

FIGURE 47. THE CHANGE IN THE TOTAL OZONE AMOUNT IN A COLUMN OF THE ATMOSPHERE DURING A SOLAR ECLIPSE

total O_3 amount, which are of course physically impossible and must presumably have been due to instrumental error. In other reported eclipse observations of O_3 in the atmosphere, discussed by Stranz (1961), slight decreases in the O_3 content seem to have occurred.

5.3.3 The reason for the discrepancy between the theoretical and experimental results

The difference between the theoretical increase in the total O_3 amount and that observed experimentally is most likely to be due to inadequacies in the Dobson spectrophotometer, which is the standard instrument used in O_3 observations. This instrument is designed to measure the ratio of two wavelengths, one centred at about 3000Å, the other at about 3300Å. The total O_3 amount in the atmosphere is obtained from the measured ratio using the following formula

$$\frac{I_1}{I_2} = \frac{I_{1,0}}{I_{2,0}} \exp\left[- (\alpha_1 - \alpha_2)\, \mu x - (\beta_1 - \beta_2)\, M \right]$$

where the various symbols have the meanings given on p.11.

Now in order to calculate the total ozone amount during an eclipse it is necessary to have a value of $I_{1,0}/I_{2,0}$, and it is normally assumed that this ratio remains constant and equal to its standard value, which is unlikely because of limb darkening of the sun. It is possible to obtain an estimate of the variation of this ratio during an eclipse using data derived as indicated in Section 5.2.3. Consider for example the "A" wavelength pair of the Dobson spectrophotometer for which the wavelengths corresponding to I_1 and I_2 are 3055Å and 3254Å respectively. Selecting the data for the nearest two 50Å wide intervals used in the present study, which are centred on 3050Å and 3250Å, the computer results indicate that at 3600 seconds the ratio of $I_{1,0}/I_{2,0}$ is 97.8% of its initial value, while at 4200 seconds it has fallen to 95.5%. By transposing the above equation it can be shown that the value of x is proportional to the difference of $I_{1,0}/I_{2,0}$ and I_1/I_2, hence any variation in the ratio of $I_{1,0}/I_{2,0}$ will affect the apparent value of x. Since this ratio decreases during an eclipse the incorporation of a limb darkening correction might be expected to reduce the value of x observed. On the spectrophotometer the wavelength intervals are only a few Angstrom units wide

for the various wavelength pairs, therefore the limb darkening results quoted above for the 50Å wide intervals will probably not be directly applicable for the "A" wavelength pair, but they should be correct as regards the fact that a reduction in $I_{1,o}/I_{2,o}$ is to be expected during an eclipse. The net result however should be to bring the theoretical and experimental results into better agreement, although the value of x which would be observed if the above corrections were incorporated is difficult to calculate because of the way the Dobson spectrophotometer data are analysed. It should be emphasized that if the theoretical results presented here are valid then no increase in the O_3 content of the atmosphere can be expected to be measured during an eclipse, because the theoretical increase of 0.6% is less then the quoted accuracy of 2% of the spectrophotometer.

Throughout this study the effect of the sun's corona has been neglected because of its low intensity, and although it is admitted that the corona would be important in determining the value of $I_{1,o}/I_{2,o}$ near totality, and therefore probably contributes to the discrepancy between theory and observation, its neglect is considered to be entirely justified despite the comments of Bezberkhny et al (1956). They state that because it can be shown the equilibrium O_3 concentration depends on the ratio of the amount of radiation absorbed by O_3 to that absorbed by O_2, then the radiation from the corona will be important because this ratio is large, although the absolute values are minute. This argument is erroneous as one is not dealing with an equilibrium situation but one in which the changes in the O_3 concentration depend on the magnitudes of the various terms in equation E1, so that absolute and not relative values are important.

It should be noted that although the theoretical study assumed the eclipse began at noon, virtually identical results would have been obtained regardless of the time of day the eclipse began, since the daylight photochemical ozone change is only 0.0002 cm S.T.P according to the results of Chapter 4. Although very rapid changes occur in the ozone and atomic oxygen concentrations at dawn and sunset, these changes should not affect any experimental observations made during an eclipse which extends into say sunset, because the sunset changes occur after observations on the sun are possible.

5.3.4 The effect on the theoretical results of neglecting limb darkening of the sun

As stated previously neglecting limb darkening altered the results obtained quantitatively, but not qualitatively. Such a result is predictable since the predominant effect occurring during an eclipse is the overall reduction in the solar radiation intensity reaching the atmosphere, the relative

change in this intensity with wavelength being of secondary importance. For about the first 3000 seconds of the eclipse the variation of the radiation intensity is essentially constant with wavelength, and is proportional to the exposed surface of the sun. Hence up to this time the neglect of limb darkening would be of minor importance, as the results were actually found to show. However, after this time the reduction in the exposed surface of the sun towards second contact progressively increases the importance of limb darkening, since the radiation becomes increasingly emitted from the limb itself. Figure 42 shows that the effect of the limb darkening is most important for the shorter wavelengths, where the radiation intensity rapidly drops towards zero as the limb is approached. The variation of $I(0)/F$ with wavelength tends to alleviate the effect of limb darkening to some extent. At a time of 3600 seconds the radiation intensity at 1800Å has fallen to about 15% of its initial value, while at the long wavelength end of the scale, 7500Å, the reduction is to only about 23% of its initial value. Now it is the shorter wavelengths, above about 3000Å, which are principally absorbed at the upper levels of the ozonosphere, resulting in the dissociation of the O_3 , hence the amount of O_3 dissociated becomes progressively less towards second contact compared with that when limb darkening is neglected. A larger increase in the total O_3 amount is therefore to be expected for the case in which limb darkening of the sun is allowed for. It should be noted that although the rate of oxygen dissociation is also reduced compared to the case with no limb darkening, this is of minor importance because this rate is very low and in each case the increase in the O_3 concentration occurs at the expense of the O "reservoir" in the atmosphere. The final result of allowing for limb darkening was found to be of little importance as regards the increase in the total O_3 amount, a rise from 0.0013 to 0.0016 cm S.T.P. being observed due to limb darkening. However, the changes in the O_3 concentration above about 70 km were more marked. Nevertheless, it is apparent that no great error would have resulted if limb darkening had been neglected and the numerical study would have been greatly simplified.

5.4 Conclusions

The theoretical study made of the changes occurring in the ozonosphere during a total eclipse of the sun has shown that an increase of less than 1% in the total O_3 amount is to be expected, compared with experimental observations of 4%. However, it appears that a correction of the experimental observations to allow for limb darkening of the sun would give better agreement

between theory and experiment. Since the theoretically predicted change in the O_3 amount is less than the experimental accuracy, it seems that when limb darkening is allowed for in the experimental results no change in the O_3 amount should be observed. Nevertheless, indirect information regarding the change in the O_3 concentration at different heights during an eclipse may be obtainable from airglow measurements, since the excitation of the hydroxyl bands and the infra red atmospheric bands of oxygen are known to result from reactions involving O_3 as discussed in Section 1.7.

From the theoretical point of view the neglect or inclusion of limb darkening of the sun in the numerical calculations was found to be of minor importance.

CHAPTER 6

A MODIFIED PHOTOCHEMICAL THEORY OF THE OZONOSPHERE

6.1 Introduction

The results presented in Chapter 3 show that it is possible to obtain fairly realistic photochemical ozone profiles with the data available at present, although there are some uncertainties in these data. As discussed in Section 3.4.5.3 the principal doubt concerns the value of the rate constant k_4 which should be used in the calculations, and it was pointed out that although the value of k_4 given by Benson and Axworthy (1957) gives unrealistic results, see Case XVI, figure 24, Clyne et al. (1963) have suggested that in spite of this the results of Benson and Axworthy are probably correct. They base this conclusion on an experimental measurement of k_4 which they found to be in agreement with the results of Leighton et al. (see Harteck and Reeves, 1961), whose value of k_4 was used for Case I. They however consider their results to be in error because of the presence of atomic hydrogen in the experimental system, and they state that a similar cause of error was probably present in the other studies of this reaction because the same type of discharge flow system was common to these studies. A noticeable exception was the work carried out by Benson and Axworthy (1957) who obtained their results from an investigation of the thermal decomposition of ozone. Clyne et al. therefore consider that the results of Benson and Axworthy, as corrected by Jones and Davidson (1962), are the best available at the present time. The discussion by Schiff (1964) of the various measurements of this rate constant would appear to support this conclusion.

The results of Clyne et al. became available after the completion of the work presented in Chapters 4 and 5, and because of the importance of the value of k_4 to the photochemistry of ozone it was apparent that a more detailed study of the reaction scheme of ozone in the atmosphere was required. Such a study is necessary in order to explain the large ozone concentrations obtained when Benson and Axworthy's (1957) data are used in photochemical ozone calculations. These high concentrations imply that there are reactions occurring which destroy ozone in the atmosphere but which to date have been neglected in the reaction scheme. It would seem unlikely that reactions involving atomic hydrogen and atomic nitrogen and their various oxides are important enough to modify substantially the ozone profile, especially in the stratosphere, and such reactions have been deliberately excluded by the limitation of an oxygen atmosphere. The additional reactions must therefore involve the destruction of ozone by excited forms of oxygen. It may be noted that Clyne et al. (1963) reported the presence of electronically excited molecular oxygen in their reaction system, as has been observed by other workers, and they concluded that an

appreciable reaction was taking place between the excited molecular oxygen and ozone. Now, it is known from studies of the airglow emission that excited oxygen exists in the atmosphere, and Vallance Jones and Gattinger (1963) have calculated that 10^{10} molecules/cm^3 of molecular oxygen in the $^1\Delta_g$ electronic state are expected to be present at a height of 50 km. In addition McGrath and Norrish (1960) have reported chain reactions occurring in the decomposition of ozone in which they consider the chain to be maintained by atomic oxygen excited to the ^{1}D state. Hence it would appear feasible that reactions between ozone and excited oxygen molecules and atoms could be of importance in the formation of the ozonosphere, and it was in order to determine the importance of such excited species that the present investigation was undertaken.

6.2 The "standard" photochemical reactions

The standard photochemical reactions were taken to be reactions R1 to R5 considered previously in Chapters 3, 4 and 5. As mentioned in Section 6.1 Jones and Davidson (1962) have revised the values of k_2 and k_4 given by Benson and Axworthy (1957) to allow for the redetermination of the dissociation energy of O_2 by Brix and Herzberg (1954). Although the correction is quite small, for the sake of completeness, equilibrium O and O_3 profiles for an overhead sun were recalculated using the new values of k_2 and k_4, these are:-

$$k_2 = 5 \times 10^{-35} \exp(1000/RT) \text{ cm}^6 \text{ molecules}^{-2} \text{ sec}^{-1}$$

$$k_4 = 5 \times 10^{-11} \exp(-5600/RT) \text{ cm}^3 \text{ molecule}^{-1} \text{ sec}^{-1}$$

For k_2 M = O_2 or N_2 and the relative efficiency of O_3 to O_2 or N_2 was taken as 1 to 0.3 (Kaufman and Kelso, 1961).

The profiles were calculated for the same height range as before, using the data selected for Case I in Chapter 3. In subsequent sections of the present chapter only the values of the various rate constants will be given, all other data being the same as that for Case I unless otherwise stated. The O and O_3 profiles for the revised values of k_2 and k_4 are given in figure 48, and are very similar to those for Case XVI of figure 24 apart from a small reduction in the total O_3 amount. The concentrations given in figure 48 are excessively high, especially above 70 km, and the total O_3 amount of 0.81 cm S.T.P. is completely unrealistic for an O_3 distribution representative of the equator. It is apparent therefore that reactions R1 to R5 are not sufficient to represent the processes actually occurring in the photochemistry of the ozonosphere, and it is necessary to investigate other possible reactions involving excited forms of oxygen. For this reason the formation

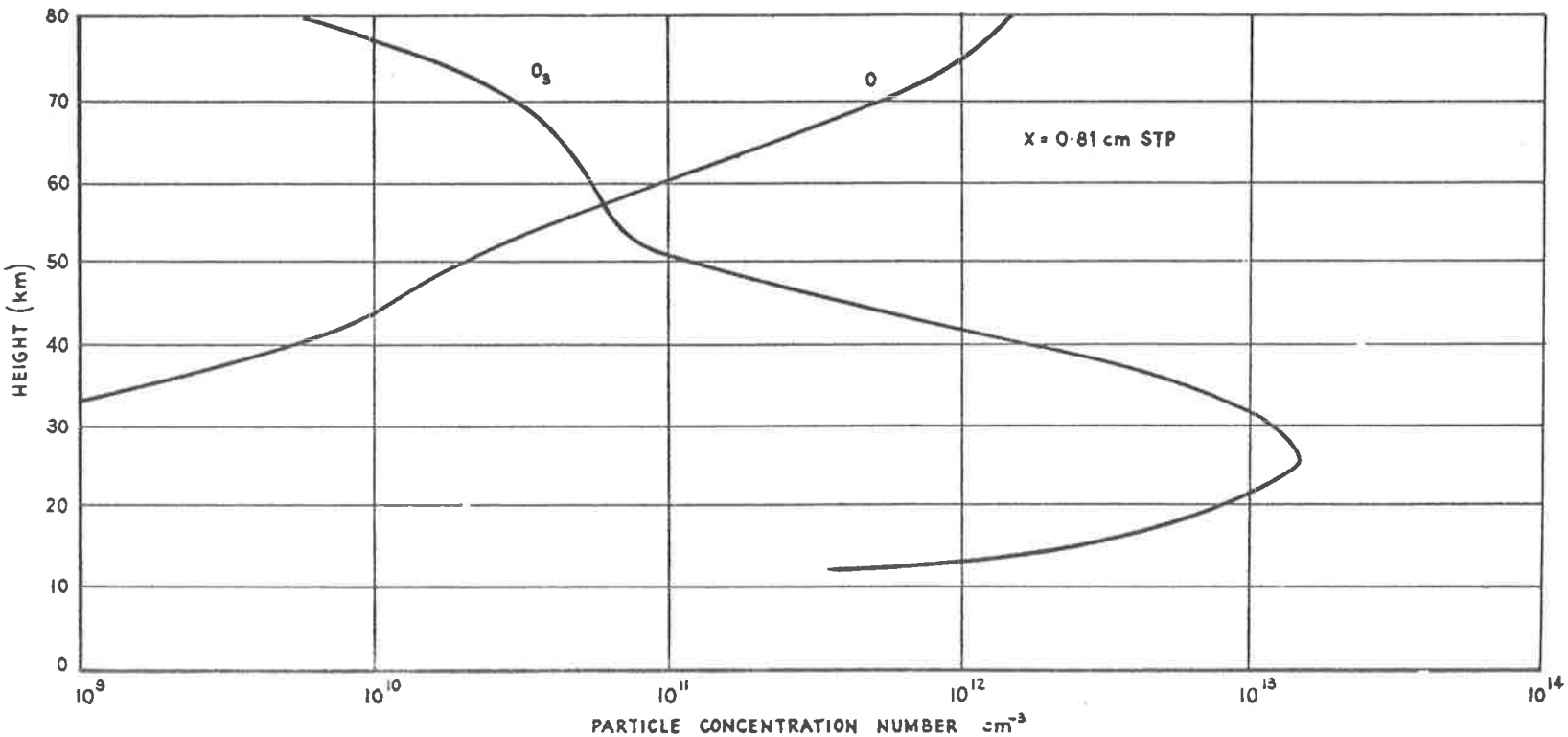

FIGURE 48. EQUILIBRIUM O AND O_3 DISTRIBUTIONS USING THE "STANDARD" REACTION SCHEME AND BENSON AND AXWORTHY'S RATE CONSTANTS

of electronically excited atomic oxygen, O (^{1}D), in the ozonosphere will now be considered.

6.3 The formation of electronically excited atomic oxygen in the ozonosphere

The lowest lying electronically excited state of atomic oxygen, O (^{1}D), cannot be produced by dissociation of O_2 in the altitude range of interest, since the shortest wavelength available, $\lambda = 1775\text{Å}$, is above that required, $\lambda = 1750\text{Å}$.

$$O_2 + h\nu \rightarrow 2O(^3P) \text{ for } 1750\text{Å} < \lambda < 2424\text{Å}$$

The excess energy for $\lambda < 2424\text{Å}$ will appear as translational energy of the ground state atoms.

In the case of O_3 dissociation, it is possible that in addition to the dissociation products being electronically excited, the O_2 formed may be rotationally or vibrationally excited. Rotational excitation can be ignored in general, and for the present the possibility of vibrational excitation of O_2 in the primary dissociation act of O_3 will be ignored also. It is therefore assumed that any energy in excess of that required to excite the electronic states will appear as translational energy only. The possible dissociation products of O_3 can be determined using the values given by Herzberg (1961) for the excitation energies of the electronic states of O and O_2. When energy and spin restrictions (O_3 is a singlet) are applied only six of the possible pairs of dissociation products of ozone for $\lambda > 1775\text{Å}$ remain feasible. These are

$$O_3 \rightarrow O(^3P) + O_2\ (^3\Sigma_g^-) \text{ for } \lambda < 11\,800\text{Å}$$

$$O_3 \rightarrow O(^1D) + O_2\ (^1\Delta_g) \text{ for } \lambda < 3100\text{Å}$$

$$O_3 \rightarrow O(^1D) + O_2\ (^1\Sigma_g^+) \text{ for } \lambda < 2670\text{Å}$$

$$O_3 \rightarrow O(^1S) + O_2\ (^1\Delta_g) \text{ for } \lambda < 1993\text{Å}$$

$$O_3 \rightarrow O(^1S) + O_2 \ (^1\Sigma_g^+) \quad \text{for } \lambda < 1800\text{Å}$$

$$O_3 \rightarrow O(^3P) + O_2 \ (^3\Sigma_u^+) \quad \text{for } \lambda < 2240\text{Å}$$

The number of possible dissociation products can be further reduced by determining whether their terms manifold are compatible with the term manifold of the O_3 molecule. The term manifold of O_3 in its ground electronic state has been given as $^1\Sigma$ (Kaufman and Kelso, 1961). Now, using tables 2 and 3 of Mulliken (1933) and tables 3 and 4 of Sponer and Teller (1941), which are derived from group theoretical considerations, it can be shown that since O_3 is a member of point group C_{2V} (Oka and Morino, 1962) its term manifold is $^1A_1$. Thence, by forming the direct products for point group C_{2V} corresponding to the term symbols of each of the various pairs of possible O_3 dissociation products, we can determine whether these products can give rise to $O_3(^1A_1)$. By these means the last pair of dissociation products listed above was eliminated.

In order to simplify the photochemical calculations as much as possible it is desirable that the ozone dissociation products be even further restricted, and for this reason the production of (^1S) atoms was neglected. This is reasonable on the ground of energy requirements, as wavelengths shorter than 1800Å or 1993Å are involved and the intensity of such radiation is very weak, as most of this radiation is absorbed above 70 km. This therefore leaves only the first three pairs of dissociation products listed above.

In the next section the presence of electronically excited states of O_2 is ignored for the time being and only the reactions of (^1D) considered. It is assumed that for each quantum of radiation absorbed by ozone for $\lambda < 3100$Å an atom of oxygen in the $O(^1D)$ state is produced. Direct evidence that $O(^1D)$ is actually produced by radiation of these wavelengths has been obtained by McGrath and Norrish (1960) and DeMore and Raper (1962). It may be noted that because of the weak absorption by ozone of radiation of wavelengths above about 3300Å the rate of production of $O(^1D)$ in the atmosphere by dissociation of ozone is greater than that of $O(^3P)$ down to about 35 km.

6.4 The reactions of $O(^1D)$ in the ozonosphere

Because of the importance of $O(^1D)$ in the atmosphere it is necessary to consider in some detail the possible reactions involving this species.

The reaction

$$O(^1D) + O_2\ (^3\Sigma_g^-) + M \rightarrow O_3(^1A_1) + M$$

cannot be a significant source of O_3 as the electronic states of ^1D and $^3\Sigma_g^-$ do not correlate to give a ground state ozone molecule. In addition since the excitation energy of $O(^1D)$ is 1.987 eV and the dissociation energy of O_3 is only 1.04 eV the formation of a stable $O\text{-}O_2$ complex involves the transfer of a considerable amount of excitation energy to the third body.

The reaction

$$O(^1D) + O(^1D) + M \rightarrow O_2 + M$$

can also be neglected because of the low concentration of $O(^1D)$ in the atmosphere, any O_2 formed by this reaction would be in an excited state.

The principal reaction of interest as far as the ozonosphere is concerned is

$$O(^1D) + O_3 \xrightarrow{k_7} 2O_2 \qquad \text{R7}$$

where the state of the O_2 formed will not be considered for the present. A value of $k_7 = 3.3 \times 10^{-12}$ cm^3 molecule^{-1} sec^{-1} has been given by Fitzsimmons and Bair (1964), which they consider to be a lower limit. Because of this, and since a high value is required for k_7, a value of 10^{-11} cm^3 molecule^{-1} sec^{-1} was actually taken. The assumption was also made that k_7 was independent of temperature since R7 is thought to have a small activation energy (Fitzsimmons and Bair, 1964). The chosen value of k_7 is in close agreement with that given by elementary kinetic theory, viz. $1.5 \times 10^{-12}\ T^{\frac{1}{2}}$ cm^3 molecule^{-1} sec^{-1}, assuming that the steric factor of 0.1 which occurs in the value of k_4 also applies to k_7.

Assuming that R7 is the major reaction involving $O(^1D)$ in the atmosphere we can determine the importance of this reaction by incorporating it into the reaction scheme which now becomes

$$O_2 + h\nu \rightarrow 2\,O(^3P) \quad \text{for } 1750\text{Å} < \lambda < 2424\text{Å} \qquad \text{R1}$$

$$O(^3P) + O_2\,(^3\Sigma_g^-) + M \xrightarrow{k_2} O_3(^1A_1) + M \qquad \text{R2}$$

$$O_3 + h\nu \rightarrow O(^3P) + O_2 \quad \text{for } 3100\text{Å} < \lambda < 11\,800\text{Å} \qquad \text{R3a}$$

$$O_3 + h\nu \rightarrow O(^1D) + O_2 \quad \text{for } 1775\text{Å} < \lambda < 3100\text{Å} \qquad \text{R3b}$$

$$O(^3P) + O_3(^1A_1) \xrightarrow{k_4} 2O_2 \qquad \text{R4}$$

$$O(^3P) + O(^3P) + M \xrightarrow{k_5} O_2\,(^3\Sigma_g^-) + M \qquad \text{R5}$$

$$O(^1D) + O_3\,(^1A_1) \xrightarrow{k_7} 2O_2 \qquad \text{R7}$$

The resulting profiles for $O(^1D)$, $O(^3P)$ and O_3 are given in figure 49 together with the O and O_3 profiles from figure 48 for comparison. The O_3 concentrations obtained are far too small and the total ozone amount of 10^{-3} cm is inadmissibly low. Hence it is apparent that other reactions must occur which compete with O_3 for the available $O(^1D)$.

Recently Raper and DeMore (1964) have discussed the deactivation of $O(^1D)$ in the atmosphere and attribute it to the reactions

$$O(^1D) + N_2 \rightleftharpoons N_2O^* \xrightarrow{k_{8a}} N_2 + O(^3P) \qquad \text{R8a}$$

and

$$O(^1D) + O_2 \rightleftharpoons O_3^* \xrightarrow{k_{8b}} O(^3P) + O_2\left(^1\Sigma_g^+\,,\,^1\Delta_g\right) \qquad \text{R8b}$$

The very fast reaction rate of 10^{-11} cm^3 molecules^{-1} sec^{-1} has been suggested by Wallace and Chamberlain (1959) for R8b based on

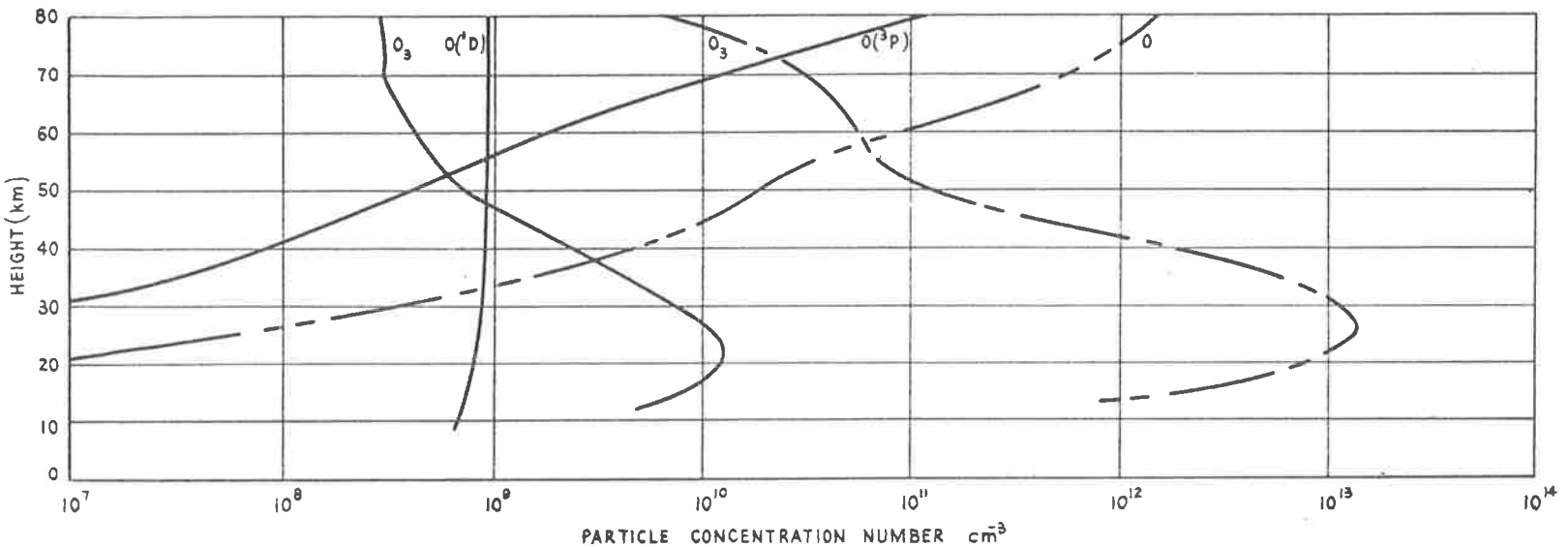

FIGURE 49. THE EFFECT OF $O(^1D)$ ON THE O_3 PROFILE

an analysis of airglow spectra originating at heights above 100 km in the atmosphere. When this value of k_{8b} was used it was found that R8b proceeded so fast with the O_2 concentrations in the ozonosphere that R7 could be completely neglected and the high O_3 concentrations of figure 48 were obtained again. It is therefore considered that no great confidence can be placed in this value for k_{8b}; Wallace and Chamberlain have, in any case, stated that k_{8b} might be considerably less at lower altitudes, a conclusion also reached by Raper and DeMore (1964).

Unfortunately no laboratory values for k_{8a} and k_{8b} are available at present, although experimental studies by DeMore and Raper (1962) and Katakis and Taube (1962) indicate that N_2 is not efficient at deactivating $O(^1D)$ in the gas phase. DeMore and Raper have however found that O_2 is 4.5 times as efficient as N_2 in deactivating $O(^1D)$, and, since the atmospheric N_2 concentration is 5 times that of O_2, it is seen that deactivation of $O(^1D)$ by O_2 and N_2 in the atmosphere will proceed at about the same rate. The combined rate is

$$O(^1D)\left(k_{8a}\,N_2 + k_{8b}\,O_2\right) = 2\,k_{8b}\,O_2\,O(^1D) = 2\,k_{8a}\,O(^1D)\,N_2$$

For convenience, calculations were made to determine an empirical value of k_{8b} which gave realistic ozone concentrations in the atmosphere. As shown in figure 50 the ozone profile is very sensitive to the value of k_{8b} and the final value selected was $k_{8b} = 2.5 \times 10^{-14}$ cm^3 molecule^{-1} sec^{-1} for which the total ozone amount was 0.33 cm S.T.P. The corresponding value for k_{8a} is 5×10^{-15} cm^3 molecule^{-1} sec^{-1}. Although these rate constants are rather low for bimolecular reactions, in view of the excited complexes N_2O^* and O_2^* involved as intermediates, it would appear that rate constants of this order are not unacceptably low. Despite the slowness of these reactions compared to that of R7 the concentration of $O(^1D)$ in the atmosphere is still controlled by R8a and R8b because of the much greater O_2 and N_2 concentrations. It is possible that both k_{8a} and k_{8b} may vary with altitude due to pressure effects but, in view of the lack of definitive data, it is considered that the assumptions made here are not unreasonable.

The concentrations of O_3, $O(^1D)$ and $O(^3P)$ for the chosen value of k_{8b} are given in figure 51. The O_3 and $O(^3P)$ concentrations are excessively high above about 60 km, partially because it was necessary to omit reaction R5 from the equations in order to simplify their numerical solution. This reaction has however

been included in the diurnal investigation reported in Section 6.7. Apart from the high concentrations above 60 km the profiles are considered to be fairly realistic for an atmosphere at rest, and a comparison of figures 48 and 51 indicates that the inclusion of reactions involving $O(^1D)$ has resulted principally in the removal of the very large O_3 concentrations below 40 km. The maximum O_3 concentration of 5.4×10^{12} molecules cm^{-3} occurs at 23 km, in agreement with Case I of Chapter 3. The concentration of $O(^1D)$ is extremely low at all altitudes, the maximum value of about 10^7 atoms cm^{-3} being reached at the highest altitude considered. Nevertheless, despite its low concentration, $O(^1D)$ effectively controls the total ozone amount in a photochemical atmosphere. This control is not achieved by reaction R7 destroying large amounts of O_3, as dissociation by solar radiation is very much more effective at all altitudes, but is due to the fact that only R4 and R7 lead to the disappearance of atomic oxygen and ozone. R7 is much more efficient in this process than R4 and as a result the equilibrium concentrations obtained are smaller than those when R7 is neglected.

No allowance has been made for reactions involving O_3 and electronically excited O_2 as suggested by Clyne et al. (1963), and in the subsequent section these reactions will be considered.

6.5 Reactions involving electronically excited molecular oxygen

Only the two lowest electronically excited states of O_2, $^1\Delta_g$ and $^1\Sigma_g^+$, were considered as these are the only excited states expected to be present in the ozonosphere in appreciable quantities. Excitation of O_2 to electronic states higher than $^1\Sigma_g^+$ in the ozonosphere seems likely to result solely from the recombination of atomic oxygen.

$$O + O + M \rightarrow O_2^* + M$$

For $O(^3P)$ Young and Sharpless (1962b) have found that although the Herzberg and Atmospheric band systems of O_2 are excited by this reaction, the excitation occurs at a negligible rate, and in any case this reaction is important only above 60 km altitude. Because of the low $O(^1D)$ concentration in the atmosphere the corresponding reaction involving $O(^1D)$ can be completely ignored.

The production of $O_2\left(^1\Delta_g\right)$ and $O_2\left(^1\Sigma_g^+\right)$ in the ozonosphere is attributed here principally to the photolysis of O_3, reaction

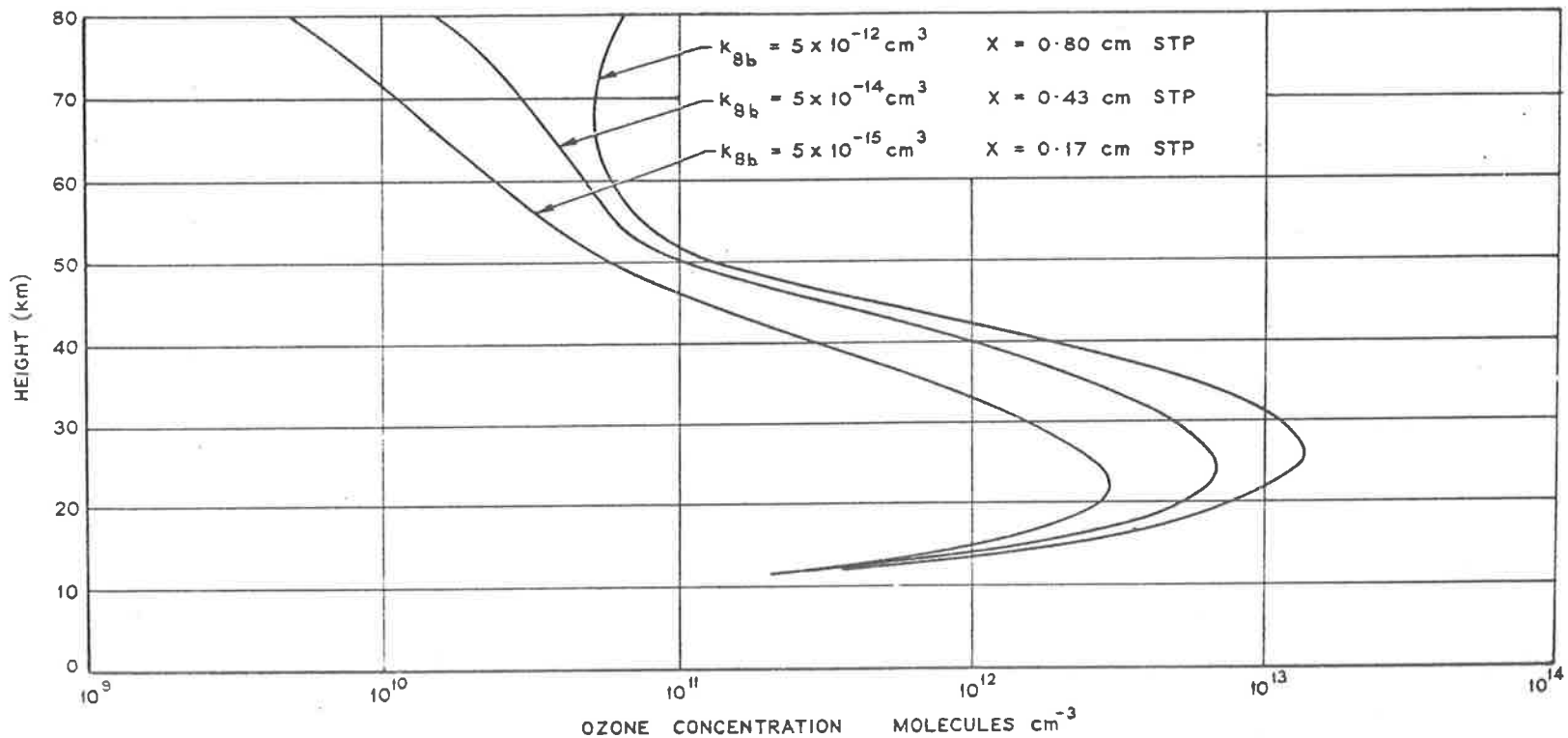

FIGURE 50. VARIATION OF THE O_3 PROFILE AND THE TOTAL O_3 AMOUNT WITH THE RATE OF DEACTIVATION OF $O(^1D)$

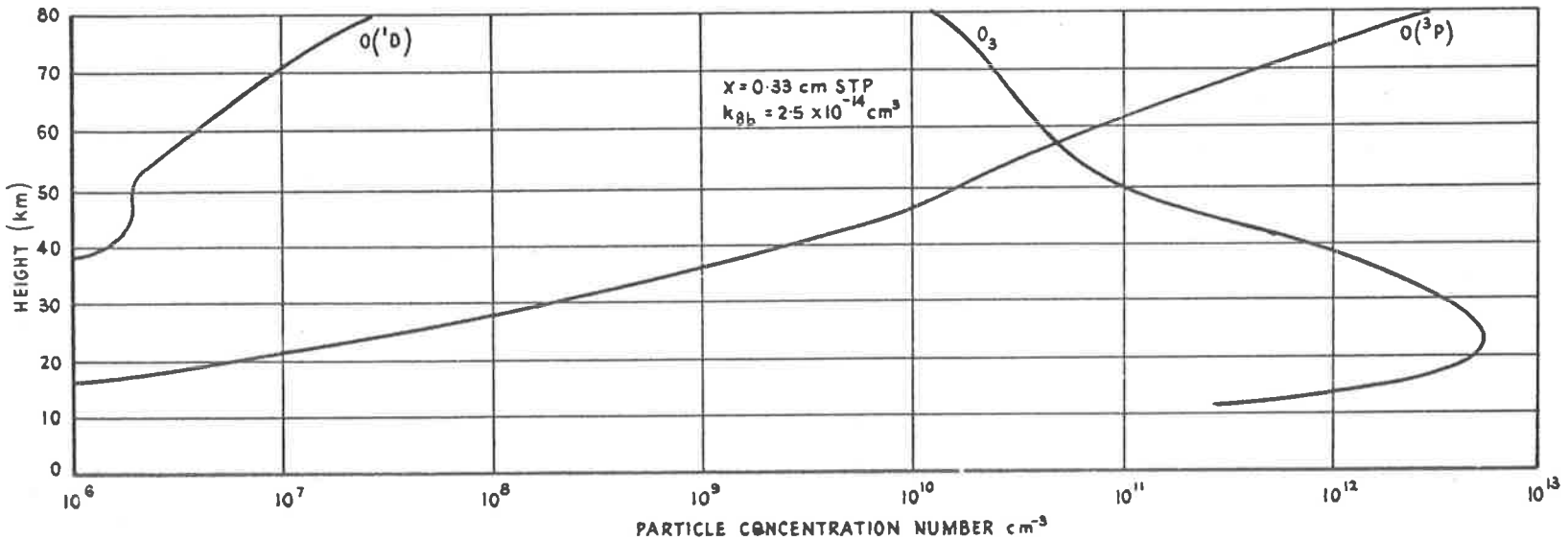

FIGURE 51. CONCENTRATIONS OF $O(^3P)$, $O(^1D)$ AND O_3 FOR SELECTED VALUE OF k_{8b}

R3b, together with the subsequent reactions of $O(^1D)$. As indicated by Raper and DeMore (1964) R8b can produce either $O_2\left(^1\Sigma_g^+\right)$ or $O_2\left(^1\Delta_g\right)$; however, because of energy requirements, it has been assumed here that only $O_2\left(^1\Sigma_g^+\right)$ actually results. As will be shown later this assumption is of little importance as regards the photochemistry of O_3. In addition, minor sources of electronically excited O_2 are reactions R4 and R7.

$$O(^3P) + O_3(^1A_1) \rightarrow O_2\left(^3\Sigma_g^-\right) + O_2\left(^1\Delta_g\right) \qquad \text{R4}$$

$$O(^1D) + O_3(^1A_1) \rightarrow O_2\left(^3\Sigma_g^-\right) + O_2\left(^1\Sigma_g^+\right) \qquad \text{R7}$$

The production of $O_2\left(^1\Delta_g\right)$ by R4 is likely on the grounds of spin conservation as suggested by McGrath and Norrish (1957). In the case of R7 production of $O_2\left(^1\Sigma_g^+\right)$ involves a spin violation.

The formation of $O_2\left(^1\Sigma_g^+\right)$ by R7 is in any case very much less than that due to reactions R3b and R8b. In both R4 and R7 the ground state O_2 molecule is observed to be vibrationally excited and McGrath and Norrish (1960) have suggested that this excitation permits the $O_2\left(^3\Sigma_g^-\right)$ to participate in chain reactions involving the destruction of O_3. In the succeeding section the possible reactions involving vibrationally excited O_2 will be discussed.

Removal of O_2 in the $^1\Sigma_g^+$ and $^1\Delta_g$ states may occur by radiative transitions or by two body collisions. In the case of radiative deactivation the following transitions are possible

$$O_2\left(^1\Delta_g\right) \xrightarrow{k_9} O_2\left(^3\Sigma_g^-\right) + h\nu \qquad \text{R9}$$

$$O_2\left(^1\Sigma_g^+\right) \xrightarrow{k_{10}} O_2\left(^1\Delta_g\right) + h\,\nu \qquad \text{R10}$$

$$O_2\left(^1\Sigma_g^+\right) \xrightarrow{k_{11}} O_2\left(^3\Sigma_g^-\right) + h\nu \qquad \text{R11}$$

The relevant radiative transition probabilities are

$k_9 = 1.5 \times 10^{-4}$ sec^{-1} Vallance Jones and Gattinger (1963)

$k_{10} = 2.5 \times 10^{-4}$ sec^{-1} Noxon (1961)

$k_{11} = 1.4 \times 10^{-1}$ sec^{-1} see Noxon (1961)

As the transition probabilities indicate, the excited states are metastable. In spite of this Young and Sharpless (1962b) consider that physical quenching of $O_2\left(^1\Sigma_g^+\right)$ is probably unimportant compared with radiative transitions and they give the rate constant of the quenching reaction.

$$O_2\left(^1\Sigma_g^+\right) + N_2 \xrightarrow{k_{12a}} O_2^* + N_2^* \qquad \text{R12a}$$

as $k_{12a} < 10^{-18}$ cm^3 molecule^{-1} sec^{-1}, implying a probability of deactivation of about 10^{-8} per gas kinetic collision. Since only physical quenching is involved in this reaction it was assumed that O_2 was equally ineffective in quenching $O_2\left(^1\Sigma_g^+\right)$ as N_2. It was also assumed that quenching resulted in deactivation of the $O_2\left(^1\Sigma_g^+\right)$ to the ground state. With the above value for k_{12a} it was found that above about 40km in the atmosphere deactivation of $O_2\left(^1\Sigma_g^+\right)$ occurred mainly by means of R11.

In the case of $O_2\left(^1\Delta_g\right)$, physical quenching is of greater importance because of the much lower radiative transition probability for R9. Arnold et al. (1964) have recently investigated a mechanism by which $O_2\left(^1\Delta_g\right)$ may be quenched which involves O_4 as an intermediate.

$$2O_2\left(^1\Delta_g\right) \underset{}{\overset{(M)}{\rightleftharpoons}} O_4^* \rightarrow \begin{matrix} O_4 \\ + \\ h\nu \end{matrix} \overset{(M)}{\rightleftharpoons} 2O_2\left(^3\Sigma_g^-\right)$$

This reaction is not of much consequence for $O_2\left(^1\Delta_g\right)$ deactivation as it involves the unstable form O_4^* which is not formed very efficiently at the low pressure existing in the upper atmosphere. Arnold et al. also found that less than 10^6 collisions did not effect the physical quenching of $O_2\left(^1\Delta_g\right)$. Now if this value is used for k_{12b} in reaction R12b

$$O_2\left(^1\Delta_g\right) + M \xrightarrow{k_{12b}} O_2\left(^3\Sigma_g^-\right) + M \qquad \text{R12b}$$

deactivation occurs so fast that the $O_2\left(^1\Delta_g\right)$ concentrations obtained are less than those stipulated by Vallance Jones and Gattinger (1963) as being required to produce the observed airglow intensities. It has therefore been assumed that $k_{12b} = 10^{-19}$ cm^3 molecules^{-1} sec^{-1}, which does not seem unreasonable when compared with the value for k_{12a} given by Young and Sharpless (1962 b). In addition to reaction R12b it has been shown by Vallance Jones and Gattinger (1963) that it is necessary to assume that selective deactivation of $O_2\left(^1\Delta_g\right)$ by atomic oxygen occurs. Such deactivation is only effective above about 50 km altitude and a value of $k_{13} = 10^{-16}$ cm^3 molecules^{-1} sec^{-1} was determined empirically for reaction R13

$$O(^3P) + O_2\left(^1\Delta_g\right) \xrightarrow{k_{13}} O(^3P) + O_2\left(^3\Sigma_g^-\right) \qquad \text{R13}$$

The deactivation is attributed to atom-atom exchange which Herron and Klein (1964) found to be a very efficient process for oxygen. In the case of $O_2\left(^1\Sigma_g^+\right)$ it is not necessary to consider such a deactivation process because of its much lower concentration in the atmosphere and its higher radiative transition probability.

The remaining mechanism for deactivation of $O_2\left(^1\Delta_g\right)$ and $O_2\left(^1\Sigma_g^+\right)$, chemical quenching, involves O_3 in the reaction scheme and is the mechanism of principal interest to this study. As suggested by Clyne et al. (1963) the reactions considered are

$$O_3\ (^1A_1) + O_2\left(^1\Sigma_g^+\right) \xrightarrow{k_{14}} 2O_2\left(^3\Sigma_g^-\right) + O(^3P) \qquad \text{R14}$$

and

$$O_3\ (^1A_1) + O_2\left(^1\Delta_g\right) \xrightarrow{k_{15}} 2O_2\left(^3\Sigma_g^-\right) + O(^3P) \qquad \text{R15}$$

Since R14 is exothermic by only 13 k cal it is impossible for any of the reaction products to be electronically excited. R15 is actually endothermic by 2.6 k cal, which is therefore the minimum activation energy of this reaction. Mathias and Schiff (1964) have measured the combined rates of what are presumed to be reactions R14 and R15 and give a value for this combined rate of $1.7 \times k_4$. This gives the combined rate at 300^oK as about 10^{-14} cm^3 $molecule^{-1}$ sec^{-1}. Therefore, approximately as an upper limit, we can take

$$k_{14} = 10^{-14}\ cm^3\ molecule^{-1}\ sec^{-1}$$

and

$$k_{15} = 10^{-14}\ \exp(-2600/RT)\ cm^3\ molecule^{-1}\ sec^{-1}.$$

Hence, incorporating the additional reactions listed above, the complete reaction scheme as defined by the controlling differential equations can be obtained as for equations E1 and E2 on p.16. Reaction R5 was again omitted for mathematical reasons and the equations were solved for equilibrium conditions, for a zenith angle of 0^{o}. The resulting concentrations of the various gases are given in figure 52. It was found that reactions R14 and R15 produced only a very minor change from the concentrations given in figure 51, because of the small rate constants and low concentrations involved. It would therefore seem that these reactions can be safely omitted from the atmospheric ozone reaction scheme.

In an attempt to reduce the high O_3 and $O(^3P)$ concentrations in the mesosphere Case I was replaced by Case II of Chapter 3 for the purposes of calculating the concentrations given in figure 52. Case II was selected as it is thought that it probably gives a more realistic representation of the O_2 dissociation processes in the Schumann-Runge absorption bands. The O_3 concentration above 50 km is less than that for Case I, as shown in figure 21, for reasons given in Section 3.4.1. Hence by substituting Case II for Case I in the present calculation it was known that smaller O_3 and $O(^3P)$ concentrations would be obtained in the mesosphere, although it turned out that the reductions were not as large as hoped. The slight change in the O_3, $O(^3P)$ and $O(^1D)$ concentrations in figure 52 compared to those of figure 51 were actually due to this change rather than the incorporation of reactions R14 and R15.

The $O_2\left(^1\Sigma_g^+\right)$ and $O_2\left(^1\Delta_g\right)$ profiles given in figure 52 call for some comment. The former profile shows that the present reaction scheme predicts a maximum concentration during the day at about 40 km, which altitude is considerably lower than that given by airglow measurements. This low level maximum concentration however rapidly disappears as sunset is approached and any nocturnal emission must originate above 80 km. The $O_2\left(^1\Delta_g\right)$ profile is not considered to be very satisfactory but this is due to the uncertainty of k_{12b} and k_{13}. Because of the unimportance of $O_1\left(^1\Delta_g\right)$ as regards the O_3 concentration, it was not considered worthwhile attempting to improve this profile at the present time. The concentrations given are of the order required to account for the Infra-red Atmospheric band intensities according to Vallance Jones and Gattinger (1963).

6.6 The production of vibrationally excited oxygen in the ozonosphere

In the discussion of the question of the quantum efficiency of photochemical O_3 reactions in Section 3.4.6, mention was made of

the work of McGrath and Norrish (1960). They found that chain reactions were occurring in the flash photolysis of O_3 which they showed to involve vibrationally excited molecular oxygen, O_2^*, in its ground electronic state. McGrath and Norrish (1957, 1960) and Fitzsimmons and Bair (1964) found that the O_2^* was produced as a result of the reaction of O_3 with both $O(^3P)$ and $O(^1D)$, and hence O_2^* must also be formed in the atmosphere. It is therefore apparent that the possibility exists that chain reactions involving the destruction of O_3 by O_2^* could be of importance in the ozonosphere, and it is necessary to discuss this possibility.

McGrath and Norrish (1960) found that a chain was not initiated in the reaction of $O(^3P)$ with O_3, in agreement with Benson and Axworthy's (1957) results on the thermal decomposition of O_3. They suggest that the chain is maintained by $O(^1D)$ in the following reaction scheme.

$$O(^1D) + O_3 \rightarrow O_2^* + O_2$$

$$O_2^*\left(^3\Sigma_g^-,\ v'' \geq 17\right) + O_3 \rightarrow 2O_2\left(^3\Sigma_g^-\right) + O(^1D)$$

As indicated, it is necessary for the O_2^* to be excited to at least the 17th vibrational level in order to produce $O(^1D)$, and McGrath and Norrish have suggested that the reason why they failed to observe O_2^* excited above the 17th level is due to the above reaction. Now, although this mechanism may give a satisfactory explanation of the laboratory results it does not follow that a chain reaction will occur in the atmosphere. The principal difference between the two environments is that the O_3 to gas ratio used in the laboratory was of the order 1 in 100, whereas in the atmosphere the corresponding ratio reaches a maximum of 1 to 10^5 at about 30 km as shown in figure 29. Hence in the atmosphere the frequency of collisions of O_2^* with O_3, all of which may not result in chemical reaction according to Jones and Davidson (1962), will be considerably lower than that in the laboratory.

Even though the deactivation of O_2^* must proceed primarily by vibrational relaxation, since O_2 is a homonuclear molecule, such de-activation is fast for highly excited vibrational levels and, according to Fitzsimmons and Bair (1964), proceeds mainly by single quantum jumps. They have also stated that the concentration of O_2^* with $v'' > 17$ is too small for these molecules to be of major importance in the reaction scheme.

The possibility that O_2^* may be formed in the primary act of O_3 dissociation has been discussed by Basco and Norrish (1961). In

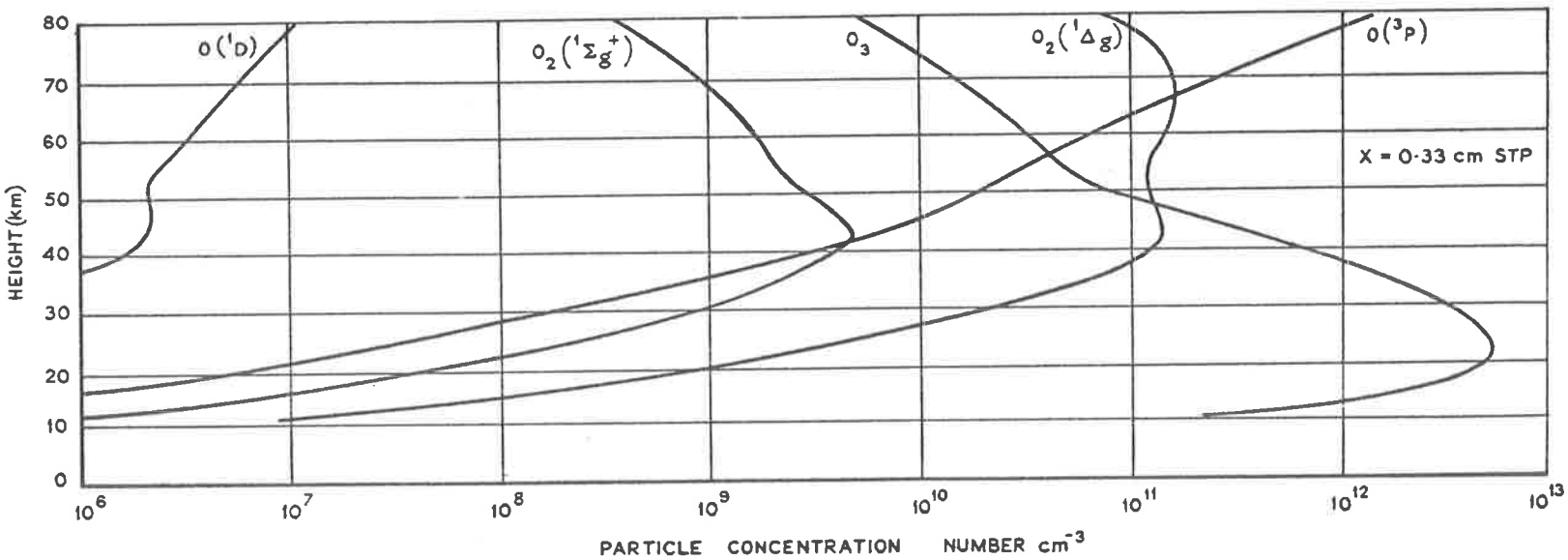

FIGURE 52. FINAL EQUILIBRIUM PROFILES

order to satisfy spin requirements any O_2^* thus formed would have to result from dissociation of O_3 for $\lambda > 3100\text{Å}$. Hence the highest vibrational level which could be expected in the atmosphere is 16, which is incapable of initiating a chain by the McGrath-Norrish mechanism. It would appear that the neglect of any reactions involving vibrationally excited O_2 is justified in the present study.

6.7 The diurnal variation of the gases in the mesosphere

In Chapter 4 an investigation of the diurnal variation of O_3 and O in the mesosphere using the "standard" O_3 reaction scheme was reported. It is therefore of some interest to repeat this investigation for the five gases involved in the present reaction scheme in order to determine their diurnal variations. The numerical methods used for this investigation were essentially the same as before, the five differential equations governing the gas concentrations being integrated simultaneously on an IBM 7090 computer. Because of time step limitations and the excessive computing time required for the present reaction scheme it was not possible to repeat the investigation in the form carried out previously. Instead attention was confined to the top layer considered (77.5 - 80 km) in order to determine the non-equilibrium concentrations, as it is for this layer that the O_3 concentration is in poorest agreement with observation, see figure 53. The extent of the departure from equilibrium is not easily determined as reaction R5 was included in the non-equilibrium calculations, and thus the reduction in the O_3 concentration due to this reaction cannot be separated from the reduction due to the diurnal effects. It was found that the O_3 concentration in the top layer at noon fell from the value of 6×10^9 molecules cm^{-3} (figure 52) to 2×10^9 molecules cm^{-3}, corresponding falls being noted for the other gases, of which $O_2\left(^1\Delta_g\right)$ showed the smallest change. It is therefore apparent that the departure from equilibrium cannot account for the discrepancy between theory and observation in the mesosphere.

Now, since the magnitude of the gas concentrations in the mesosphere are excessive, the magnitudes given for the diurnal variation of these gases in figure 54 will not be representative of actual conditions, but the form of the variation should be fairly realistic. The O_3 and $O(^3P)$ variations are similar to those obtained previously in Chapter 4 with marked changes occurring at dawn and dusk, although the build up in the concentrations during the day is not so apparent as before. At lower levels the dawn and dusk variations would be smaller and at about 50 km no diurnal variation would be expected. The $O(^1D)$ and $O_2\left(^1\Sigma_g^+\right)$ concentrations fall very

very rapidly to zero at sunset even at 80 km, and thus no airglow contributions can be expected from these gases below 80 km. At dawn there is an extremely fast rise in the concentration of these gases and marked "spikes" occur in the profiles which can be attributed to the dissociation at this time of the very high O_3 concentrations. These spikes disappear within 30 minutes and almost constant values for the concentrations are maintained throughout the day. At lower altitudes these spikes would be much less noticeable. The $O_2\left(^1\Delta_g\right)$ concentration shows a much slower rate of decrease at sunset than that of $O_2\left(^1\Sigma_g^+\right)$. The reduction occurs throughout the whole night and is greater than two orders of magnitude. The concentration very soon returns to its daytime value at dawn, and a much broader spike is obtained than those for $O(^1D)$ and $O_2\left(^1\Sigma_g^+\right)$. At lower levels the $O_2\left(^1\Delta_g\right)$ concentration is expected to fall to zero because of the greater physical quenching at these levels. The diurnal variation of this gas is not very realistically represented here because of doubts concerning the rates of deactivation.

6.8 Concluding remarks

The modified photochemical ozone theory presented here cannot, unfortunately, be considered proven until the rates of deactivation of $O(^1D)$ by O_2 and N_2, as determined here, are substantiated experimentally. Despite this uncertainty the theory, besides explaining the otherwise unacceptable O_3 profile in figure 48 obtained with the standard O_3 reaction scheme, also has an advantage over other previously "acceptable" photochemical O_3 profiles. The advantage is that higher O_3 concentrations are obtained in the stratosphere, resulting in better agreement with rocket measurements between 35 and 50 km than the previous photochemical profiles given in figure 31. However, above about 50 km the situation is reversed, and very poor agreement is found between the present theory and observation. This failing is attributed to the limitation of an oxygen atmosphere and the discrepancy between theory and observation indicates that this limitation must be more restrictive than hitherto thought. In the actual atmosphere atomic hydrogen reacts with O_3 as discussed in Chapter 2, and produces the hydroxyl airglow bands which have been shown by Packer (1961) to be situated mainly around 80 km altitude. It is known that the reaction of H with O_3 is very fast, Kaufman (1964), hence the high O_3 values in the mesosphere shown in figure 53 can be expected to be somewhat reduced when this reaction is considered. Since it is likely that

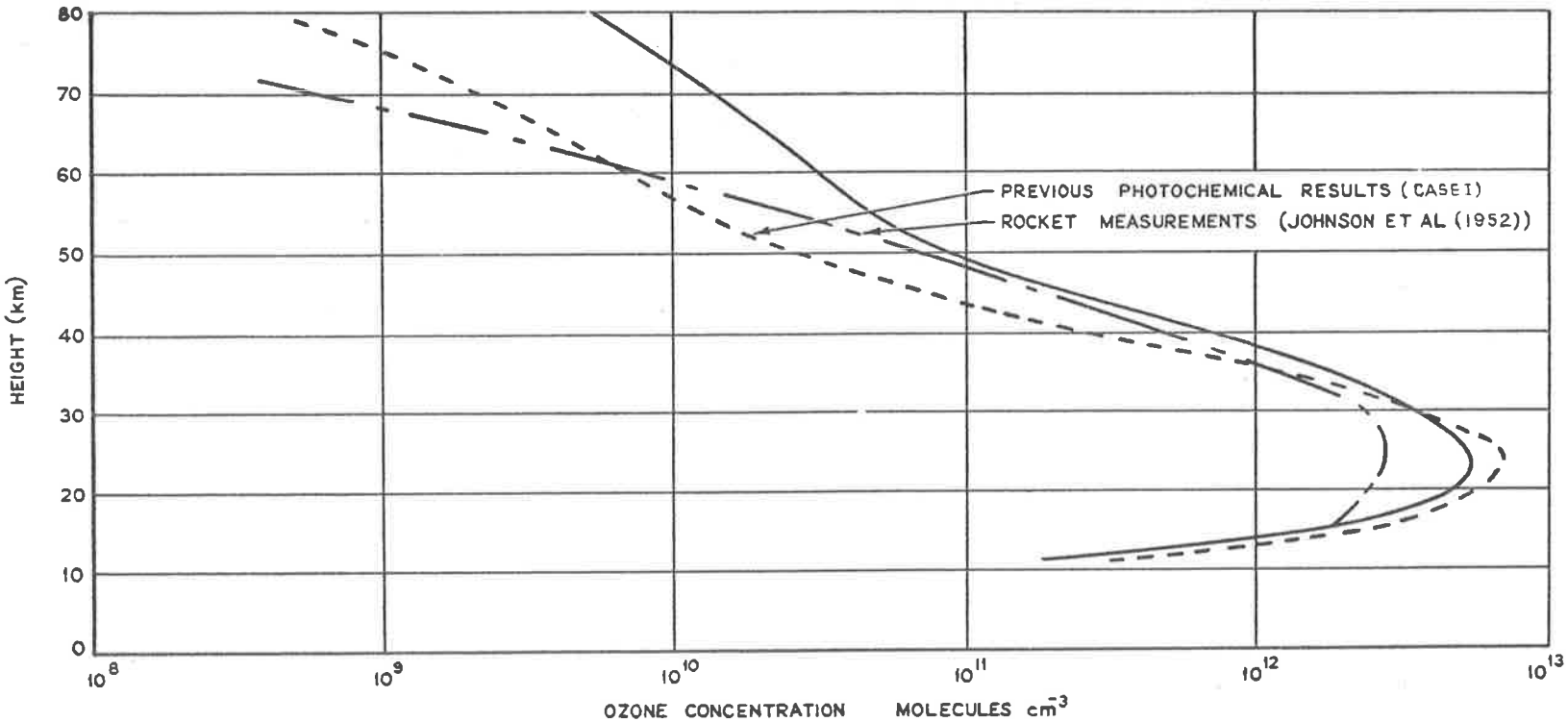

FIGURE 53. COMPARISON OF RESULTS WITH ROCKET MEASUREMENTS AND PREVIOUS PHOTOCHEMICAL CALCULATIONS

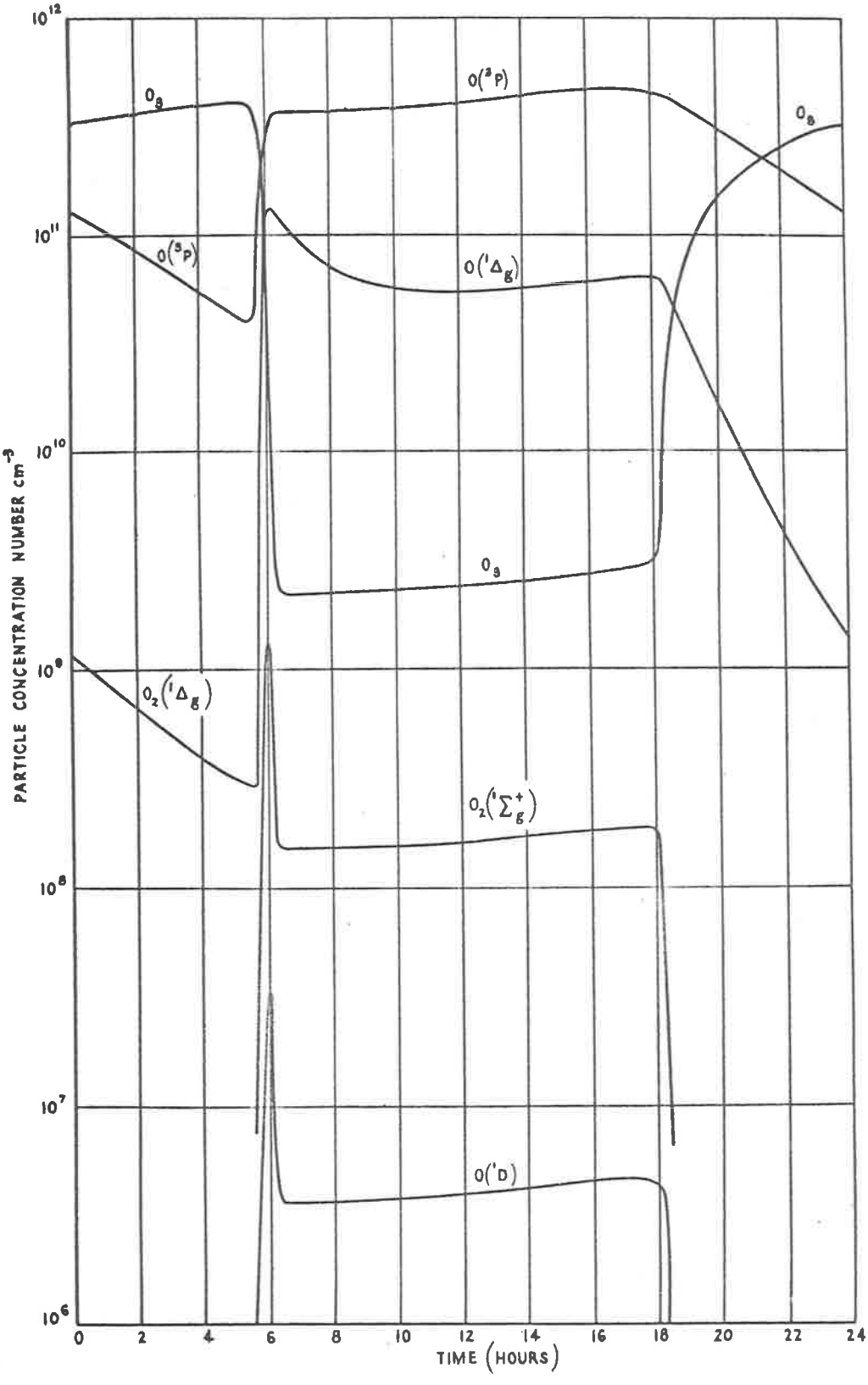

FIGURE 54. THE DIURNAL VARIATION OF THE GASES AT 80 KM

most of the H in the mesosphere results from dissociation of water vapour, it is noteworthy that such dissociation should be able to occur, with diminishing effectiveness, down to altitudes of about 50 km because of the wavelengths involved.

A further advantage of the present theory stems from the high O_3 concentrations obtained in the mesosphere. This advantage is that previous photochemical O_3 profiles, including those given in the preceding chapters, do not require reactions involving H and O_3 in order to obtain O_3 concentrations in agreement with observation in the mesosphere, i.e. these O_3 profiles for oxygen atmospheres satisfactorily account for the observed O_3 distribution. However the O_3 values obtained in this chapter for an oxygen atmosphere do require reactions between O_3 and H, (or some other mechanism for O_3 removal) in order to reduce the O_3 values and produce profiles in agreement with observation. Hence the presence of H in the mesosphere, as indicated by the OH emission bands, is a necessity of the present theory, and can readily be included in any extension to a hydrogen-oxygen atmosphere of the results presented here. If reactions involving H were included in the reaction schemes of previous photochemical O_3 calculations it would appear that unreasonably low O_3 concentrations would be obtained in the mesosphere.

It must be emphasized that the results presented in the preceding section would be substantially modified by the inclusion of these additional reactions. Similar remarks of course apply to a much lesser extent to the results of Chapters 4 and 5. In each case different numerical values to those quoted previously are to be expected, but in all cases essentially the same form of diurnal variation or eclipse variation would be obtained. A departure from equilibrium in the mesosphere would still be expected because of the influence of reactions involving H in the radiation free time at night.

It is admitted that the reaction mechanism presented in this chapter does not of course prove that $O(^1D)$ is of major importance in the photochemistry of ozone as advocated here, but it is difficult to find any reasonable alternative at the present moment. Thus reactions involving H and N cannot be of importance in the stratosphere because there is no way of producing these atoms at this level. For similar reasons reactions involving excited molecules other than O_2 can also be neglected, especially as such reactions do not in general result in a reduction in the number of odd forms of oxygen, as is required in order to remove the O_3. There remains the possibility that ion reactions may be of importance but it would seem that ion concentrations are too low in the ozonosphere to be of much consequence. A further alternative is that the atmospheric O_3 profile is entirely controlled by meteorological factors, and that any excessive O_3 concentrations are rapidly removed by atmospheric motions. Such a possibility seems highly unlikely since, as similar

photochemical profiles are to be expected at all latitudes above about 35km, the removal of any excess O_3 involves identical atmospheric motions at all latitudes, which of course is impossible.

An aspect of some importance which should be mentioned concerns the consequences to airglow studies of the rate of deactivation of $O(^1D)$ in the ozonosphere as required here to account for the O_3 concentrations in the stratosphere. No observable emission from $O(^1D)$ would result from its presence in the ozonosphere, as its lifetime in this altitude region is considerably less than its radiative lifetime of about 100 seconds. For this reason radiative transitions involving $O(^1D)$ have been neglected throughout the present study. However above 100km a high rate of deactivation of $O(^1D)$ is required in order to account for the low observed intensity of its airglow emission at 6300Å. Thus the requirements of the airglow theory are at variance with those of the O_3 theory. In order to resolve this disagreement laboratory measurements are required for the rate of deactivation of $O(^1D)$ over a pressure range representative of the altitude regions discussed here. The little information which exists at present, as mentioned in Section 6.4, supports the slow rate of deactivation of $O(^1D)$ proposed here.

In conclusion it therefore appears that future photochemical O_3 calculations must take account of the reaction of $O(^1D)$ with O_3, although reactions involving electronically and vibrationally excited O_2 can be omitted. It also seems that with this reaction scheme the limitation of an oxygen atmosphere imposes an unacceptable restriction above about 50km altitude, and a more realistic reaction scheme including hydrogen is required. However, definitive laboratory studies of reactions involving O_3 and $O(^1D)$, and also experimental measurements of the O_3 profile in the atmosphere, are needed to supply vital information bearing on this proposed reaction scheme before it can be considered proven.

APPENDIX I

TABLE 1. OXYGEN ABSORPTION COEFFICIENTS (cm^2 molecule^{-1} base 'E')

Derived from Ditchburn and Young's data (1962)

$$\alpha_2 = \alpha_o + \frac{p}{po} \cdot \Delta\alpha$$

Wavelength $\lambda \pm 25$Å	α_o (The values of α_2 for p = 0)	$\Delta\alpha$ (per atmosphere) (The increase in α_2 for a pressure change p/po)	$\alpha_2 = \alpha_o + \Delta\alpha$ (α_2 for pressure p = po)
2400	1.0×10^{-24}	1.9×10^{-24}	2.9×10^{-24}
2350	1.8	2.6	4.4
2300	3.1	3.8	6.9
2250	4.6	5.0	9.6
2200	6.4	5.6	1.2×10^{-23}
2150	7.9	6.4	1.4
2100	9.6	8.1	1.8
2050	1.1×10^{-23}	1.0×10^{-23}	2.1
2000	1.3	1.4	2.7

Derived from Watanabe et al's data (1953)

Wavelength $\lambda \pm 25$Å	1950	1900	1850	1800
α_2	60×10^{-23}	1.0×10^{-21}	8.0×10^{-21}	3.0×10^{-20}

TABLE 1 (Continued)

Derived from Ditchburn and Young's (1962) extrapolation of their data for the Herzberg continuum

Wavelength $\lambda \pm 25\text{Å}$	1950	1900	1850	1800
α_2	1.5×10^{-23}	1.53×10^{-23}	1.53×10^{-23}	1.5×10^{-23}

Derived from Watanabe et al's data (1953) assuming a continuum to underlie the Schumann-Runge bands as proposed by Wilkinson and Mulliken (1957)

Wavelength $\lambda \pm 25\text{Å}$	1950	1900	1850	1800
α_2	3.0×10^{-23}	2.0×10^{-22}	1.0×10^{-21}	5.0×10^{-21}

TABLE 2. OZONE ABSORPTION COEFFICIENTS (cm^2 $molecule^{-1}$, base 'E')

Wavelength $\lambda \pm 25$Å	α_3	Wavelength $\lambda \pm 25$Å	α_3	α_3 temperature correction
1800	7.7×10^{-19}	2700	7.77×10^{-18}	
1850	6.8	2750	5.7	
1900	5.3	2800	3.84	
1950	4.2	2850	2.44	0.94
2000	3.3	2900	1.39	0.93
2050	3.52	2950	7.44×10^{-19}	0.94
2100	5.49	3000	3.84	0.93
2150	9.86	3050	1.96	0.92
2200	1.75×10^{-18}	3100	1.02	0.91
2250	2.89	3150	5.36×10^{-20}	0.82
2300	4.45	3200	2.94	0.80
2350	6.25	3250	1.46	0.80
2400	8.05	3300	7.04×10^{-21}	0.75
2450	9.8	3350	3.82	0.75
2500	1.09×10^{-17}	3400	1.94	
2550	1.13	3450	7.04×10^{-22}	
2600	1.08	3500	2.74	
2650	9.56×10^{-18}			

Wavelength $\lambda \pm 250$Å	α_3
4750	4.8×10^{-22}
5250	2.06×10^{-21}
5750	3.98
6250	3.66
6750	1.53
7250	5.23×10^{-22}

TABLE 3. THE INTENSITY OF THE SOLAR RADIATION

Wavelength $\lambda \pm 25$Å	Extra-terrestrial radiation ergs $cm^{-2}\ sec^{-1}\ (50A)^{-1}$	Radiation intensity at 80 km ergs $cm^{-2}\ sec^{-1}\ (50A)^{-1}$	Radiation intensity at 80 km quanta $cm^{-2}\ sec^{-1}\ (50A)^{-1}$
1800	19	4.76	4.31×10^{11}
1850	28	19.36	1.80×10^{12}
1900	41	39.15	3.75
1950	55	54.85	5.38
2000	70	69.96	7.04
2050	90	89.95	9.28
2100	145	144.9	1.53×10^{13}
2150	240	239.9	2.60
2200	310	309.9	3.43
2250	350	349.9	3.96
2300	360	359.9	4.17
2350	320	319.9	3.79
2400	340	339.9	4.11

Wavelength $\lambda \pm 25$Å	Extra-terrestrial radiation ergs $cm^{-2}\ sec^{-1}\ (50A)^{-1}$	Extra-terrestrial radiation quanta $cm^{-2}\ sec^{-1}\ (50A)^{-1}$
2450	390	4.81×10^{13}
2500	380	4.78
2550	560	7.19
2600	700	9.16
2650	1000	1.33×10^{14}
2700	1350	1.84
2750	1212	1.68
2800	979	1.38
2850	1603	2.30
2900	2863	4.18
2950	3000	4.46
3000	3050	4.61
3050	3350	5.14
3100	3800	5.93
3150	4050	6.42
3200	4350	7.01
3250	5100	8.35
3300	5650	9.39
3350	5600	9.45
3400	5600	9.59
3450	5750	9.99
3500	5900	1.04×10^{15}

TABLE 3 (Continued)

Wavelength $\lambda \pm 250\text{A}^{\circ}$	Extra-terrestrial radiation ergs $cm^{-2}\ sec^{-1}\ (500A)^{-1}$	Extra-terrestrial radiation quanta $cm^{-2}\ sec^{-1}\ (500A)^{-1}$
4750	1.01×10^{5}	2.41×10^{16}
5250	9.80×10^{4}	2.59
5750	9.35	2.71
6250	8.40	2.64
6750	7.70	2.62
7250	6.75	2.46

BIBLIOGRAPHY

A

AHMED, S.J. and Halim, A., Jour. Geophys. Res., 66, 3213, 1961.

ARDC Model Atmosphere, 1959, Airforce Surveys in Geophysics No.115, Geophysics Research Directorate.

ARNOLD, S.J., Ogryzlo, E.A. and Witzke, H., Jour. Chem. Phys., 40, 1769, 1964.

B

BALLIF, J.R. and Venkateswaran, S.V., Jour. Atmos. Sci., 20, 1, 1963 a.

BALLIF, J.R. and Venkateswaran, S.V., Jour. Atmos. Sci., 20, 251, 1963 b.

BARTH, C.A. "Chemical Reactions in the Lower and Upper Atmosphere". (Interscience, New York, 1961), Chapt. 20.

BARTH, C.A., Abstract from COSPAR, 1964.

BASCO, N. and Norrish, R.G.W., Nature, 189, 455, 1961.

BATES, D.R., "The Earth as a Planet" ed. by G.P. Kuiper, (Chicago University Press, 1954), Chapt. 12.

BATES, D.R. and Moiseiwitsch, B.L., Jour. Atmos. Terr. Phys., 8, 305, 1956.

BATES, D.R. and Nicolet, M., Jour. Geophys. Res., 55, 301, 1950.

BATES, D.R. and Witherspoon, A.E., Mon. Not. R. Astrom. Soc., 112, 101, 1952.

BENSON, S.W. and Axworthy, A.E., Jour. Chem. Phys., 26, 1718, 1957.

BEZBERKHNY, Sh. A., Osherovich, A.L. and Rodionov, S.F., Akad. nauk SSSR Doklady (Geophysics), 106, 651, 1956.

BREWER, A.W., Quart. J.R. Met. Soc., 75, 351, 1949.

BREWER, A.W. and Milford, J.R., Proc. Roy. Soc., 256, 470, 1960.

BRIGGS, J. and Roach, W.T., Quart. J.R. Met. Soc., 89, 225, 1963.

BRIX, P. and Herzberg, G., Can. Jour. Phys., 32, 110, 1964.

BUTLER, S.T. and Small, K.A., Proc. Roy. Soc., 274, 91, 1963.

C

CASTELLANO, E. and Schumacher, H.J., Jour. Chem. Phys., 36, 2238, 1962.

CARROLL, P.K., Astrophys. Jour., 129, 794, 1959.

CHAMBERLAIN, J.W., "Physics of the Aurora and the Airglow" (Academic Press, New York, 1961).

CHAPMAN, S., Proc. Phys. Soc., 43, 483, 1931.

CLYNE, M.A.A., Thrush, B.A. and Wayne, R.P., Nature, 199, 1057, 1963.

CRAIG, R.A., Met. Mono., 1, 2, 1950.

D

DEB, S., Jour. Atmos. Terr. Phys., 2, 309, 1952.

DEMORE, W. and Raper, O.F., Jour. Chem. Phys., 37, 2048, 1962.

DETWILER, C.R., Garret, D.L., Purcell, J.D. and Tousey, R., Ann. Geophys., 17, 263, 1961.

DITCHBURN, R.W. and Young, P.A., Jour. Atmos. Terr. Phys., 24, 127, 1962.

DOBSON, G.M.B., Ann. I.G.Y., V, 46, 1957.

DOBSON, G.M.B., Brewer, A.W. and Cwilong, B.M., Proc. Roy. Soc., 185, 144, 1946.

DOBSON, G.M.B., Harrison, D.N. and Lawrence, J., Proc. Roy. Soc., 122, 456, 1929.

DOBSON, G.M.B. and Normand, C., Jour. Geophys. Res., 67, 4093, 1962.

DOERING, J.P. and Mahan, B.H., "Chemical Reactions in the Lower and Upper Atmosphere". (Interscience, New York, 1961), Chapt. 21.

DUNKELMAN, L. and Scolnik, R., Jour. Opt. Soc. Amer., 49, 536, 1959.

DÜTSCH, H.U., Archiv. f. Met., Geoph. und Biokl., A.9, 87, 1956.

DÜTSCH, H.U., Final Report, Contract No. AF 61 (514) - 905, 1959.

DÜTSCH, H.U., "Chemical Reactions in the Lower and Upper Atmosphere". (Interscience, New York, 1961), Chapt. 11.

E

EBDON, R.A., Quart. J.R. Met. Soc., 87, 322, 1961.

F

FITZSIMMONS, R.V. and Bair, E.J., Jour. Chem. Phys., 40, 451, 1964.

FOURNIER d'Albe, E.M., and Rasool, S.I., Ann. Geophys., 12, 72, 1956.

FUNK, J.P. and Garnham, G.L., Tellus, 14, 378, 1962.

G

GODSON, W.L., Quart, J.R. Met. Soc., 86, 301, 1960.

GODSON, W.L., Quart. J.R. Met. Soc., 88, 220, 1962.

GOLDBERG, L. "The Earth as a Planet" ed. by G.P. Kuiper, (Chicago University Press, 1954), Chapt. 9.

GOODY, R.M. "The Physics of the Stratosphere". (Cambridge University Press, 1954), Chapt. 6.

GOTZ, F.W.P., "Compendium of Meteorology" (Amer. Meteor. Soc., Boston, 1951) p. 275.

GOWAN, E.H., Proc. Roy. Soc., 190, 219, 1947a.

GOWAN, E.H., Proc. Roy. Soc., 190, 227, 1947b.

H

HARTECK, P. and Dondes, S. Phys. Rev., 95, 320, 1954.

HARTECK, P. and Reeves, R., "Chemical Reactions in the Lower and Upper Atmosphere". (Interscience, New York, 1961), Chapt. 14.

HEARN, A.G., Proc. Phys. Soc., 87, 932, 1961.

HERRON, J.F. and Klein, F.S., Jour. Chem. Phys., 40, 2731, 1964.

HERZBERG, G., "Spectra of Diatomic Molecules". (Van Nostrand, New Jersey, 1961).

HERZBERG, G. and Herzberg, L., Nature, 161, 283, 1948.

HUNT, B.G., Weapons Research Establishment, T.N. PAD 86, 1964.

I

INN, E.C.Y. and Tanaka, Y., Jour. Opt. Soc. Amer., 43, 870, 1953.

J

JOHANSEN, H., Spec. Suppl., Jour. Atmos. Terr. Phys., 189, 1957.

JOHNSON, F.S., Bull. Amer. Met. Soc., 34, 106, 1953.

JOHNSON, F.S., Jour. Met., 11, 431, 1954.

JOHNSON, F.S., Purcell, J.D. and Tousey, R., Jour. Geophys. Res. 56, 583, 1951.

JOHNSON, F.S., Purcell, J.D., Watanabe, K. and Tousey, R., Jour. Geophys. Res., 57, 157, 1952.

JONES, W.N. and Davidson, N., Jour. Amer. Chem. Soc., 84, 2862, 1962.

JURSA, A.S., Tanaka, Y., and LeBlanc, F., Plan. Space Sci., 1, 161, 1959.

K

KATAKIS, D. and Taube, H., Jour. Chem. Phys., 36, 416, 1962.

KAUFMAN, F., Ann. Geophys., 20, 106, 1964.

KAUFMAN, F. and Kelso, J.R., "Chemical Reactions in the Lower and Upper Atmosphere." (Interscience, New York, 1961), Chapt. 16.

KHALEK, A. and Vassy, A., Comptes Rendus, 235, 737, 1952.

KOCKARTS, G. and Nicolet, M., Ann. Geophys., 18, 269, 1962.

KRASSOVSKY, V.I., "The Airglow and the Aurorae" ed. by E.B. Armstrong and A. Dalgarno, (Pergamon Press, London, 1955), p. 197.

KRASSOVSKY, V.I., COSPAR III, ed. by W. Priester, (North-Holland Publishing Co., Amsterdam, 1963) p. 96.

KROENING, J.L. and Ney, E.P., Jour. Geophys. Res., 67, 1867, 1962.

KULKARNI, R.N., Nature, 198, 1189, 1963.

L

LEOVY, C., Jour. Atmos. Sci., 21, 238, 1964.

LONDON, J. and Haurwitz, M.W., Jour. Geophys. Res., 68, 795, 1963.

LONDON, J. and Prabhakara, C., Final Report, Contract No. AF 19 (604) - 5492, AFCRL - 62 - 672, 1962.

LYTLE, E.A. and Hampson, J., Nature, 202, 76, 1964.

M

MACDOWALL, J., Proc. Roy. Soc., 265, 149, 1960.

MCGRATH, W.D. and Norrish, R.G.W., Proc. Roy. Soc., 242, 265, 1957.

MCGRATH, W.D. and Norrish, R.G.W., Proc. Roy. Soc., 254, 317, 1960.

MCKINLEY, J., Garvin, D. and Boudart, M., Jour. Chem. Phys., 23, 784, 1955.

MATEER, C.L. and Godson, W.L., Quart, J.R., Met. Soc., 86, 512, 1960.

MATHIAS, A. and Schiff, H.I., Jour. Chem. Phys., 40, 3118, 1964.

MATTHEWS, D.L., Phys. of Fluids, 2, 170, 1959.

MITCHELL, W.E., Astrophys. Jour., 129, 93, 1959.

MULLIKEN, R.S., Phys. Rev., 43, 279, 1933.

MURGATROYD, R.J. and Goody, R.M., Quart, J.R. Met. Soc., 84, 225, 1958.

MURGATROYD, R.J. and Singleton, F., Quart. J.R. Met. Soc., 87, 125, 1961.

N

NEWELL, R.E., Quart. J.R. Met. Soc., 89, 167, 1963.

NICHOLLS, L.A., Weapons Research Establishment, T.N. SAD 85, 1962.

NICOLET, M., "The Earth as a Planet" ed. by G.P. Kuiper, (Chicago University Press, 1954), Chapt. 13.

NICOLET, M., Bull. Soc. Chim. Belg., 71, 665, 1962.

NICOLET, M. and Aikin, A.C., Jour. Geophys. Res., 65, 1469, 1960.

N (Continued)

NICOLET, M. and Mange, P., Jour. Geophys. Res., 59, 15, 1954.

NORMAND, C., Quart. J.R. Met. Soc., 79, 39, 1953.

NOXON, J.F., Can. Jour. Phys., 39, 1110, 1961.

O

OHRING, G. and Muench, H.S., Jour. Met., 17, 195, 1960.

OKA, T. and Morino, Y., Jour. Mol. Spectry., 8, 9, 1962.

P

PACKER, D.M., Ann. de Geophys., 17, 67, 1961.

PAETZOLD, H.K., Jour. Atmos. Terr. Phys., 3, 125, 1953.

PAETZOLD, H.K., "Chemical Reactions in the Lower and Upper Atmosphere." (Interscience, New York, 1961), Chapt. 12.

PAETZOLD, H.K. and Kulcke, W., Ann. Meteor., 8, 47, 1957.

PEYTURAUX, R., Ann. Astrophys., 18, 34, 1955.

PHILLIPS, L.F. and Schiff, H.I., Jour. Chem. Phys., 36, 1509, 1962.

PIERCE, A.K. and Waddell, J.H., Mem. R. Astron. Soc., LXVIII, 1961.

PIERCE, A.K., Handbuch der. Physik, LII, 1959.

PLASS, G.N., Quart. J.R. Met. Soc., 82, 30, 1956 a.

PLASS, G.N., Quart. J.R. Met. Soc., 82, 310, 1956 b.

PRESSMAN, J., Jour. Met., 12, 87, 1955.

PURCELL, J.D. and Tousey, R., Mem. Soc. R. Sci. Liege, 4, 283, 1961.

R

RAMANATHAN, K.R., Quart, J.R. Met. Soc., 89, 540, 1963.

RAMANATHAN, K.R. and Kulkarni, R.N., Quart. J.R. Met. Soc., 86, 144, 1960.

R (Continued)

RAMANATHAN, K.R., Shah, G.M. and Angreji, P.D., IUGG Monograph No.19, 13, 1961.

RANK, D.H., Slomba, A.F., Gardner, E.F. and Wiggins, T.A., Jour. Opt. Soc. Amer., 52, 858, 1962.

RAPER, O.F., DeMore, W., Astrophys. Jour., 139, 1381, 1964.

RAWCLIFFE, R.D., Meloy, G.E., Friedman, R.M. and Rogers, E.H., Jour. Geophys. Res., 68, 6425, 1963.

REED, R.J., Jour. Met., 7, 263, 1950.

REED, R.J. and Rogers, D.G., Jour. Atmos. Sci., 19, 127, 1962.

REEVES, R.R., Manella, G. and Harteck, P., Jour. Chem. Phys., 32, 632, 1960.

REGENER, V.H., Advances in Chem., 21, 124, 1959.

S

SCHIFF, H.I., Bull. Soc. Chim. Belg., 71, 670, 1962.

SCHIFF, H.I., Ann. Geophys., 20, 115, 1964.

SEATON, M.J., Astrophys. Jour., 127, 67, 1958.

SHAPIRO, R. and Ward, F., Jour. Atmos. Sci., 19, 506, 1962.

SPONER, H. and Teller, E., Rev. Mod. Phys., 13, 75, 1941.

STALEY, D.O., Jour. Atmos. Sci., 20, 506, 1963.

STRANZ, D., Tellus, 13, 276, 1961.

STROUD, W.G. and Nordberg, W., NASA, T.N. D-703, 1961.

T

De TURVILLE, C.M., Nature, 190, 156, 1961.

TANAKA, Y., Inn, E.C.Y. and Watanabe, K., Jour. Chem. Phys., 21, 1651, 1952.

V

VALLANCE JONES, A. and Gattinger, R.L., Plan. Space Sci., 11, 961, 1963.

VASSY, A., "The Threshold of Space" ed. by M. Zelikoff, (Pergamon Press, New York, 1951), p. 73.

VENKATESWARAN, S.V., "Rocket and Satellite Meteorology" ed. by H. Wexler and J.E. Caskey, (North-Holland Publishing Co., Amsterdam, 1963), p. 199.

VIGROUX, E., Ann. de Phys., 8, 709, 1952.

W

WALLACE, L., Jour. Atmos. Sci., 19, 1, 1962.

WALLACE, L. and Chamberlain, J.W., Plan. Space Sci., 2, 60, 1959.

WATANABE, K., Inn, E.C.Y. and Zelikoff, M., Jour. Chem. Phys., 21, 1027, 1953.

WEXLER, H., Jour. Met., 7, 370, 1950.

WILKINSON, P.G. and Mulliken, R.S., Astrophys. Jour., 125, 594, 1957.

WILLETT, H.C., Jour. Geophys. Res., 67, 661, 1962.

WILSON, N.L., Tousey, R., Purcell, J.D., Johnson, F.S. and Moore, C.E., Astrophys. Jour., 119, 590, 1954.

Y

YOUNG, R.A. and Sharpless, R.L., Jour. Geophys. Res., 67, 2581, 1962 a.

YOUNG, R.A. and Shaprless, R.L., Jour. Geophys. Res., 67, 3871, 1962 b.

YOUNG, C. and Epstein, E.S., Jour. Atmos. Sci., 19, 435, 1962.

Z

ZASLOWSKY, J.A., Private Communication, 1962.

ZASLOWSKY, J.A., Urbach, H.B., Leighton, F., Wnuk, R.J. and Wojtowicz, J.A., Jour. Amer. Chem. Soc., 82, 2682, 1960.